Carl von Ossietzky Universität Oldenburg

Fakultät für Mathematik und Naturwissenschaften

The impact of ocean acidification on marine dissolved organic matter

---

An der Fakultät für Mathematik und Naturwissenschaften der Carl von Ossietzky Universität Oldenburg zur Erlangung des Grades und Titels eines Doktors der Naturwissenschaften (Dr. rer. nat.) angenommene Dissertation von Frau

Maren Zark (geb. Stumm)

geboren am 12.03.1987 in Rotenburg Wümme

1. Gutachter: Prof. Dr. Thorsten Dittmar

2. Gutachter: Prof. Dr. Meinhard Simon

Tag der Disputation: 11.02.2016

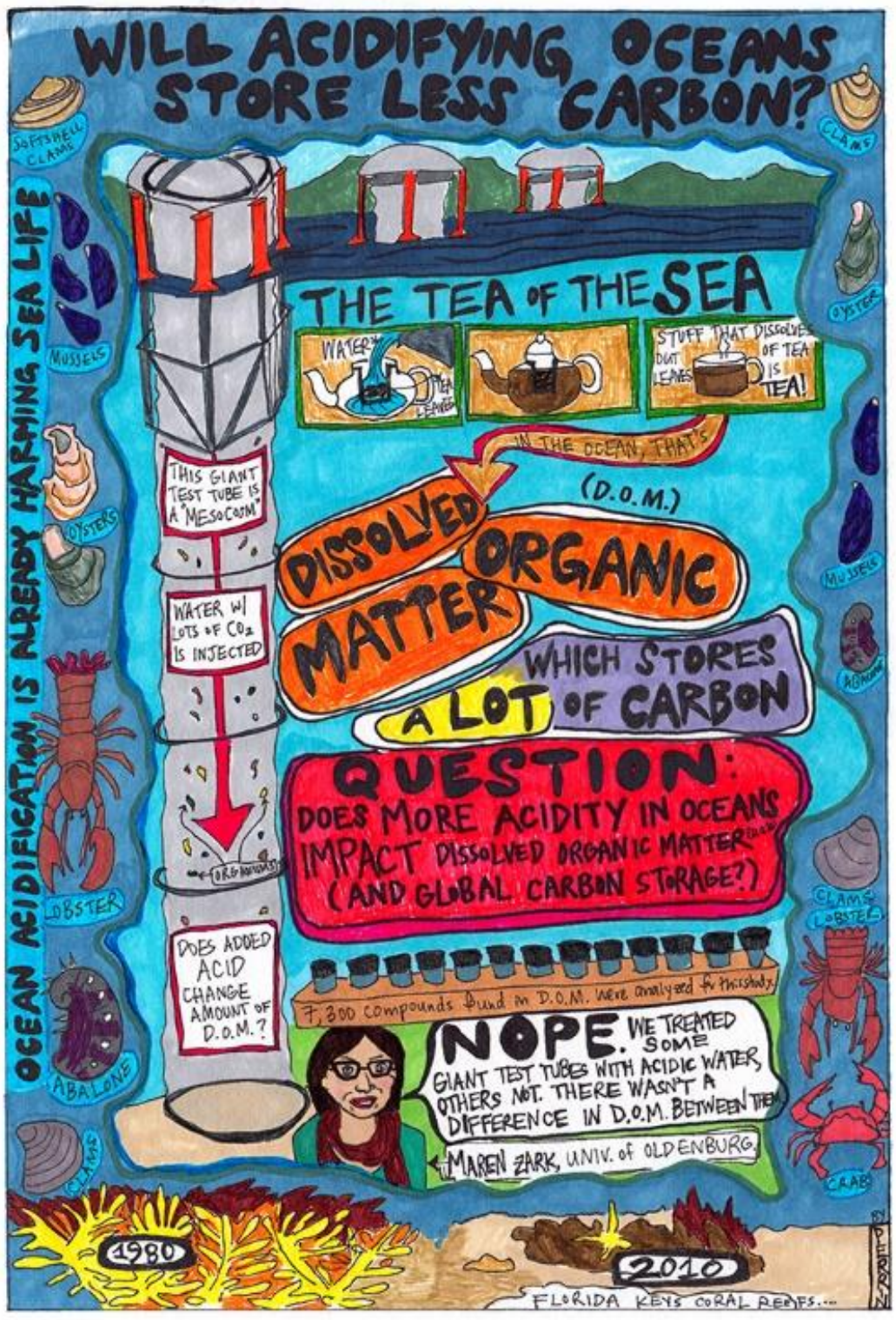

The artist Perrin Ireland illustrated parts of the results presented in this thesis in the above picture with the title “Just how bitter is the tea of the sea”.

Perrin Ireland is a senior science communications specialist at the National Resources Defense Council (NRDC), located in New York, USA. The picture was published online in October 2015 on www.onearth.com.

ABSTRACT

Marine dissolved organic matter (DOM) is one of the largest active carbon pools on earth and an important factor in the global carbon cycle. Shifts in its pool size or reactivity have the potential to affect the earth's climate in general, and the biogeochemical cycling of matter and energy in marine food webs in particular. The overarching goal of this thesis was to study the effects of ocean acidification on marine DOM, both in terms of the amount of carbon that is stored in DOM and in terms of its molecular composition. The essential results are described in four chapters, each of which corresponds to a full manuscript. One manuscript was already published, one submitted, and two are close to submission.

The first part evaluates the influence of elevated pCO_2 levels on DOM based on experiments in a Swedish Fjord (Manuscript I) and in the subtropical North Atlantic Ocean (Manuscript II). Large-scale pelagic mesocosm units were artificially enriched in CO_2 to simulate future ocean conditions. The production and consumption of individual molecular compounds was monitored over the succession of phytoplankton blooms via ultrahigh-resolution Fourier-transform ion cyclotron resonance mass spectrometry (FT-ICR-MS). Whereas a clear succession could be observed for individual molecules being produced or consumed over time, no differences were detected in molecular DOM composition related to CO_2 concentrations for both studies. Indications were found for enhanced dissolved organic carbon concentratios starting from target CO_2 levels of 1250 µatm. However, this trend was not statistically significant. The combined results suggest that the marine DOM pool may not be affected by ocean acidification within the next century.

The second part of the work (Manuscript III) focuses on a systematic comparison of chemical structures in DOM between different marine environments. To date, only a low percentage of compounds constituting the DOM pool are fully characterized, but a better understanding of structural features will be inevitable to assess the effects of ocean acidification on a global scale. Fragmentation experiments were performed via FT-ICR-MS on a range of samples, including the deep sea and water from a eutrophic lake. The fragmentation patterns serve as fingerprints for the structure of the isolated compounds and were surprisingly

similar. The analysis of relative fragment intensities indicated the presence of a large pool of compounds with common structural features in DOM among aquatic environments. A cascade of degradation pathways may hence be the ultimate source for a common refractory DOM background with undistinguishable molecular properties.

The last part of the dissertation (Manuscript IV) deals with the diversity of DOM on a molecular level. The major fraction of DOM is highly persistent towards microbial degradation and remains in the oceans for thousands of years. If this persistence was revoked as a response to ocean acidification, huge amounts of carbon could be released from the ocean interior. It has been hypothesized e.g. that the persistence could be due to either very stable chemical structures or a high diversity of compounds with concentrations too low to serve as a substrate for microorganisms. From regular FT-ICR-MS analysis alone it is not possible to extract the number of compounds present in a mixture because each detected molecular formula could represent a multitude of isomers with the same elemental composition but different chemical structures. Fragmentation experiments with deep-sea DOM, which is respresentative for the refractory fraction, provided evidence that each molecular formula is represented by a number of possible isomers. This is evidence for the fact that high diversity is more likely the source for the persistence of DOM than stable individual structures. Hence, ocean acidification will presumably not trigger the release of large amounts of carbon due to changes of specific structural features in DOM.

ZUSAMMENFASSUNG

Im Meerwasser gelöstes organisches Material („dissolved organic matter“, DOM) spielt als einer der größten aktiven Speicher für Kohlenstoff auf der Erde eine wichtige Rolle im globalen Kohlenstoffkreislauf. Veränderungen in Menge oder Reaktivität des DOM könnten das Erdklima allgemein und speziell den biogeochemischen Kreislauf von Stoffen und Energie in marinen Nahrungsnetzen beeinflussen. Das übergeordnete Ziel der vorliegenden Dissertation war es die Auswirkungen von Ozeanversauerung auf die Menge des in Form von DOM im Meer gespeicherten Kohlenstoffs und auf dessen molekulare Zusammensetzung zu untersuchen. Der Kern der Ergebnisse wird in vier Kapiteln dargestellt. Jedes Kapitel entspricht jeweils einem vollständigen Manuskript, von denen eines veröffentlicht und eines eingereicht wurde. Zwei weitere Manuskripte sind bereit für die Veröffentlichung.

Im ersten Teil der Dissertation wurde der Einfluss von erhöhten CO_2 Konzentrationen auf DOM anhand von Experimenten in einem schwedischen Fjord (Manuskript I) und im subtropischen Nordatlantischen Ozean (Manuskript II) untersucht. Große pelagische Mesokosmen wurden künstlich mit CO_2 angereichert um so die Bedingungen im zukünftigen Ozean zu simulieren. Über den Verlauf mehrerer Phytoplanktonblüten wurden Produktion und Abbau einzelner Stoffe mittels ultrahochauflösender Fouriertransformation-Ionencyclotronresonanz-Massenspektrometrie (FT-ICR-MS) auf molekularer Ebene beobachtet. In beiden Studien konnten deutliche Trends einzelner Verbindungen über die Zeit beobachtet werden, während keine Effekte auf die molekulare Zusammensetzung des DOM nachweisbar waren. Es wurden des Weiteren Hinweise darauf gefunden, dass ab einer CO_2 Konzentrationen von 1250 µatm pCO_2 mehr gelöster organischer Kohlenstoff angereichert wurde. Diese Beobachtung konnte jedoch nicht statistisch belegt werden. Zusammengefasst deuten die gesammelten Ergebnisse darauf hin, dass Ozeanversauerung innerhalb des nächsten Jahrhunderts keinen Einfluss auf das im Meerwasser gelöste DOM haben wird.

Im Fokus des zweiten Teils der Arbeit (Manuskript III) steht ein systematischer Vergleich der chemischen Strukturen, die in DOM Proben aus unterschiedlichen aquatischen Gebieten vorkommen. Nur ein geringer Prozentsatz der Verbindungen,

die in DOM auftreten, ist bisher vollständig charakterisiert worden. Ein besseres Verständnis der strukturellen Merkmale ist jedoch erforderlich um die Auswirkungen von Ozeanversauerung auf globaler Ebene besser einschätzen zu können. DOM aus unterschiedlichen Gewässern, einschließlich der Tiefsee und einem eutrophen See, wurde durch Fragmentierung anhand von tandem FT-ICR-MS untersucht. Die Fragmentierungsmuster der jeweiligen isolierten Verbindungen dienen als Fingerabdruck für ihre Struktur und zeigten eine überraschende Ähnlichkeit über alle Proben hinweg. Die Auswertung der relativen Fragmentintensitäten wies auf eine Kette von Abbauprozessen hin, die zur Bildung eines gemeinsamen refraktären DOM Hintergrunds mit nicht unterscheidbaren molekularen Eigenschaften führen könnte.

Der letzte Teil der Dissertation (Manuskript IV) behandelt die Diversität von DOM auf molekularer Ebene. Der größte Teil des DOM ist hochresistent gegenüber mikrobiellem Abbau und verbleibt über tausende von Jahren im Ozean. Wenn diese Persistenz durch Umwelteinflüsse wie Ozeanversauerung aufgehoben würde, könnten große Mengen Kohlenstoff aus dem Meer freigesetzt werden. Eine mögliche Erklärung für die Persistenz von DOM ist, dass hauptsächlich sehr stabile chemische Strukturen vorliegen könnten. Des Weiteren wäre es denkbar, dass die Diversität der vorliegenden Komponenten sehr hoch und damit die jeweilige Konzentration zu gering ist um als Substrat für Mikroorganismen geeignet zu sein. Anhand von FT-ICR-MS Analysen allein ist es nicht möglich die Anzahl der vorhandenen Verbindungen zu ermitteln, da jede detektierte Summenformel eine Vielzahl von unterschiedlichen Isomeren mit derselben Elementzusammensetzung repräsentieren könnte. Fragmentierungsexperimente an DOM aus der Tiefsee, welches charakteristisch für den persistenten Anteil in DOM ist, lieferten Hinweise darauf, dass eine Vielzahl möglicher Isomere mit unterschiedlichen chemischen Strukturen vorliegt. Dies deutet auf eine hohe Diversität von Verbindungen in DOM als Ursache für dessen Persistenz hin. Es ist somit unwahrscheinlich, dass Ozeanversauerung Veränderungen in der chemischen Struktur des DOM hervorrufen und infolgedessen Auslöser für die Freisetzung größerer Mengen an Kohlenstoff sein könnte.

ACKNOWLEDGEMENTS

First and foremost I would like to thank my advisor, Thorsten Dittmar, for guidance during this thesis work. Thank you for the Friday afternoon brainstormings and for being a great source of motivation. You have been a fantastic supervisor with many fresh and inspiring ideas. I would further like to thank Meinhard Simon for reviewing this thesis and for his guidance during Polarstern cruise ANT XVIII/5, which was one of the most exciting experiences of my career as a marine scientist this far. Thank you, Hans Brumsack, for agreeing to be part of my doctorate committee.

Ulf Riebesell, head of the two KOSMOS experiments, has contributed to this work with a lot of scientific expertise on ocean acidification, which had been a completely new chapter for me when I started my PhD. Thank you for getting this huge team of researchers together and for being such a visionary and motivating person.

My working group, the “geochems”: you have been a great source of help, inspiration and joy. I am especially grateful to Jutta Niggemann for scientific discussions and for support during project meetings or conferences. More special thanks go to my aquarium officemates Helena Osterholz, Maren Seibt and Hannelore Waska for advice, discussions and for just making my day brighter! Your support with the planning of field trips, labwork, and solving R problems was incredibly helpful. In this sense, I would further like to thank Marcus Manecki who helped a lot with statistics and forced me to use R in the first place. Thank you Pamela Rossel, Michael Seidel, and Jeff Hawkes for sharing your endless knowledge and advice on scientific and other life-related problems during morning coffees. A huge THANKS to my PhD fellows: Beatriz Noriega, Anika Pohlabeln, Nadine Broda, Maria del Carmen Igarza Tagle, Andrea Mentges, Gonzalo Gómez Sáez, and Jomar Marques da Silva for organizing container BBQs, exchanging survival tips and for making workdays a lot more fun! I would further like to thank Susanne Wendeling for help with institutional paperwork, billings and for her friendly assistance. Thank you, Ina Ulber, Matthias Friebe, and Kathrin Klaproth for technical support in the lab, for sending equipment to any place in the world, for the analysis of DOC samples, and for help with FT-ICR-MS analyses. I am

incredibly fortunate to be a member of this team and I have met many wonderful people in the Dittmar lab – thank you all for having such a great time!

As I spent some time of my PhD in the field I would also like to thank the KOSMOS mesocosm crew from both experiments in Sweden 2013 and Gran Canaria 2014. An enormous THANK YOU goes to Andrea Ludwig who was the heart and soul of both experiments. Thank you also Dana Hellemann, Meri Algueró, Micha Sswat, Jan Büdenbender, Jan Czerny, Lennart Bach, Tim Boxhammer and Thomas Hornick for fikas, enjoyable sampling trips, fawesome dinners and being such good friends within the KOSMOS. I hope we can add some more destinations on our list. I would further like to thank Maike Nicolai for making great effort to communicate our science to the broad public.

To my friends: Crispin and Julia, thank you for reading manuscripts and for sharing daily PhD problems. Susanne, thank you for the cake and motivation flowers – their shouting did a great job! Elly, thank you for being such a great friend for so many years. Aaron and Laura, thank you for Friday evenings and for going down so many roads together.

Most importantly, I would like to thank my family for their love and guidance. Thank you mom for care packages, Sunday visits and encouraging words. Dad, thank you for introducing me to the wonderful and exciting world of chemistry. And finally, I would like to thank my husband Patrick who had to share his wife for some time with this thesis. Sorry for that. Thank you for listening to my thoughts and problems and also for cooking Frikadellen mit Erbsen on Sunday evenings.

TABLE OF CONTENTS

LIST OF ABBREVIATIONS

AABW	Antarctic Bottom Water
A_T	Total alkalinity
CRAM	Carboxyl-rich alicyclic molecules
DIC	Dissolved inorganic carbon
DOC	Dissolved organic carbon
DOM	Dissolved organic matter
EMW	Eurafrican Mediterranean Water
ESI	Electrospray ionization
FOCE	Free ocean CO_2 experiment
FT-ICR-MS	Fourier-transform ion cyclotron resonance mass spectrometry
HMW	High molecular weight (> 1 kDa)
KOSMOS	Kiel off-shore mesocosms for future ocean simulations
LMW	Low molecular weight (< 1 kDa)
pCO_2	Partial pressure of CO_2
NADW	North Atlantic Deep Water
NEqPIW	North Equatorial Pacific Intermediate Water
NMR	Nuclear magnetic resonance
PCA	Principal components analysis
R	Revelle factor
SPE	Solid phase exctraction
TDN	Total dissolved nitrogen
TEP	Transparent exopolymer particles
[ ]	concentration

1. Introduction

Within the last decade, ocean acidification has emerged to one of the fastest growing fields of marine research with a steep increase in research effort (Riebesell and Gattuso, 2015). Scientists as well as policy-makers have recognized the urge for a better understanding of ocean acidification and its consequences as it has the potential to cause major long-term changes in the global environment. In addition to prominent examples such as decalcification of mussel shells and corals, ocean acidification may affect the planet in manifold ways, for example, by causing changes to the marine ecosystems and their services to humankind (Dupont and Pörtner, 2013) or by impacts on the global carbon cycle (Falkowski et al., 2000). The changes in seawater chemistry, induced by elevated levels of atmospheric carbon dioxide, could directly or indirectly affect organisms or element pools. Despite the fact that impacts on the global climate will presumably not become visible before the end of the century, it is important for modern societies to think ahead and be aware of what might affect future generations. Models providing valuable information by determining the magnitude of potential effects (Sarmiento et al., 2004; Oschlies et al., 2008) and obtaining sufficient scientific data for future ocean models are thus of utmost importance in order to make valid projections for the next centuries.

One of the largest active carbon pools on earth and important for carbon storage and key biogeochemical processes in the marine carbon cycle is marine dissolved organic matter (DOM). Changing environmental conditions such as ocean acidification have the potential to impact the marine DOM pool in its quantity and composition. Due to its great size, shifts in reactivity or partitioning of carbon species could induce negative feedbacks on the future climate. The major fraction of DOM in seawater, however, remains chemically uncharacterized and our understanding of the chemical structures in DOM is still at its beginning. In summary, it is not known whether the DOM pool can change in size and what would drive these changes.

The goal of this dissertation was to gain a better understanding of the molecular structure of dissolved organic matter in different marine environments and to

identify the potential impacts of ocean acidification as environmental stressor on this important carbon pool on earth.

1.1 Dissolved organic matter in the marine environment

1.1.1 Inventory and fluxes

Each liter of seawater in the global oceans contains about 0.5-1 mg dissolved organic compounds (Repeta, 2015), about as much as a few crumbs of ground coffee. These compounds make up a rather small fraction if compared to the amount of 35 g salt that is dissolved in each liter, for example. But as the oceans cover a large proportion of the earth's surface, the small amounts per liter result in a total mass of about 662 Pg carbon, which is similar in size to all living biomass on earth (Hansell et al., 2009). Marine dissolved organic matter is thus among the most important active pools within the global carbon cycle and its fate is an important factor influencing global climate.

The ultimate source of organic matter in the open oceans is primary production in the euphotic zone by algal communities, e.g. diatoms (Fig. 1.1) which release the fixed carbon as DOM either directly into the water or after cell-death (Carlson, 2002). About 0.24 Pg C yr^{-1} is transported to the oceans via riverine, tidal, and fluvial input from the continents (Dittmar and Stubbins, 2014). These terrestrial sources, however, are probably of minor importance to the marine DOM cycle as it was suggested by global ocean models (Hansell et al., 2012, 2009). Dissolved organic carbon (DOC) as a quantitative measure of DOM is high at 60 – 80 µmol L^{-1} in the surface layer of the ocean where production takes place. DOC concentration then decrease with depth to minimum values of about 34 µmol L^{-1} in the deep sea (Hansell et al., 2009). Annual net DOM production is most evident in oceanic regions that experience phytoplankton blooms and particularly coastal seas constitute one of the biologically most productive marine areas, accounting for 10-15% of oceanic net primary production (Cloern et al., 2014). Both, quantity and quality of the produced DOM varies between bloom events and is likely controlled by factors such as nutrient status and phytoplankton community structure (Carlson et al., 1998).

1.1.2 Size and reactivity fractions

Marine DOM compounds show a spectrum of reactivities, based on their chemical structure, and can be divided into different reactivity fractions (Hansell et al., 2009). Labile and semi-labile DOM constitute only a small fraction (~1%) of the bulk DOM pool on the global scale (Hansell et al., 2009), but serves as the key link between larger phytoplankton and marine heterotrophic microorganisms, which use DOM as substrate and immediately respire it to CO_2. The turnover time for these compounds is within minutes up to days for labile DOM and from months up to more than a year for semi-labile DOM (Hansell et al., 2012). About half of the carbon fixed by primary production in the surface ocean (~30 Pg C yr^{-1}) is shunted via labile DOM to marine microorganisms that are grazed in turn by Protozoa (Azam and Malfatti, 2007; Williams, 2000). Within this "microbial loop" concept, microorganisms make elements and energy fixed by marine primary production available to higher trophic levels (Fig. 1.1). Labile DOM thus forms the organic bottom of the marine food web.

A smaller but significant fraction of DOM production (~2 Pg C yr^{-1}) escapes fast decomposition by microbial degradation and is transformed to resistant compounds that accumulate in the ocean on time scales ranging from hours to millennia (Hansell, 2013). This refractory DOM represents by far the largest DOC pool (~99%) in terms of carbon inventory (Hansell et al., 2012). Its mean apparent radiocarbon age is ~6000 years in the deep sea, which exceeds the circulation time of the ocean several times and makes it an important component of the global carbon cycle on historic time scales (Bauer et al., 1992; Williams and Druffel, 1987).

Refractory DOM concentration is homogenous throughout the water column and represents about 60% of the surface DOC in stratified systems (Hansell, 2013). Its unreactive character remains enigmatic, considering the amount of energy that it could supply to marine microbes (Dittmar, 2015). The processes that lead to the formation of refractory DOM are not completely understood either. UV exposure can alter the chemical composition of DOM (Kujawinski et al., 2009) and may partially lead to the formation of persistent structures. But the largest fraction of refractory DOM is presumably formed as a byproduct of the heterotrophic

microbial processing of labile DOM. This hypothesis is also referred to as the "microbial carbon pump" concept, as the produced compounds are stored in the ocean interior for months to millennia (Jiao et al., 2010). In other terms, if labile DOC is responsible for fueling the microbial food web, refractory DOC is important for carbon export and sequestration.

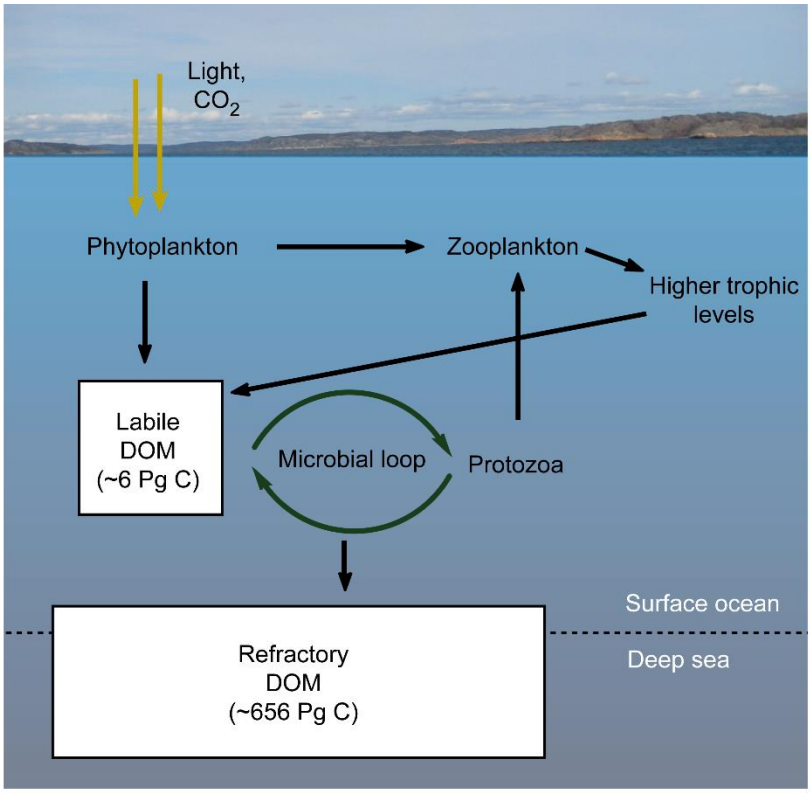

Figure 1.1: A simplified schematic of the ocean carbon cycle and the microbial loop. Primary production is the major DOM source in the oceans (Carlson, 2002). The microbial loop (Azam and Malfatti, 2007) makes the fixed carbon available to higher trophic levels. Labile (including conceptual semi-labile species) and refractory (including conceptual semi-refractory and ultra-refractory species) DOM pools are displayed in boxes in relation to their carbon inventories. Labile DOM is mostly processed within the surface ocean while refractory DOM occurs uniformly distributed throughout the water column (Hansell et al., 2012).

DOM can be roughly divided into two size fractions: colloidal material of high molecular weight (HMW, > 1kDa) and truly dissolved molecules of low molecular weight (LMW, < 1kDa). LMW-DOM comprises 60-80 % of the marine DOM pool and partly consists of labile compounds such as amino acids or monosaccharides but to the greater extent of refractory, structurally uncharacterized molecules

(Hansell, 2013). The remaining 20-35 % of the bulk carbon in DOM is categorized as HMW-DOM. Marine bacteria, however, are limited to the uptake of sufficiently small LMW-DOM (up to ~600 Da). Extracellular enzymes can convert HMW-DOM to smaller compounds, and thus play a key role for the fate of the organic matter produced in marine systems (Arnosti, 2011; Simon et al., 2002).

While the classical definition restricts DOM to be smaller than 0.2 to 0.7 µm, a new concept has emerged that considers DOM rather as a size continuum (Fig. 1.2) and challenges the paradigm of seawater as a homogenous mixture (Verdugo et al., 2004). The size scale of organic components in seawater ranges from individual molecules, through gel networks, to larger sinking aggregates.

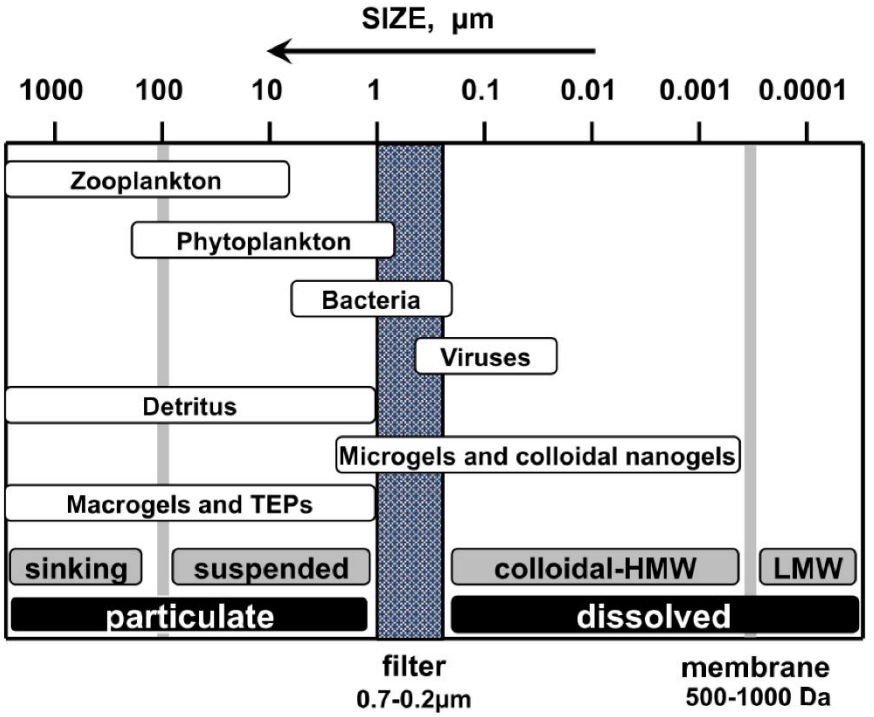

Figure 1.2: Size continuum of marine organic matter. Dissolved and particulate organic matter are operationally separated by filter size (0.2 to 0.7 µm). The cut-off between high molecular weight (HMW) and low molecular weight (LMW) DOM is 1 kDa. Macrogels and transparent exoppolymer particles (TEP) are formed by aggregation processes. Reprinted from: Álvarez-Salgado and Arístegui, 2015.

The individual components may be transformed on short timescales from minutes to hours and bridge the dissolved-particulate continuum (Verdugo et al., 2012). For example, carbohydrates are important precursors for the abiotic

formation of transparent exopolymeric particles (TEP) that have a sticky character and share characteristics with marine microgels (Passow, 2002). This process is also referred to as “abiotic loop” because the formed particles are large enough to be taken up by marine organisms (Alldredge et al., 1993). Larger marine microgels can form in situ through aggregation of smaller precursors and represent metabolic hotspots for the microbial loop (Azam, 1998; Azam and Malfatti, 2007). Biological processes are hence partially shaping the size spectrum of organic matter. Refractory DOM, for example, was observed to be more persistent and aged with smaller size. This relationship between the size, reactivity, and chemical composition of marine organic matter was summarized in a “size-reactivity continuum” model (Benner and Amon, 2015).

1.1.3 Elucidating the chemical structure of DOM

A central task of today’s biogeochemists is to improve the understanding of why DOM persists in the deep sea. The reactivity of compounds is driven by their chemical structure, but despite its importance, only very little is known about the structural composition of marine DOM. One of the main problems is that DOM represents a highly complex organic mixture. Natural DOM samples comprise thousands of molecular masses, with a high number of isomers potentially possible for each mass (Hertkorn et al., 2008). This vast structural diversity poses a challenge to modern analytical methods, reflected in the fact that less than 7% of marine organic carbon can currently be assigned to specific compound groups. Targeted derivatization or break down of specific compound groups (e.g. oxidation of lignins) coupled to the subsequent detection of resulting products via chromatographic methods reduces molecular complexity and allows for the detection of molecular building blocks (Opsahl and Benner, 1997). However, only 1% of bulk DOM accounts for quantifiable small biopolymers such as carbohydrates, fatty acids, and amino acids, that can be isolated from the mixture (Kaiser and Benner, 2012, 2009). A complete separation of all compounds present in DOM samples by chromatographic methods is not possible to date, due to the very low concentration of each individual component (Arrieta et al., 2015). The main fraction thus remains uncharacterized on the molecular level.

Optical techniques using UV-visible absorption and fluorescence have proven to be powerful tools in describing qualitative changes in bulk DOM. However, they are limited to the chromophoric fraction and do not give detailed structural information. Non-target analytical techniques such as nuclear magnetic resonance (NMR) spectroscopy or Fourier-transform ion cyclotron resonance mass spectrometry (FT-ICR-MS) are advantageous as they are unselective and have the power to characterize the entire pool of compounds present in DOM samples (Hertkorn et al., 2013; Mopper et al., 2007).

These information-rich detection methods, however, require samples with high DOM concentrations and low amounts of inorganic salts. In principle, there are three classes of isolation methods available to separate the organic molecules from dissolved inorganic salts: ultrafiltration (Amon and Benner, 1996), solid phase extraction (SPE) as the most commonly used isolation method (Dittmar et al., 2008; Minor et al., 2014), and reverse osmosis (e.g. Vetter et al., 2007). Good DOC recoveries of ~60% can be achieved for SPE by using a commercially available styrene-divinylbenzene polymer (Varian PPL) as resin (Dittmar et al., 2008). For PPL, the extracted compounds cover a broad range of polarities and are representative for the entire DOM pool (Dittmar et al., 2008). However, a major part of DOM is lost from the analytical window and none of the isolation methods allows for 100% recovery of DOC, which has to be considered for later data interpretation.

Nuclear magnetic resonance (NMR) spectroscopy is widely applied for chemical characterization of marine DOM samples (Dittmar and Stubbins, 2014). It provides detailed information about the linkages and proximities of the nuclei of individual stable isotopes within DOM (e.g. ^{1}H, ^{13}C) by interaction with extremely weak electromagnetic radiation in the radio waveband. The obtained chemical shifts can be related to specific chemical structures and functional groups within substances (Fig. 1.3). NMR is applicable to any molecular size class of organic molecules and can be performed on liquid or solid DOM samples (Simpson et al., 2011).

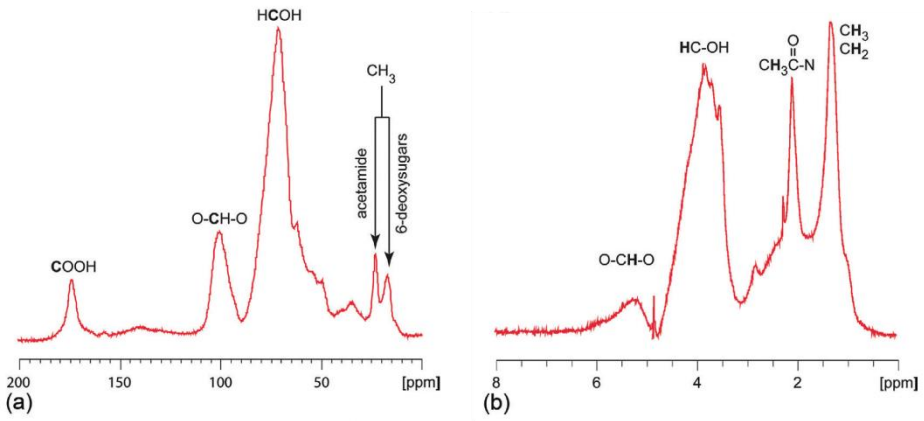

Figure 1.3: Nuclear magnetic resonance spectra of ultrafiltered DOM samples from surface seawater collected in the North Pacific Ocean. (a) ^{13}C NMR, and (b) ^{1}H NMR spectra with functionalities assigned to the chemical shifts. Adapted from: Repeta et al., 2015.

Information on specific functionalities alone is insufficient to establish the complete structure of molecules in complex mixtures but provides major constraints on the average structural characteristics of DOM. By the use of ^{13}C NMR it was possible to identify carbohydrates (C-O resonance at 72 ppm; O-C-O resonance at 100 ppm, Fig. 1.3a) as an abundant DOM fraction in surface waters that decreases rapidly with increasing depth. However, carbohydrates were not completely absent in samples from the deep sea, providing evidence for a refractory DOM pool of carbohydrate-like molecules (Benner et al., 1992; Hedges et al., 1992). Another important contribution to the field was the identification of carboxyl-rich alicyclic molecules (CRAM) from two-dimensional NMR spectroscopy combined with FT-ICR-MS analysis and it was estimated that CRAM constitutes ~8% of the DOM pool (Hertkorn et al., 2006). Hence, it represents the largest fraction of DOM identified to date. Its biogeochemical origin and formation mechanism, however, remain unclear (Hertkorn et al., 2006).

Solid-state ^{13}C NMR analysis of North Pacific Deep Water DOM, which is considered to be among the most degraded DOM samples and thus most representative for refractory DOM (Hansell et al., 2009), suggests a higher structural diversity than in DOM from shallower depths (Dittmar and Stubbins, 2014). A similar complexity was indicated by novel two-dimensional NMR techniques, which allowed the identification of around 1500 structural moieties in DOM (Hertkorn et al., 2013). But as any analytical technique is limited to its

window, the molecular diversity of DOM surpasses the resolving capabilities of NMR (Hertkorn et al., 2013). The original molecular structures of the DOM compounds remain elusive by using NMR spectroscopy because the detected structural features cannot be assigned to individual molecules.

Ultrahigh resolution mass spectrometry has emerged to one of the most commonly used techniques to characterize the DOM pool on a molecular level. Fourier-transform ion cyclotron resonance mass spectrometry (FT-ICR-MS) coupled to electrospray ionization (ESI) has the power to fully resolve intact DOM compounds down to the level of individual masses (Fig. 1.4). The resolution power and mass accuracy are very high (0.1 mDa) and even exceed the mass of single electrons (0.5 mDa). As every elemental isotope has a unique mass defect, molecular formulae can be assigned to each mass within an error of < 1ppm (Koch et al., 2005; Stenson et al., 2003, 2002). Even though the number of structural isomers with identical molecular formulae may be high (Hertkorn et al., 2008), basic structural features and abundance patterns can be derived for each specific mass.

Parameters such as saturation state (H/C elemental ratio), the number of double bond equivalents or an aromaticity index give structural information about the compound groups present in DOM (Koch and Dittmar, 2006; Šantl-Temkiv et al., 2013, Stenson et al., 2003). One of the first studies separating compound groups by molecular parameters found a significant fraction of polyaromatic molecules present in DOM samples from the Southern Ocean (Dittmar and Koch, 2006) that are highly resistant to biodegradation and likely originate from thermogenic processes in the seafloor or from wildfires on land (Dittmar and Paeng, 2009). This group is characterized by very low hydrogen and oxygen content and a high number of double bond equivalents, which can be inferred from molecular formulae alone. Further, the detected masses in FT-ICR-MS spectra of terrestrial plant-derived and marine algal-derived DOM samples overlap to a high degree, based on presence/absence (Koch et al., 2005; Rossel et al., 2013). Thus, it was proposed that there may exist a common degradation pathway that ultimately leads to the formation of similar compounds regardless of the origin of the sources of organic material (Rossel et al., 2013).

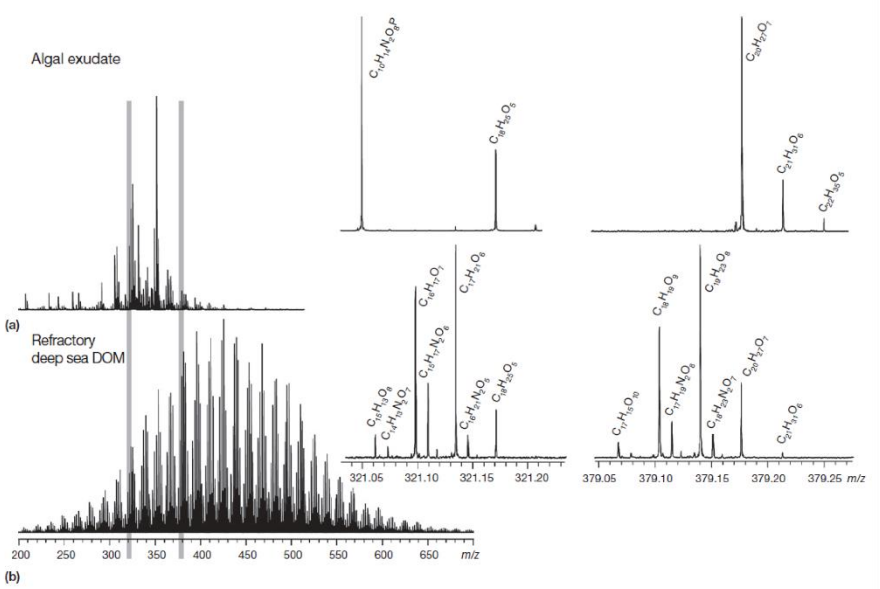

Figure 1.4: The molecular fingerprint of (a) freshly produced DOM (algal exudate) and (b) refractory DOM (deep-sea water) analyzed via ultrahigh resolution mass spectrometry (FT-ICR-MS). The whole mass spectra and two exemplary nominal masses are shown (321 and 379 Da). Due to very high mass accuracies it is possible to assign individual molecular formulae to the detected masses. Reprinted from: Dittmar and Stubbins, 2014.

A valuable tool for the visualization of the high amount of data points obtained from FT-ICR-MS analysis, and to summarize the molecular composition of DOM samples, is the Van Krevelen plot. Every detected molecular formula is graphed in the van Krevelen space according to its elemental H/C and O/C ratio. This way, it can be compared how empirical formulae overlap with general compound classes (Fig. 1.5) that are grouped according to their saturation and oxidation state. For example, condensed hydrocarbons “black carbon” (Dittmar and Koch, 2006) or CRAM (Hertkorn et al., 2006) each occupy a specific region in the plot. It has to be noted that formulae plotting e.g. in the area of proteins may also represent other compound classes with similar elemental composition.

In summary, elemental composition or parameters inferred from the molecular formula restrict the possible options for the chemical set-up in a molecule. The information itself, however, is not derived from structure but from molecular weight.

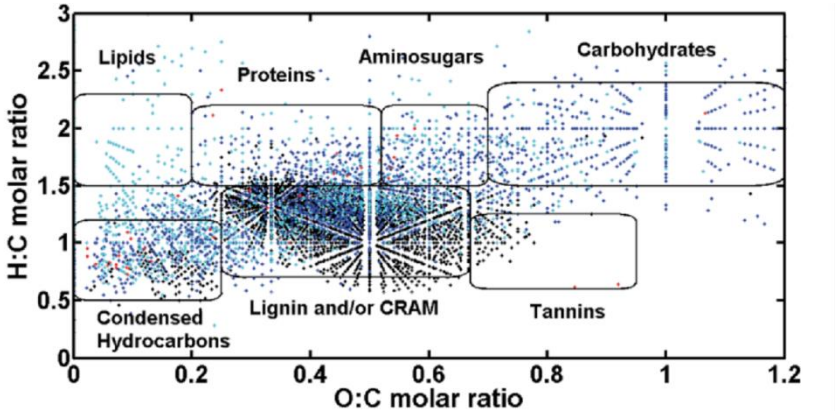

Figure 1.5: Exemplary Van Krevelen diagram illustrating the molecular composition of DOM from a lake surface water sample by elemental H/C and O/C ratios. Each dot represents an individual molecular formula that was assigned to a detected mass from FT-ICR-MS analysis. Formulae are grouped according to their saturation and oxidation state. Black boxes mark areas where compounds from individual chemical building blocks occur. Adapted from: Minor et al., 2014.

Tandem FT-ICR-MS can provide structural information on DOM compounds by applying excess energy to the detected ions, for example by collision with argon gas. The ions then become energetically unstable and dissociate into substructures that are specific for individual organic compounds because different amounts of energy are required to break down different chemical structures. The fragmentation patterns (Fig. 1.6) can thus be considered as a structural fingerprint and give important insight into the structures of the fragmented ions (Witt et al., 2009).

If analyzed under the same conditions, fragmentation patterns are comparable between samples. By using this approach it was for example possible to reveal that microbial derived DOM from an incubation study and deep-sea DOM, which are almost identical based on the molecular fingerprint mass spectra obtained by conventional FT-ICR-MS, do not share the same molecular structure (Osterholz et al., 2015). Another advantage of fragmentation pattern fingerprints is that they can be compared to data bases. This approach, however, has not yet lead to the identification of compounds, either due to a high amount of different isomers for each molecular formula or because data bases do not yet contain sufficient components that occur in the complex DOM mixture (Cortés-Francisco and Caixach, 2015). Apart from the comparative analysis of structural differences between DOM samples, fragmentation patterns provide direct evidence for abundant structural features within the molecules, which can be inferred from the

type of occurring neutral losses (Stenson et al., 2003). Tandem FT-ICR-MS in ESI negative mode revealed that natural organic matter contains a high proportion of hydroxyl and carboxyl functional groups as mostly CO_2 and H_2O neutral losses (Fig. 1.6) were observed (Plancque et al., 2001; Stumm, 2011; Witt et al., 2009). Other neutral losses, such as CH_2O from the fragmentation of lignin-derived structures, could serve as a structural biomarker for detecting the respective origin of DOM (Liu et al., 2011).

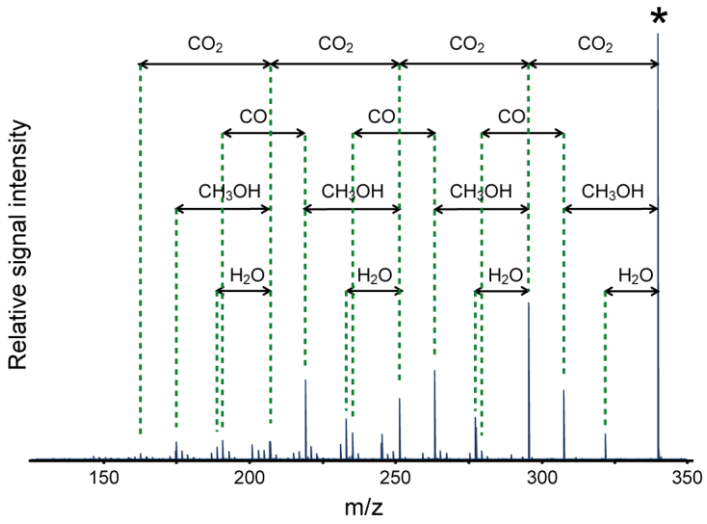

Figure 1.6: Tandem FT-ICR-MS fragmentation pattern in ESI negative mode of DOM from North Equatorial Pacific Intermediate Water with assigned neutral losses for a precursor ion with m/z = 339 Da, indicated by asterisk (*). Adapted from: Stumm, 2011.

On the whole, FT-ICR-MS analyses have proven that DOM is among the most complex mixtures known and more than 10,000 different elemental formulae have been identified within DOM to date (Dittmar and Stubbins, 2014; Hertkorn et al., 2006; Koch et al., 2005). The application of NMR and FT-ICR-MS have helped to identify possible structures for DOM components (Fig. 1.7) and molecular characterization on a structural level is a fast developing field in DOM research.

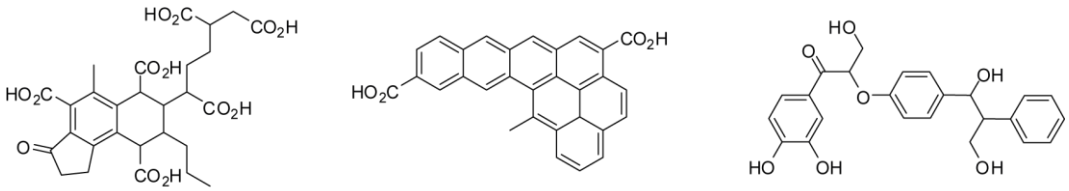

1 2 3

Figure 1.7: Proposed molecular structures from (tandem) FT-ICR-MS and NMR analysis of DOM for **1** CRAM (Hertkorn et al., 2006), **2** "black carbon" (Dittmar and Paeng, 2009), and **3** a lignin-derived degradation product (Stenson et al., 2003).

Future advances and novel applications for high-resolution fingerprinting techniques will broaden our knowledge of DOM on a structural level to great extent. The application of, e.g., ^{1}H NMR to natural water samples without a prior concentration step (Lam and Simpson, 2008), or the interpretation of large FT-ICR-MS data sets in analogy to biodiversity concepts ("chemodiversity"; Kellerman et al., 2014) are promising approaches towards a more holistic understanding of the marine DOM pool. Recent developments in data processing allow further to compare mass spectra from a high number of samples to detect changes with environmental gradients or across experiments (e.g. Singer et al., 2012; Stubbins et al., 2014). Ultimately, the combination of both, NMR spectroscopy and FT-ICR-MS, could elucidate the complete DOM structure (Hertkorn et al., 2008; Woods et al., 2011). However, it is not yet possible to isolate individual molecular formulae for NMR spectroscopy and linking the two techniques can only be achieved via statistical methods this far.

1.2 Ocean acidification

Atmospheric carbon dioxide concentrations ranged from 172 to 300 parts per million per volume (ppmv) during the past 800,000 years (Lüthi et al., 2008). Since the era of industrialization, anthropogenic fossil fuel burning has been superimposed on the natural CO_2 flux causing an overall increase in its global atmospheric concentration (Fig. 1.8). In May 2013, a historical level of 400 ppmv was reached at Mauna Loa observatory, Hawaii (Tans and Keeling, 2015). This is an outstanding problem for the modern society as accumulation of CO_2 in the atmosphere may increase the global greenhouse effect. Future atmospheric CO_2

levels will depend on the development of emissions but were projected to reach approximately 1000 ppmv under business-as-usual conditions at the end of the century (representative concentration pathway 8.5; IPCC, 2013).

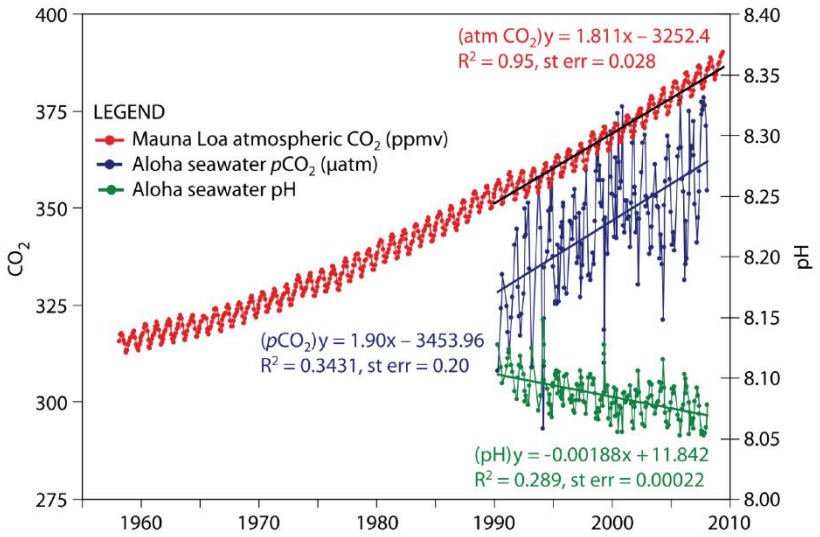

Figure 1.8: Time series of atmospheric CO_2 at the Mauna Loa observatory, Hawaii (red). Seawater pCO_2 (blue), and sea surface pH (green) records are from the ALOHA time series station in the subtropical North Pacific Ocean. Reprinted from: Feely et al., 2009.

A major sink for anthropogenic CO_2 in the atmosphere are the global oceans. From the year 1800 to present, they have taken up about 118 Pg C, which accounts for ~48% of the carbon generated by human activities during this time (Sabine et al., 2004). By taking this CO_2 away from the atmosphere, the oceans serve as a buffer for climatic changes. But the downside of CO_2 being absorbed in seawater is a shift in seawater chemistry through formation of carbonic acid. Protons are released and form hydroxonium ions (H_3O^+) in water. As pH is a function of H_3O^+ concentration ($pH = -\log(H_3O^+)$), seawater pH decreases and the oceans become more acidic. This process is also named “ocean acidification”, even though surface waters will remain alkaline (Caldeira and Wickett, 2003).

Ocean acidification will occur everywhere but in different rates among oceanic regions. The sea-air flux of CO_2 is mainly dependent on temperature among other physical and thermodynamic processes and more CO_2 is soluble in colder waters. While large regions of the tropical oceans represent a net source to the atmosphere,

waters at high latitudes are a major sink (Fig. 1.9). Accordingly, changes in seawater chemistry are expected to be most pronounced in the Arctic Ocean (Steinacher et al., 2009).

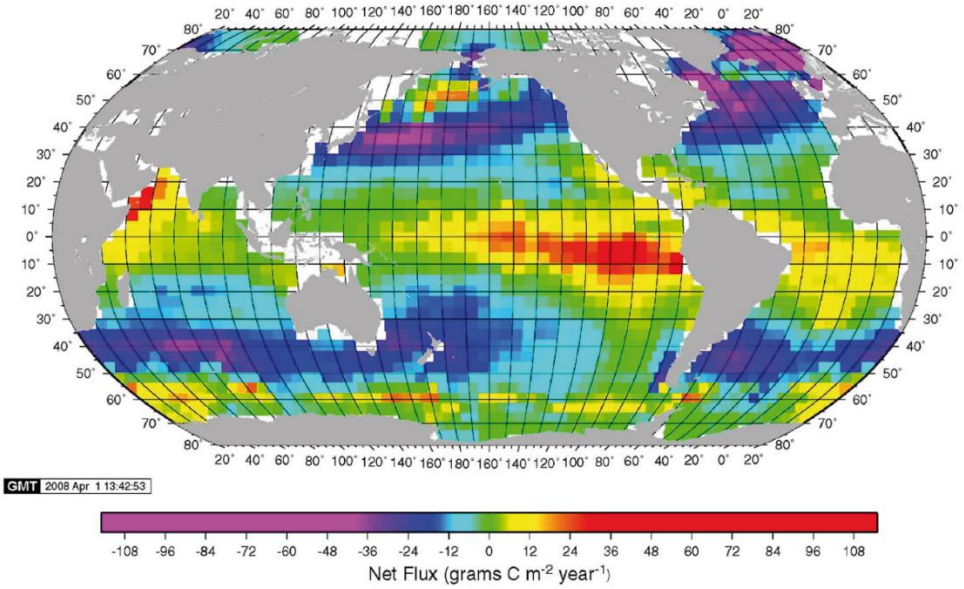

Figure 1.9: Mean annual sea-air flux of CO_2 for the reference year 2000. The values are based on measurements of pCO_2 in the surface ocean and the gas exchange mass transfer coefficient determined from wind speed. The net global air-sea flux is 1.42 Pg C yr^{-1}. Reprinted from: Takahashi et al., 2009.

1.2.1 The seawater-carbonate system

One of the most important components for the control of seawater pH is the carbonate system (Emerson and Hedges, 2008). Once dissolved in water, CO_2 forms carbonic acid (H_2CO_3, equation 1). Carbonic acid reacts to bicarbonate (HCO_3^-) and a hydroxonium ion (H_3O^+) in a following step (see equation 2).

$$CO_2 + H_2O \rightleftharpoons H_2CO_3 \qquad (1)$$

$$H_2CO_3 + H_2O \rightleftharpoons HCO_3^- + H_3O^+ \qquad (2)$$

Carbonic acid in its original form (H_2CO_3) is present in seawater in very low concentrations compared to dissolved CO_2 and HCO_3^-. The equations (1) and (2) can thus be combined to equation (3). Bicarbonate can release another hydroxonium

ion to form carbonate (CO_3^{2-}) in an equilibrium reaction (4). Chemical equilibria in seawater are described by the respective equilibrium constants *K*'.

$$CO_2 + 2\,H_2O \overset{K'_1}{\rightleftharpoons} HCO_3^- + H_3O^+ \qquad K'_1 = \frac{[HCO_3^-]\,[H_3O^+]}{[CO_2]\,[H_2O]^2} \qquad (3)$$

$$HCO_3^- + H_2O \overset{K'_2}{\rightleftharpoons} CO_3^{2-} + H_3O^+ \qquad K'_2 = \frac{[CO_3^{2-}]\,[H_3O^+]}{[HCO_3^-]\,[H_2O]} \qquad (4)$$

The three dissolved inorganic carbon species in seawater (CO_2, HCO_3^-, and CO_3^{2-}) are in chemical equilibrium on time scales shorter than a few minutes. Their concentrations depend primarily on the equilibrium constant *K*' and the concentration of the ions that are contributing to the equilibria. Because hydroxonium ion concentrations are part of the equations for equilibrium constants K'_1 and K'_2, seawater pH partly controls the concentration of the inorganic carbon species. The concentration of ions on the left side of the equilibrium (reactants) and on the right side (products) are equal at pH = p*K*' ($pK'_1 = 5.85$, $pK'_2 = 8.97$ at T = 25 °C, and S = 35; Emerson and Hedges, 2008). Anthropogenic ocean acidification affects the speciation of inorganic carbon species and increases the overall concentration of HCO_3^- while CO_3^{2-} concentration decreases (Fig. 1.10). The concentration of the different species is further dependent on temperature, salinity, and pressure. Accordingly, there are natural differences in the concentrations of inorganic carbon species between different oceanic environments.

The easiest way to describe the marine carbonate system in a specific setup is by the use of two conservative tracers, total alkalinity A_T (5) and total dissolved inorganic carbon (DIC) (6). While the total alkalinity is related to the charge balance in seawater, total dissolved inorganic carbon describes the sum of concentrations of the dissolved carbonate species.

$$A_T = [HCO_3^-] + 2\,[CO_3^{2-}] + [B(OH)_4^-] + [OH^-] - [H_3O^+] + \text{minor ions} \qquad (5)$$

$$DIC = [CO_2] + [HCO_3^-] + [CO_3^{2-}] \qquad (6)$$

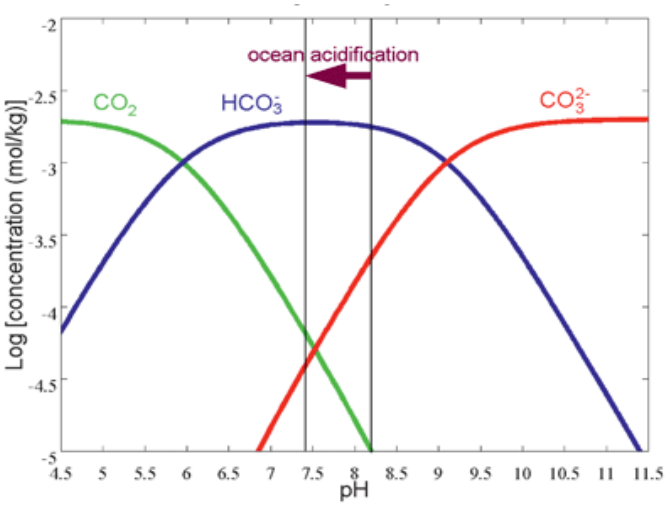

Figure 1.10: Concentrations of the three inorganic carbon species of the ocean carbonate system versus pH (Bjerrum plot) for DIC = 2100 µmol L^{-1}, S = 35 psu, and T = 25 °C. The expected amount in pH decline under a business-as-usual emission scenario is illustrated by the purple arrow. Reprinted from: Hofmann and Schellnhuber, 2010, with permission of The Royal Society of Chemistry.

Anthropogenic CO_2 that is added to the atmosphere dissolves in seawater, but it does not remain in its dissolved form like most other gases (e.g. oxygen). Instead it reacts to form HCO_3^- and CO_3^{2-} , resulting in higher DIC concentrations. Referring to the overall increase in DIC, ocean acidification could also be named "ocean carbonation" (Bach et al., 2011). The buffer capacity of the oceans for anthropogenic CO_2, however, is limited and decreases with increasing amounts of CO_2 already taken up. The so-called "Revelle factor" *R* (Revelle and Suess, 1957), serves as a measure for this buffer capacity and describes the change of partial pressure of CO_2 for a given change in DIC (7).

$$R = \frac{\partial\, pCO_2 \,/\, pCO_2}{\partial\, \mathrm{DIC} \,/\, \mathrm{DIC}} = \frac{\partial \ln pCO_2}{\partial \ln \mathrm{DIC}} \qquad (7)$$

The Revelle factor is inversely proportional to the capacity of seawater to take up anthropogenic CO_2 from the atmosphere. Revelle factors are comparatively low in tropical regions, whereas high latitudes are characterized by high Revelle factors. Therefore, the highest concentrations of anthropogenic CO_2 can be found in subtropical Atlantic surface waters (Sabine et al., 2004).

The seawater pH decreased since pre-industrial times by about 0.1 units, corresponding to an increase in hydroxonium ion concentration of about 30%

(Raven et al., 2005). Based on model results it was estimated that the surface ocean pH could further drop in the future by about 0.7 units (Caldeira and Wickett, 2003). The calculated changes in seawater pH are measurable in the oceans. Data from three time series stations show a decrease in pH by 0.0014 to 0.0019 units per year during the last decades (Bates, 2007; González-Dávila et al., 2010; Dore et al., 2009). From the geological record it is known that ocean chemistry has experienced higher variability by some orders of magnitude in the past (Zachos et al., 2008). This, however, happened on comparatively long time scales. The rate at that acidification is happening in modern times is unprecedented (Zeebe et al., 2011) and, thus, marine organisms will potentially not have sufficient time to adapt to these changes. This could affect the functioning of marine ecosystems and biogeochemical cycles.

1.3 Marine carbon cycle feedback on elevated atmospheric CO_2

The marine carbon cycle is an essential component of the earth system and the global oceans are by far the largest reservoir for carbon, apart from sedimentary rocks (Falkowski et al., 2000). It is driven by two main processes: the solubility pump and the biological carbon pump.

In general, the concentration of DIC is about 10 – 15% higher in the deep sea (Feely et al., 2001) than in surface ocean waters. It was estimated that one-third of this surface-to-depth gradient of DIC is generated by the solubility pump (Riebesell and Tortell, 2011). As the solubility of CO_2 is more than two times higher under low temperatures, cold water transports atmospheric CO_2 to the deep ocean via deep water formation in high latitudes (Feely et al., 2001). The formed deep water then carries a high CO_2 load which is transported towards lower latitudes. The other two thirds of the gradient are generated by the biological carbon pump. DIC is fixed in the upper ocean layer by primary producers through photosynthesis, reducing CO_2 concentrations in surface waters. If the formed organic material was subsequently degraded in the surface layer and respired back to CO_2, the concentration of inorganic carbon would be restored. This, however, is not the case as some particles sink out through the water column and escape from the euphotic zone. During sinking, they are partly degraded by microbes and 1 to 40% of the formed particles

reach the ocean floor (Ducklow et al., 2001). This way, a gradient is created towards higher DIC with increasing depths.

In a similar process, DOM can be transported to the deeper layers of the ocean. Compounds that were transformed into refractory DOM in the euphotic zone, e.g. by the proposed "microbial carbon pump" concept (see chapter 1.1.2), are carried through deep water formation to the deep sea with an estimated flux of 2 Pg C yr^{-1} (Christian and Anderson, 2002). The formation of refractory DOC may thus play an important role for the long-term sequestration of atmospheric CO_2 (Jiao et al., 2010).

1.3.1 Effects on carbon fixation

Microscopic phytoplankton in the surface mixed layer carry out photosynthesis by fixing inorganic carbon. They mainly use CO_2 dissolved in seawater as substrate for a reaction that is catalyzed by ribulose-1,5-bisphosphate carboxylase, also known as "RubisCo" (Hartmann and Harpel, 1994; Riebesell, 2000). This enzyme has a relatively low affinity to CO_2 and its optimum CO_2 concentration is well above the current level in the open ocean. Some organisms have developed mechanisms to concentrate CO_2 in their cells in an energy consuming process (Badger et al., 1998). If the concentration of CO_2 in seawater is higher, the energy consumed for pre-concentration will decrease. Thus, it is expected that primary production will increase under elevated CO_2 concentrations. This hypothesis was supported by experiments with single plankton species (e.g. Riebesell et al., 1993) and natural assemblages in the field (e.g. Hein and Sand-Jensen, 1997) or in mesocosm experiments (e.g. Riebesell et al., 2007). However, other studies reported no or very small effects of elevated CO_2 on photosynthesis and carbon fixation (Czerny et al., 2009; Langer and Geisen, 2006).

Phytoplankton taxa differ in their photosynthetic apparatus and carbon-concentrating mechanisms. Rising CO_2 levels therefore have the potential to alter competitive relationships between phytoplankton types and to significantly change community structure (Dutkiewicz, 2015; Rost et al., 2008). Shifts in species composition may impact the cycling of elements and the flow of nutrients and energy through the marine food web, either diminishing or amplifying the impacts

of changes in primary productivity on carbon export. But it has to be kept in mind that phytoplankton taxa can also adapt to ocean acidification as it was recently shown for an important calcifying phytoplankton type (Lohbeck et al., 2012).

Overall, mostly positive or no feedbacks were observed for phytoplankton under elevated CO_2 concentrations and an overall increase in primary production is indicated. The magnitude, however, must be better constrained, especially at community level under in situ conditions.

1.3.2 Effects on respiration by heterotrophic marine microorganisms

Compared to phytoplankton, there is only little information available on the impacts of ocean acidification on marine microbes (Weinbauer et al., 2011). Growth optima and physiological functions of marine microorganisms are dependent on pH (Yamada and Suzumura, 2010) and could be directly affected by ocean acidification, whereas indirect effects are likely to occur due to changes in substrate, i.e. DOM quality. In this context it is important to consider that the pH of surface waters underlies high natural variations in time and space as a result of biological activity. The average pH decline in surface waters predicted for the end of the century in response to ocean acidification already occurs in some locations in the oceans at present, and marine microbes are thus likely capable to adapt to these shifts (Joint et al., 2011).

A high tolerance towards low pH was indicated in studies using isolates (Labare et al., 2010; Takeuchi et al., 1997). Whereas no or only small effects of elevated pCO_2 were detected on the total bacterial abundance in several mesocosm studies (Allgaier et al., 2008; Grossart et al., 2006; Rochelle-Newall et al., 2004), a positive response was observed for bacterial production (Grossart et al., 2006). However, no enhanced bacterial production occurred under similar conditions in culture experiments and field assays (Allgaier et al., 2008). In a follow-up mesocosm study in the Baltic Sea bacteria showed enhanced growth rates if exposed to comparatively high concentrations of CO_2 (Endres et al., 2014). Studies on the impact of elevated CO_2 on enzyme activities reveal a similar controversy as for bacterial production and some enzymes showed higher activity (Grossart et al., 2006) while negative effects were reported for others (Yamada and Suzumura,

2010). Extracellular enzyme activities, on the other hand, are likely to increase at higher pCO_2 in the future ocean and to stimulate the processing of organic matter, such as polysaccharides (Piontek et al., 2010).

In a nutshell, there are still large uncertainties concerning the impact of ocean acidification on marine microorganisms with most studies reporting no or positive effects. Further, adaption to environmental change by genetic modification plays a key role in this aspect as it can assumingly occur faster in microbes than in multicellular organisms (Labare et al., 2010). Ocean-acidification induced shifts in microbial diversity could further impact the functioning of the species within ecosystems (Bell et al., 2005). However, data is not yet available on long-term experiments and studies mimicking a gradual increase in the open ocean over longer timescales will be crucial for a better understanding of microorganism performance in a high-CO_2 ocean.

1.3.3 Effects on organic matter dynamics

Contradictory results were found for the effects of elevated pCO_2 on DOC concentrations. No significant effects were observed in mesocosm studies with natural plankton assemblages (Engel et al., 2014, 2004), while elevated pCO_2 led to increased DOC production under nutrient depleted conditions in a mesocosm study in the Arctic (Czerny et al., 2013; Engel et al., 2013). Ship-based incubation experiments on the other hand pointed towards reduced DOC accumulation (MacGilchrist et al., 2014). Overall, elevated pCO_2 levels are assumed to enhance DOC production (Riebesell et al., 2013a).

As some DOM molecules are precursors for the formation of TEP, increased production of DOC may also be coupled to higher TEP formation. In several studies, TEP production was shown to be affected positively by high CO_2 concentrations (Engel, 2002; Engel et al., 2004; Mari, 2008), which is likely a result of increased concentrations of carbohydrate-type DOM precursors that aggregate to particles on short timescales. In accordance, no elevated DOC concentrations were detected at the same time (Engel et al., 2004). Another measure for the quality of DOM produced under acidification conditions are elemental C/N ratios in freshly produced DOC. Marine primary producers normally incorporate the elements

C/N/P in a ratio of 106/16/1 also known as the Redfield ratio (Redfield, 1958). The C/N stoichiometry of DOM differs from the ratio of fresh particulate organic matter (POM, C/N ~6.6) and is relatively constant at 13.6 (±2.8) at the sea surface and 14.7 (±2.8) in the deep sea (Bronk, 2002; Hopkinson and Vallino, 2005). The ratio, however, may shift if excess carbon relative to nitrogen is incorporated into freshly released DOM. Production of such carbon rich DOM can be observed under nutrient depleted conditions (Fig. 1.11) in bottle incubation experiments (Carlson and Hansell, 2015). An increase of the C/N ratio was further observed with environmental stressors such as elevated CO_2 conditions in natural phytoplankton assemblages for POC (Engel et al., 2005) and inferred from excess DIC drawdown in a mesocosm study (Bellerby et al., 2008; Riebesell et al., 2007). Increases of the C/N ratio can also occur for both, POC and DOC, as response to higher temperatures (Taucher et al., 2012).

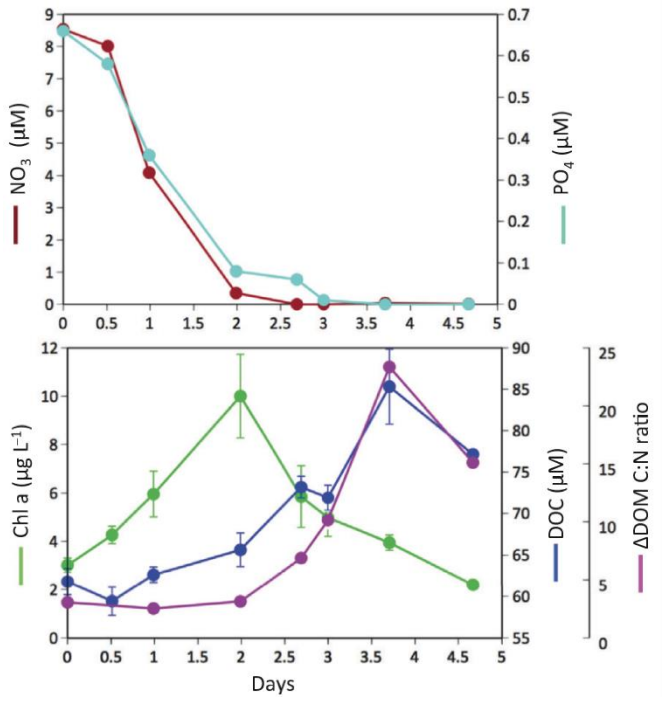

Figure 1.11: Results of a bottle incubation study conducted with a mixture of 1:1 (v/v) surface water with nutrient enriched water from 75 m depth. While net DOC accumulation was relatively minor during nutrient replete conditions, DOC concentrations increase after nutrients are depleted and the produced DOM becomes richer in carbon. Reprinted from: Carlson and Hansell, 2015.

No studies focusing on changes in the DOM composition on a molecular level and only few studies including the analysis of labile building block compounds such as carbohydrates and amino acids (Engel et al., 2014) have been performed so far.

1.3.4 Biogeochemical implications for the marine carbon cycle

An overall increase in primary productivity is likely to enhance the biological carbon pump, providing a negative climate feedback. The extent to which the carbon fixed in the surface ocean is exported to the deep sea is partly dependent on the partitioning between organic carbon species (POC-DOC) in the future ocean. DOC produced in excess could either serve as substrate for higher trophic levels or aggregate to larger particles, e.g. TEP (Engel, 2002; Engel et al., 2004) and ultimately enhance vertical organic matter flux (Riebesell et al., 2007). This effect would be even more pronounced if C-rich DOM with elevated C/N ratios was produced and exported as aggregates (Arrigo, 2007). The quality of the produced organic matter is very important in this context because the ability to form fast sinking aggregates could be reduced, in turn reducing the efficiency of the biological carbon pump (Mari, 2008).

Excess carbon could be sequestered in the deep sea by export of extremely carbon-rich DOM (Hopkinson and Vallino, 2005). This way, increased C/N drawdown will likely cause an overall negative feedback on the atmospheric CO_2 concentration with an estimated carbon uptake of 34 Gt C under business-as-usual conditions (Oschlies et al., 2008). Results from the same model show that oceanic suboxic regimes are expected to increase by 50% in connection to enhanced respiration of the carbon-rich organic matter at depth. Higher bacterial abundance and production as well as enhanced extracellular enzyme activities may reduce the passive sinking of carbon (Grossart et al., 2006; Simon et al., 2002). A strengthened microbial loop could hence counteract the biological pump. The net accumulation of DOC as well as shifts in reactivity will presumably depend to a great extent on the environmental settings such as nutrient availability (Fig. 1.12).

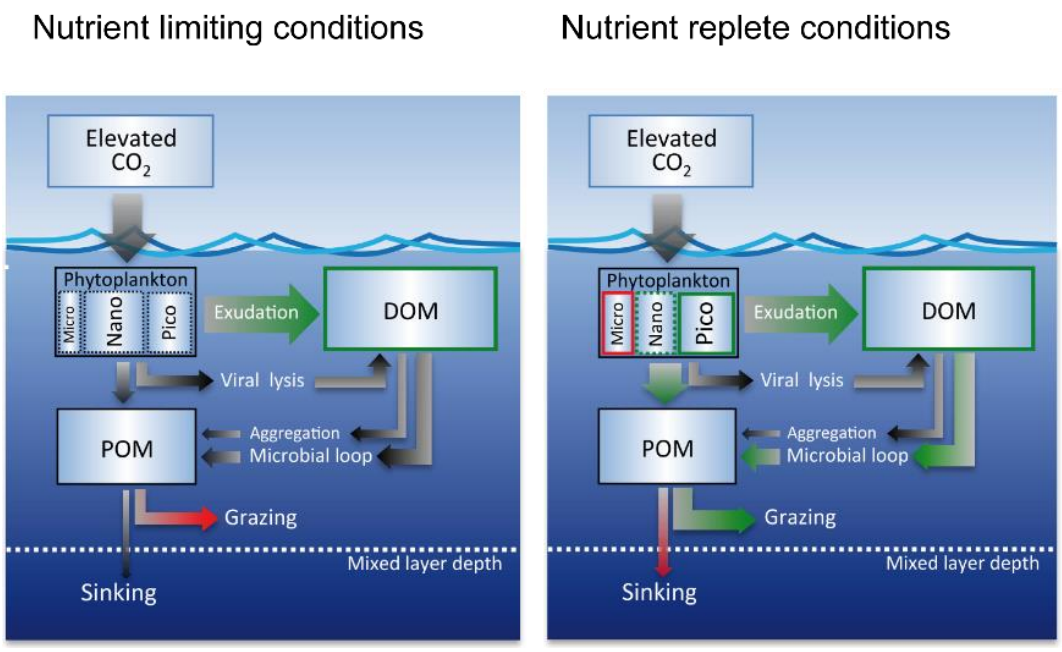

Figure 1.12: Potential scenarios for the marine carbon cycle under elevated pCO_2 for nutrient limiting and nutrient replete conditions. Green arrows indicate a positive, red arrows negative responses. Adapted from: Riebesell et al., 2013a.

In this context, it is important to consider the enigmatic stability of refractory DOM. It was hypothesized that the stability of the chemical structures within refractory DOM or the high molecular diversity could lead to inhibition of microbial degradation (Dittmar, 2015). Considering the great size of the refractory DOM pool, the global climate could be affected if this inhibition was revoked due to changing physical parameters (Sexton et al., 2011). For example, higher elemental C/N ratios of produced DOM, as well as the strengthening of the microbial loop could alter the structure of refractory DOM. Hence, it may become accessible for degradation, similar to the fast decomposition of huge carbon reservoirs in peat as a response to warming (Dorrepaal et al., 2009). The situation for refractory DOM, however, is different as it is not locked away from phytoplankton and marine bacteria. With this in mind, the essential need for more structural and compositional information on this huge inactive carbon pool in the world's oceans becomes clearly visible.

1.4 Mesocosm studies

The current developments in ocean acidification research have clearly improved our understanding of effects on single organisms. However, observations derived from these studies may not easily be extrapolated to natural systems. Due to the complexity and interaction of different marine carbon pools, it is necessary to study ecosystems as a whole including different trophic levels and the potential for evolutionary adaptation of marine organisms. It was stated by Riebesell and Gattuso (2015) in a recent publication on the current state of ocean acidification research that priorities for future studies are to "expand (1) from single to multiple drivers, (2) from single species to communities and ecosystems, and (3) from acclimation to adaption", in order to fill the current knowledge gaps.

Laboratory based short-term incubation experiments provide valuable information on single marine organisms or specific communities and well-controlled conditions facilitate the interpretation of responses. However, they may not be suited for studies using multiple organisms as incubation bottles with low volumes are too small to adequately sample higher trophic levels such as larger phytoplankton. A good alternative to classical lab based studies are field studies on naturally CO_2-rich sites or using free ocean CO_2 enrichment (FOCE). As a drawback, these can only be performed on benthic communities and perturbations with the surrounding water body could tamper results. Large scale experimental approaches, such as mesocosm studies, are well suited to address point (2) and will be discussed in this chapter.

The use of mesocosm enclosures for CO_2 perturbation experiments is advantageous because pelagic communities as well as benthic assemblages can be studied and the closed character allows for a well-defined control of carbonate chemistry. The mesocosm approach provides the closest approximation to natural conditions and takes direct as well as indirect effects of elevated pCO_2 levels on natural plankton assemblages into account (Riebesell et al., 2010). Another advantage is the possibility for replicate measurements and the investigation of multiple pCO_2 levels if more than one mesocosm system is used. The disadvantages include high costs, time, and effort in order to maintain controlled conditions and to avoid biofilm growth. Enclosure effects may further alter the food web dynamics

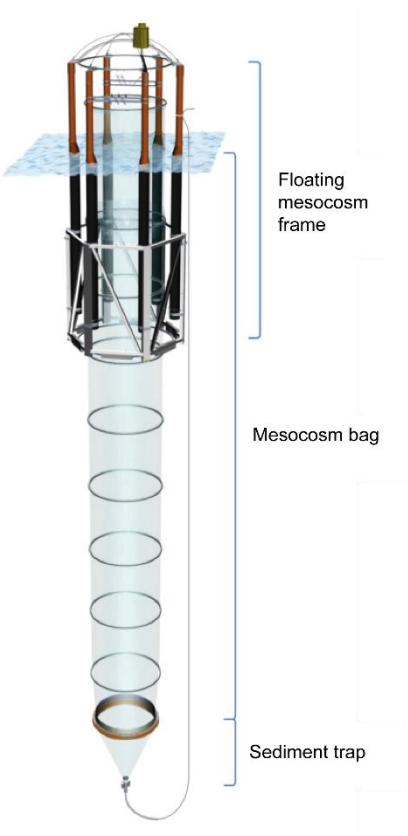

Figure 1.13: KOSMOS Mesocosm sketch drawing. The floating frame holds a plastic bag with 15-20 m depth and 2 m diameter. The bottom is closed with a sediment trap. Adapted from: Paul, AJ et al., 2015.

and reduce the vertical mixing, that occurs under natural conditions. Despite drawbacks, mesocosm enclosures represent one of the best approaches to manipulate multi-trophic plankton assemblages over long time periods.

In general, two system types have developed in the recent past. Laboratory-based mesocosms are installed in a fixed location and can be filled with water from the respective study site (e.g. “indoor mesocosms”, Paul, C et al., 2015). On the other hand, mesocosm systems that were invented for the application in the field can be used in a wide range of hydrographic regions considered to be sensitive for ocean acidification. One of these systems is the Kiel Offshore Mesocosms for Future Ocean Simulation (KOSMOS) facility (see Riebesell et al., 2013b for a complete description of the setup). It includes 9 to 10 sea-going mesocosm units that consist of large bags made from polyurethane with an attached floatation frame (Fig. 1.13). The bags are 2 m in diameter and reach depths of 15-20 m (~50-75 m^3 volume) with a sediment trap attached to the bottom in order to allow the study of carbon export. Manipulations are performed by the addition of CO_2 enriched water that is mixed into the entire water column. The systems are open to the atmosphere and CO_2 gradients have to be maintained by the readjustments of pCO_2.

The systems were applied for the first time in 2010 during a pilot study in the Arctic off Svalbard (Riebesell et al., 2013a, Schulz et al., 2013). Since then, several follow-up studies investigating the effects of ocean acidification on natural plankton communities were performed (e.g. Paul, AJ et al., 2015). Important findings from studies using this setup were the first report of enhanced biological carbon consumption (Riebesell et al., 2007), the enhanced formation of TEP (Engel

et al., 2014) and indications for DOC accumulation (Czerny et al., 2013; Engel et al., 2013) in a natural assemblage. Overall, mesocosm studies have already provided valuable insights into the effects of ocean acidification under close-to-natural conditions and will further improve our understanding of the applicability of results from studies using single species and single stressors.

1.5 Objectives

This thesis includes published and unpublished results of four studies. The primary goal was to assess the impact of ocean acidification on marine DOM, in terms of the global pool of carbon that is stored in DOM and in terms of DOM molecular composition that determines the biogeochemical cycling of matter and energy in marine food webs. More specifically, ocean acidification has the potential to trigger changes in the size of the global bioresistant DOM pool or to change the proportion of primary production that is routed as bioavailable DOM through the microbial loop. As a consequence, a different amount of energy would be available to higher trophic levels.

In order to study the changes of the DOM pool under future ocean conditions, samples were collected from two large-scale mesocosm studies using the novel KOSMOS mesocosm setup. The first study was performed in 2013 in a Swedish fjord for a total duration of more than three months. It was designed to accurately assess the possible impacts of ocean acidification within the next century for future ocean projections (5 replicates with “ambient” and 5 replicates with “year 2100” target pCO_2 levels). The results are discussed in Manuscript I. In order to compare the extent to which ocean acidification affects different ecosystems, a second study was performed in 2014 in the subtropical North Atlantic where marine organisms are presumably less adapted towards natural changes in ocean pH (Manuscript II). A phytoplankton bloom was induced by an artificial upwelling event. In order to test for threshold effects, mesocosms were manipulated along a gradient of CO_2 levels (within the range from 600-2000 µatm target pCO_2). The molecular composition of the DOM pool was analyzed via FT-ICR-MS and compared between different CO_2 treatments for both studies.

The second goal of the dissertation was to improve the current understanding of DOM structural features. This is essential because, at present, studies analyzing the molecular composition of DOM via FT-ICR-MS are mostly performed by comparing detected molecular formulae. However, compounds that share the same elemental composition do not necessarily have identical chemical structures. There may e.g. be regional differences in the chemical structure of compounds with the same elemental composition. It is important to identify these differences in order to produce valid statements about the applicability of the results from KOSMOS mesocosm studies to other regions in the global oceans. In this context, it is further important to obtain an estimate about the number of individual isomers represented by each molecular formula detected by FT-ICR-MS in DOM. Manuscript III deals with fragmentation experiments performed on DOM from a wide range of aquatic environments in order to compare chemical structures. Manuscript IV describes a fragmentation experiment performed on refractory DOM from the deep sea that is compared to a number of model compounds to assess the diversity of the individual molecular formulae that are detected by FT-ICR-MS.

The stated aims of this thesis can be summarized in the following overall research questions:

(1) What are the regional and overall impacts of ocean acidification on DOM accumulation and molecular composition?

(2) Are there natural differences in DOM molecular composition among aquatic environments in terms of its chemical structure?

(3) To what extent do common molecular formulae detected by FT-ICR-MS represent identical chemical structures in the different oceanic environments?

(4) Are detected molecular formulae representing single structures or a higher number of different isomers?

1.6 References

Alldredge, A.L., Passow, U., Logan, B.E., 1993. The abundance and significance of a class of large, transparent organic particles in the ocean. Deep Sea Res. Part 1 40, 1131−1140.

Allgaier, M., Riebesell, U., Vogt, M., Thyrhaug, R., Grossart, H.-P., 2008. Coupling of heterotrophic bacteria to phytoplankton bloom development at different pCO_2 levels: a mesocosm study. Biogeosciences 5, 1007−1022.

Álvarez-Salgado, X.A., Arístegui, J., 2015. Organic matter dynamics in the canary current, in: Valdés, L., Déniz-González, I. (Eds.), Oceanographic and biological features in the Canary Current Large Marine Ecosystem. IOC Technical Series 115, IOC-UNESCO, pp. 151−159.

Amon, R.M.W., Benner, R., 1996. Bacterial utilization of different size classes of dissolved organic matter. Limnol. Oceanogr. 41, 41−51.

Arnosti, C., 2011. Microbial extracellular enzymes and the marine carbon cycle. Annu. Rev. Mar. Sci. 3, 401−425.

Arrieta, J.M., Mayol, E., Hansman, R.L., Herndl, G.J., Dittmar, T., Duarte, C.M., 2015. Dilution limits dissolved organic carbon utilization in the deep ocean. Science 348, 331−333.

Arrigo, K.R., 2007. Carbon cycle: marine manipulations. Nature 450, 491−492.

Azam, F., 1998. Microbial control of oceanic carbon flux: the plot thickens. Science 280, 694−696.

Azam, F., Malfatti, F., 2007. Microbial structuring of marine ecosystems. Nat. Rev. Microbiol. 5, 782−791.

Bach, L.T., Riebesell, U., Schulz, K.G., 2011. Distinguishing between the effects of ocean acidification and ocean carbonation in the coccolithophore Emiliania huxleyi. Limnol. Oceanogr. 56, 2040−2050.

Badger, M.R., Andres, T.J., Whitney, S.M., Ludwig, M., Yellowlees, D.C., Leggat, W., et al., 1998. The diversity and coevolution of Rubisco, plastids, pyrenoids, and chloroplast-based CO_2-concentrating mechanisms in algae. Can. J. Botany. 76, 1052−1071.

Bates, N.R., 2007. Interannual variability of the oceanic CO_2 sink in the subtropical gyre of the North Atlantic Ocean over the last 2 decades. J. Geophys. Res. 112, C09013.

Bauer, J.E., Williams, P.M., Druffel, E.R.M., 1992. ^{14}C activity of dissolved organic carbon fractions in the north-central Pacific and Sargasso Sea. Nature 357, 667−670.

Bell, T., Newman, J.A., Silverman, B.W., Turner, S.L., Lilley, A.K., 2005. The contribution of species richness and composition to bacterial services. Nature 436, 1157−1160.

Bellerby, R.G.J., Schulz, K.G., Riebesell, U., Neill, C., Nondal, G., Heegaard, E., et al., 2008. Marine ecosystem community carbon and nutrient uptake stoichiometry under varying ocean acidification during the PeECE III experiment. Biogeosciences 5, 1517−1527.

Benner, R., Amon, R., 2015. The size-reactivity continuum of major bioelements in the ocean. Annu. Rev. Mar. Sci. 7, 185−205.

Benner, R., Pakulski, J.D., McCarthy, M., Hedges, J.I., Hatcher, P.G., 1992. Bulk chemical characteristics of dissolved organic matter in the ocean. Science 255, 1561−1564.

Bronk, D.A., 2002. Dynamics of DON, in: Hansell, D.A., Carlson, C.A., (Eds.), The biogeochemistry of marine dissolved organic matter. Academic Press, San Diego, pp. 153−247.

Caldeira, K., Wickett, M.E., 2003. Anthropogenic carbon and ocean pH. Nature 425, 365.

Carlson, C.A., 2002. Production and removal processes, in: Carlson, D.A., Hansell, C.A., (Eds.), The biogeochemistry of marine dissolved organic matter. Academic Press, San Diego, pp. 91−151.

Carlson, C.A., Ducklow, H.W., Hansell, D.A., Smith, W.O., 1998. Organic carbon partitioning during spring phytoplankton blooms in the Ross Sea polynya and the Sargasso Sea. Limnol. Oceanogr. 43, 375−386.

Carlson, C.A., Hansell, D.A., 2015. DOM sources, sinks, reactivity, and budgets, in: Hansell, D.A., Carlson, C.A., (Eds.), The biogeochemistry of marine dissolved organic matter, 2nd edition. Academic Press, San Diego, pp. 369−388.

Christian, J.R., Anderson, T.R., 2002. Modeling DOM biogeochemistry, in: Hansell, D.A., Carlson, C.A., (Eds.), The biogeochemistry of marine dissolved organic matter, Academic Press, San Diego, pp. 717−756.

Cloern, J.E., Foster, S.Q., Kleckner, A.E., 2014. Phytoplankton primary production in the world's estuarine-coastal ecosystems. Biogeosciences 11, 2477−2501.

Cortés-Francisco, N., Caixach, J., 2015. Fragmentation studies for the structural characterization of marine dissolved organic matter. Anal. Bioanal. Chem. 407, 2455−2462.

Czerny, J., Barcelos e Ramos, J., Riebesell, U., 2009. Influence of elevated CO_2 concentrations on cell division and nitrogen fixation rates in the bloom-forming cyanobacterium *Nodularia spumigena*. Biogeosciences 6, 1865−1875.

Czerny, J., Schulz, K.G., Boxhammer, T., Bellerby, R.G.J., Büdenbender, J., Engel, A., et al., 2013. Implications of elevated CO_2 on pelagic carbon fluxes in an Arctic mesocosm study – an elemental mass balance approach. Biogeosciences 10, 3109−3125.

Dittmar, T., 2015. Reasons behind the long-term stability of dissolved organic matter, in: Hansell, D.A., Carlson, C.A., (Eds.), The biogeochemistry of marine dissolved organic matter, 2nd edition. Academic Press, San Diego, pp. 369−388.

Dittmar, T., Koch, B.P., 2006. Thermogenic organic matter dissolved in the abyssal ocean. Mar. Chem. 102, 208−217.

Dittmar, T., Koch, B.P., Hertkorn, N., Kattner, G., 2008. A simple and efficient method for the solid-phase extraction of dissolved organic matter (SPE-DOM) from seawater. Limnol. Oceanogr.: Methods 6, 230−235.

Dittmar, T., Paeng, J., 2009. A heat-induced molecular signature in marine dissolved organic matter. Nat. Geosci. 2, 175−179.

Dittmar, T., Stubbins, A., 2014. Dissolved organic matter in aquatic systems, in: Birrer, B., Falkowski, P., Freeman, K., (Eds.), Treatise of Geochemistry, 2nd edition. Academic Press, Oxford, pp. 125−156.

Dore, J.E., Lukas, R., Sadler, D.W., Church, M.J., Karl, D.M., 2009. Physical and biogeochemical modulation of ocean acidification in the central North Pacific. Proc. Natl. Acad. Sci. U S A 106, 12235−12240.

Dorrepaal, E., Toet, S., Van Logtestijn, R.S.P., Swart, E., Van de Weg, M.J., Callaghan, T.V., et al., 2009. Carbon respiration from subsurface peat accelerated by climate warming in the subarctic. Nature 460, 616−619.

Ducklow, H.W., Steinberg, D.K., Buesseler, K.O., 2001. Upper ocean carbon export and the biological pump. Oceanography 14, 50−58.

Dupont, S., Pörtner, H.-O., 2013. A snapshot of ocean acidification research. Mar. Biol. 160, 1765−1771.

Dutkiewicz, S., Morris, J.J., Follows, M.J., Scott, J., Levitan, O., Dyhrman, S.T., et al., 2015. Impact of ocean acidification on the structure of future phytoplankton communities. Nature Clim. Change 5, 1002−1006.

Emerson, S.R., Hedges, J.I., 2008. Chemical oceanography and the marine carbon cycle, Cambridge University Press, New York, pp. 103−112.

Endres, S., Galgani, L., Riebesell, U., Schulz, K.G., Engel, A., 2014. Stimulated bacterial growth under elevated pCO_2: results from an off-shore mesocosm study. PLoS ONE 9, e99228.

Engel, A., 2002. Direct relationship between CO_2 uptake and transparent exopolymer particles production in natural phytoplankton. J. Plankton Res. 24, 49−53.

Engel, A., Borchard, C., Piontek, J., Schulz, K.G., Riebesell, U., Bellerby, R.G.J., 2013. CO_2 increases ^{14}C primary production in an Arctic plankton community. Biogeosciences 10, 1291−1308.

Engel, A., Delille, B., Jacquet, S., Riebesell, U., Rochelle-Newall, E., Terbrüggen, A., et al., 2004. Transparent exopolymer particles and dissolved organic carbon production by *Emiliania huxleyi* exposed to different CO_2 concentrations: A mesocosm experiment. Aquat. Microb. Ecol. 34, 93−104.

Engel, A., Piontek, J., Grossart, H.-P., Riebesell, U., Schulz, K.G., Sperling, M., 2014. Impact of CO_2 enrichment on organic matter dynamics during nutrient induced coastal phytoplankton blooms. J. Plankton Res. 36, 641−657.

Engel, A., Zondervan, I., Aerts, K., Beaufort, L., Benthien, A., Chou, L., et al., 2005. Testing the direct effect of CO_2 concentration on a bloom of the coccolithophorid *Emiliania huxleyi* in mesocosm experiments. Limnol. Oceanogr. 50, 493−507.

Falkowski, P., Scholes, R.J., Boyle, E., Canadell, J., Elser, J., Gruber, N., et al., 2000. The global carbon cycle: a test of our knowledge of earth as a system. Science 290, 291−296.

Feely, R.A., Doney, S.C., Cooley, S.R., 2009. Ocean acidification: present conditions and future changes in a high-CO_2 world. Oceanography 22, 36−47.

Feely, R.A., Sabine, C.L., Takahashi, T., Wanninkhof, R., 2001. Uptake and storage of carbon dioxide in the ocean: the global CO_2 survey. Oceanography 14, 18−32.

González-Dávila, M., Santana-Casiano, J.M., Rueda, M.J., Llinás, O., 2010. The water column distribution of carbonate system variables at the ESTOC site from 1995 to 2004. Biogeosciences 7, 3067−3081.

Grossart, H.-P., Allgaier, M., Passow, U., Riebesell, U., 2006. Testing the effect of CO_2 concentration on the dynamics of marine heterotrophic bacterioplankton. Limnol. Oceanogr. 51, 1−11.

Hansell, D.A., 2013. Recalcitrant dissolved organic carbon fractions. Annu. Rev. Mar. Sci. 5, 421−445.

Hansell, D.A., Carlson, C.A., Repeta, D.J., Schlitzer, R., 2009. Dissolved organic matter in the ocean: a controversy stimulates new insights. Oceanography 22, 202−211.

Hansell, D.A., Carlson, C.A., Schlitzer, R., 2012. Net removal of major marine dissolved organic carbon fractions in the subsurface ocean. Global Biogeochem. Cycles 26, GB1016.

Hartmann, F.C., Harpel, M.R., 1994. Structure, function, regulation, and assembly of D-ribulose-1,5-bisphosphate carboxylase/oxygenase. Annu. Rev. Biochem. 63, 197−234.

Hedges, J.I., Hatcher, P.G., Ertel, J.R., Meyers-Schulte, K.J., 1992. A comparison of dissolved humic substances from seawater with Amazon River counterparts by ^{13}C-NMR spectrometry. Geochim. Cosmochim. Ac. 56, 1753−1757.

Hein, M., Sand-Jensen, K., 1997. CO_2 increases oceanic primary production. Nature 388, 526−527.

Hertkorn, N., Benner, R., Frommberger, M., Schmitt-Kopplin, P., Witt, M., Kaiser, K., et al., 2006. Characterization of a major refractory component of marine dissolved organic matter. Geochim. Cosmochim. Ac. 70, 2990−3010.

Hertkorn, N., Frommberger, M., Witt, M., Koch, B.P., Schmitt-Kopplin, P., Perdue, E.M., 2008. Natural organic matter and the event horizon of mass spectrometry. Anal. Chem. 80, 8908−8919.

Hertkorn, N., Harir, M., Koch, B.P., Michalke, B., Schmitt-Kopplin, P., 2013. High-field NMR spectroscopy and FTICR mass spectrometry: powerful discovery tools for the molecular level characterization of marine dissolved organic matter. Biogeosciences 10, 1583−1624.

Hofmann, M., Schellnhuber, H.J., 2010. Ocean acidification: a millennial challenge. Energy Environ. Sci. 3, 1883−1896.

Hopkinson, C.S., Vallino, J.J., 2005. Efficient export of carbon to the deep ocean through dissolved organic matter. Nature 433, 142−145.

IPCC, 2013. Climate Change 2013: The Physical Science Basis. Contribution of Working Group 1 to the Fifth Assessment Report of the Intergovernmental Panel on Climate Change, in: Stocker, T.F., Qin, D., Plattner, G.-K., Tignor, M., Allen, S.K., Boschung, J., Nauels, A., Xia, Y., Bex, V., Midgley, P.M., (Eds.), Cambridge University Press, Cambridge and New York, p. 1096.

Jiao, N., Herndl, G.J., Hansell, D.A., Benner, R., Kattner, G., Wilhelm, S.W., et al., 2010. Microbial production of recalcitrant dissolved organic matter: long-term carbon storage in the global ocean. Nat. Rev. Microbiol. 8, 593−599.

Joint, I., Doney, S.C., Karl, D.M., 2011. Will ocean acidification affect marine microbes? ISME 5, 1−7.

Kaiser, K., Benner, R., 2009. Biochemical composition and size distribution of organic matter at the Pacific and Atlantic time-series stations. Mar. Chem. 113, 63−77.

Kaiser, K., Benner, R., 2012. Organic matter transformations in the upper mesopelagic zone of the North Pacific: chemical composition and linkages to microbial community structure. J. Geophys. Res.: Oceans 117, C01023.

Kellerman, A.M., Dittmar, T., Kothawala, D.N., Tranvik, L.J., 2014. Chemodiversity of dissolved organic matter in lakes driven by climate and hydrology. Nat. Comm. 5, 3804.

Koch, B.P., Dittmar, T., 2006. From mass to structure: an aromaticity index for high-resolution mass data of natural organic matter. Rapid Commun. Mass Spectrom. 20, 926−932.

Koch, B.P., Witt, M., Engbrodt, R., Dittmar, T., Kattner, G., 2005. Molecular formulae of marine and terrigenous dissolved organic matter detected by electrospray ionization Fourier transform ion cyclotron resonance mass spectrometry. Geochim. Cosmochim. Ac. 69, 3299−3308.

Kujawinski, E.B., Longnecker, K., Blough, N.V., del Vecchio, R., Finlay, L., Kitner, J.B., et al., 2009. Identification of possible source markers in marine dissolved organic matter using ultrahigh resolution mass spectrometry. Geochim. Cosmochim. Ac. 73, 4384−4399.

Labare, M.P., Bays, J.T., Butkus, M.A., Snyder-Leiby, T., Smith, A., Goldstein, A., et al., 2010. The effects of elevated carbon dioxide levels on a *Vibrio* sp. isolated from the deep-sea. Environ. Sci. Pollut. Res. 17, 1009−1015.

Lam, B., Simpson, A.J., 2008. Direct ^{1}H NMR spectroscopy of dissolved organic matter in natural waters. Analyst 133, 263−269.

Langer, G., Geisen, M., 2006. Species-specific responses of calcifying algae to changing seawater carbonate chemistry. Geochem. Geophy. Geosy. 7, 9.

Liu, Z., Sleighter, R.L., Zhong, J., Hatcher, P.G., 2011. The chemical changes of DOM from black waters to coastal marine waters by HPLC combined with ultrahigh resolution mass spectrometry. Estuar. Coast. Shelf S. 92, 205−216.

Lohbeck, K.T., Riebesell, U., Reusch, T.B.H., 2012. Adaptive evolution of a key phytoplankton species to ocean acidification. Nat. Geosci. 5, 346−351.

Lüthi, D., Le Floch, M., Bereiter, B., Blunier, T., Barnola, J.-M., Siegenthaler, U., et al., 2008. High-resolution carbon dioxide concentration record 650,000-800,000 years before present. Nature 453, 379−382.

MacGilchrist, G.A., Shi, T., Tyrell, T., Richier, S., Moore, C.M., Dumousseaud, C., et al., 2014. Effect of enhanced pCO_2 levels on the production of dissolved organic carbon and transparent exopolymer particles in short-term bioassay experiments. Biogeosciences 11, 3695−3706.

Mari, X., 2008. Does ocean acidification induce an upward flux of marine aggregates? Biogeosciences 5, 1023−1031.

Minor, E.C., Swenson, M.M., Mattson, B.M., Oyler, A.R., 2014. Structural characterization of dissolved organic matter: a review of current techniques for isolation and analysis. Environ. Sci.: Processes Impacts 16, 2064−2079.

Mopper, K., Stubbins, A., Ritchie, J.D., Bialk, H.M., Hatcher, P.G., 2007. Advanced instrumental approaches for characterization of marine dissolved organic matter: extraction techniques, mass spectrometry, and nuclear magnetic resonance spectroscopy. Chem. Rev. 107, 419−442.

Opsahl, S., Benner, R., 1997. Distribution and cycling of terrigenous dissolved organic matter in the ocean. Nature 386, 480−482.

Oschlies, A., Schulz, K.G., Riebesell, U., Schmittner, A., 2008. Simulated 21st century's increase in oceanic suboxia by CO_2-enhanced biotic carbon export. Global Biogeochem. Cy. 22, GB4008.

Osterholz, H., Niggemann, J., Giebel, H.-A., Simon, M., Dittmar, T., 2015. Inefficient microbial production of refractory dissolved organic matter in the ocean. Nat. Comm. 6, 7422.

Paul, A.J., Bach, L.T., Schulz, K.-G., Boxhammer, T., Czerny, J., Achterberg, E.P., et al., 2015. Effect of elevated CO_2 on organic matter pools and fluxes in a summer Baltic Sea plankton community. Biogeosciences 12, 6181−6203.

Paul, C., Matthiessen, B., Sommer, U., 2015. Warming, but not enhanced CO_2 concentration, quantitatively and qualitatively affects phytoplankton biomass. Mar. Ecol. Prog. Ser. 528, 39−51.

Passow, U., 2002. Production of transparent exopolymer particles (TEP) by phyto- and bacterioplankton. Mar. Ecol. Prog. Ser. 236, 1−12.

Piontek, J., Lunau, M., Händel, N., Borchard, C., Wurst, M., Engel, A., 2010. Acidification increases microbial polysaccharide degradation in the ocean. Biogeosciences 7, 1615−1624.

Plancque, G., Amekraz, B., Moulin, V., Toulhat, P., Moulin, C., 2001. Molecular structure of fulvic acids by electrospray with quadrupole time-of-flight mass spectrometry. Rapid Commun. Mass Spectrom. 15, 827−835.

Raven, J., (chair), Caldeira, K., Elderfield, H., Hoegh-Guldberg, O., Liss, P., Riebesell, U., et al. (2005) Ocean acidification due to increasing atmospheric carbon dioxide. The Royal Society, Document 12/05.

Redfield, A.C., 1958. The biological control of chemical factors in the environment. Am. Sci. 46, 205−221.

Repeta, D.J., 2015. Chemical characterization and cycling of dissolved organic matter, in: Hansell, D.A., Carlson, C.A., (Eds.), The biogeochemistry of marine dissolved organic matter, 2nd edition. Academic Press, San Diego, pp. 21−63.

Revelle, R., Suess, H.E., 1957. Carbon dioxide exchange between atmosphere and ocean and the question of an increase of atmospheric CO_2 during the past decades. Tellus 9, 18−27.

Riebesell, U., 2000. Carbon fix for a diatom. Nature 407, 959−960.

Riebesell, U., Czerny, J., von Bröckel, K., Boxhammer, T., Büdenbender, J., Deckelnick, M., et al., 2013b. Technical note: a mobile sea-going mesocosm system – new opportunities for ocean change research. Biogeosciences 10, 1835−1847.

Riebesell, U., Gattuso, J.-P., 2015. Lessons learned from ocean acidification research. Nature Clim. Change 5, 12−14.

Riebesell, U., Gattuso, J.-P., Thingstad, T.F., Middelburg, J.J., 2013a. Preface "Arctic ocean acidification: pelagic ecosystem and biogeochemical responses during a mesocosm study". Biogeosciences 10, 5619−5626.

Riebesell, U., Lee, K., Nejstgaard, J.C., 2010. Pelagic mesocosms, in: Riebesell, U., Fabry, V., Hansson, L., Gattuso, J.-P., (Eds.), Guide to best practices in ocean acidification research and datareporting. Office for Official Publications of the European Communities, Luxembourg, pp. 81–98.

Riebesell, U., Schulz, K.G., Bellerby, R.G.J., Botros, M., Fritsche, P., Meyerhöfer, M., et al., 2007. Enhanced biological carbon consumption in a high CO_2 ocean. Nature 450, 545−548.

Riebesell, U., Tortell, P.D., 2011. Effects of ocean acidification on pelagic organisms and ecosystems, in: Gattuso, J.-P., Hansson, L., (Eds.), Ocean acidification. Oxford University Press, New York, pp. 99−116.

Riebesell, U., Wolf-Gladrow, D.A., Smetacek, V., 1993. Carbon dioxide limitation of marine phytoplankton growth rates. Nature 361, 249−251.

Rochelle-Newall, E., Delille, B., Frankignoulle, M., Gattuso, J.-P., Jacquet, S., Riebesell, U., et al., 2004. Chromophoric dissolved organic matter in experimental mesocosms maintained under different pCO_2 levels. Mar. Ecol. Prog. Ser. 272, 25−31.

Rossel, P.E., Vähätalo, A.V., Witt, M., Dittmar, T., 2013. Molecular composition of dissolved organic matter from a wetland plant (*Juncus effusus*) after photochemical and microbial decomposition (1.25 yr): common features with deep sea dissolved organic matter. Org. Geochem. 60, 62−71.

Rost, B., Zondervan, I., Wolf-Gladrow, D., 2008. Sensitivity of phytoplankton to future changes in ocean carbonate chemistry: current knowledge, contradictions and research directions. Mar. Ecol. Prog. Ser. 373, 227-237.

Sabine, C.L., Feely, R.A., Gruber, N., Key, R.M., Lee, K., Bullister, J.L., et al., 2004. The oceanic sink for anthropogenic CO_2. Science 305, 367−371.

Šantl-Temkiv, T., Finster, K., Dittmar, T., Hansen, B.M., Thyrhaug, R., Nielsen, N.W., et al. (2013) Hailstones: a window into the microbial and chemical inventory of a storm cloud. PLoS ONE 8, e53550.

Sarmiento, J.L., Slater, R., Barber, R., Bopp, L., Doney, S.C., Hirst, A.C., et al., 2004. Response of ocean ecosystems to climate warming. Global Biogeochem. Cy. 18, GB3003.

Schulz, K.G., Bellerby, R.G.J., Brussaard, C.P.D., Büdenbender, J., Czerny, J., Engel, A., et al., 2013. Temporal biomass dynamics of an Arctic plankton bloom in response to increasing levels of atmospheric carbon dioxide. Biogeosciences 10, 161−180.

Sexton, P.F., Norris, R.D., Wilson, P.A., Pälike, H., Westerhold, T., Röhl, U., et al., 2011. Eocene global warming events driven by ventilation of oceanic dissolved organic carbon. Nature 471, 349−352.

Simon, M., Grossart, H.-P., Schweitzer, B., Ploug, H., 2002. Microbial ecology of organic aggregates in aquatic ecosystems. Aquat. Mirob. Ecol. 28, 175−211.

Simpson, A.J., McNally, D.J., Simpson, J., 2011. NMR spectroscopy in environmental research: from molecular interactions to global processes. Prog. Nucl. Mag. Res. Sp. 58, 97−175.

Singer, G.A., Fasching, C., Wilhelm, L., Niggemann, J., Steier, P., Dittmar, T., et al., 2012. Biogeochemically diverse organic matter in Alpine glaciers and its downstream fate. Nat. Geosci. 5, NGEO1581.

Steinacher, M., Joos, F., Frölicher, T.L., Plattner, G.-K., Doney, S.C., 2009. Imminent ocean acidification in the Arctic projected with the NCAR global coupled carbon cycle-climate model. Biogeosciences 6, 515−533.

Stenson, A.C., Landing, W.M., Marshall, A.G., Cooper, W.T., 2002. Ionization and fragmentation of humic substances in electrospray ionization Fourier transform-ion cyclotron resonance mass spectrometry. Anal. Chem. 74, 4397−4409.

Stenson, A.C., Marshall, A.G., Cooper, W.T., 2003. Exact masses and chemical formulas of individual Suwannee River fulvic acids from ultrahigh resolution electrospray ionization Fourier transform ion cyclotron resonance mass spectra. Anal. Chem. 75, 1275−1284.

Stubbins, A., Lapierre, J.-F., Berggren, M., Prairie, Y.T., Dittmar, T., del Giorgio, P.A., 2014. What's in an EEM? Molecular signatures associated with dissolved organic fluorescence in boreal Canada. Environ. Sci. Technol. 48, 10598−10606.

Stumm, M., 2011. First mass spectrometric steps towards molecular structure assignments in marine dissolved organic matter. Master Thesis, Carl von Ossietzky University Oldenburg.

Takahashi, T., Sutherland, S.C., Wanninkhof, R., Sweeney, C., Feely, R.A., Chipman, D.W., 2009. Climatological mean and decadal change in surface ocean pCO_2, and net sea-air CO_2 flux over the global oceans. Deep-Sea Res. Pt. II 56, 554−577.

Takeuchi, K., Fujioka, Y., Kawasaki, Y., Shirayama, Y., 1997. Impacts of high concentration of CO_2 on marine organisms; a modification of CO_2 ocean sequestration. Energy Convers. Mgmt 38, S337−S341.

Tans, P., Keeling, R., 2015. NOAA/ESRL Global monitoring division. Available from: www.esrl.noaa.gov/gmd/ccgg/trends/. [6 November 2015].

Taucher, J., Schulz, K.G., Dittmar, T., Sommer, U., Oschlies, A., Riebesell, U., 2012. Enhanced carbon overconsumption in response to increasing temperatures during a mesocosm experiment. Biogeosciences 9, 3531−3545.

Verdugo, P., 2012. Marine Microgels. Annu. Rev. Mar. Sci. 4, 375−400.

Verdugo, P., Allredge, A.L., Azam, F., Kirchman, D.L., Passow, U., Santschi, P.H., 2004. The oceanic gel phase: a bridge in the DOM-POM continuum. Mar. Chem. 92, 67−85.

Vetter, T.A., Perdue, E.M., Ingall, E., Koprivnjak, J.F., Pfromm, P.H., 2007. Combining reverse osmosis and electrodialysis for more complete recovery of dissolved organic matter from seawater. Sep. Purif. Technol. 56, 383−387.

Weinbauer, M.G., Mari, X., Gattuso J.-P., 2011. Effects of ocean acidification on the diversity and activity of heterotrophic marine microorganisms, in: Gattuso, J.-P., Hansson, L., (Eds.), Ocean acidification. Oxford University Press, New York, pp. 83−98.

Williams, P.J., 2000. Heterotrophic bacteria and the dynamics of dissolved organic material, in: Kirchman, D.L., (Ed.), Microbial ecology of the oceans, Wiley-Liss, New York, pp. 153−200.

Williams, P.M., Druffel, E.R.M., 1987. Radiocarbon in dissolved organic matter in the central North Pacific Ocean. Nature 330, 246−248.

Witt, M., Fuchser, J., Koch, B.P., 2009. Fragmentation studies of fulvic acids using collision induced dissociation Fourier transform ion cyclotron resonance mass spectrometry. Anal. Chem. 81, 2688−2694.

Woods, G.C., Simpson, M.J., Koerner, P.J., Napoli, A., Simpson, A.J., 2011. HILIC-NMR: towards the identification of individual molecular components in dissolved organic matter. Environ. Sci. Technol. 45, 3880−3886.

Yamada, N., Suzumura, M., 2010. Effects of seawater acidification on hydrolytic enzyme activities. J Oceanogr 66, 233−241.

Zachos, J.C., Dickens, G.R., Zeebe, R.E., 2008. An early Cenozoic perspective on greenhouse warming and carbon-cycle dynamics. Nature 451, 279−283.

Zeebe, R.E., Ridgwell, A., 2011. Past changes in ocean carbonate chemistry, in: Gattuso, J.-P., Hansson, L., (Eds.), Ocean acidification. Oxford University Press, New York, pp. 21−40.

Manuscript I:

Effects of ocean acidification on marine dissolved organic matter are not detectable over the succession of phytoplankton blooms

Maren Zark,[1] Ulf Riebesell,[2] and Thorsten Dittmar[1]

This chapter corresponds to a full published manuscript in
Science Advances (2015) 1:e1500531; doi:10.1126/sciadv.1500531.

[1] Institute for Chemistry and Biology of the Marine Environment (ICBM), Research Group for Marine Geochemistry (ICBM-MPI Bridging Group), Carl von Ossietzky University of Oldenburg, Carl-von-Ossietzky-Straße 9-11, 26129 Oldenburg, Germany.

[2] GEOMAR Helmholtz Centre for Ocean Research Kiel, Düsternbrooker Weg 20, 24105 Kiel, Germany.

The manuscript „Effects of ocean acidification on marine dissolved organic matter are not detectable over the succession of phytoplankton blooms" (Manuscript I) presents the results from a long-term mesocosm study in a Swedish Fjord. The experiment was conducted over a period of more than three months with CO_2 concentrations projected for the year 2100 (IPCC 2013). We found no indications for changes in the molecular DOM composition with elevated CO_2 concentration. All authors designed the study. M. Zark and U. Riebesell did fieldwork. M. Zark analyzed samples and performed statistical data evaluation together with T. Dittmar. M. Zark wrote the paper and all authors discussed the results and commented on the manuscript.

This manuscript was published in *Science Advances* (doi: 10.1126/-sciadv.1500531) and is presented with adjusted formatting according to the style of this thesis.

2.1 Abstract

Marine dissolved organic matter (DOM) is one of the largest active organic carbon reservoirs on Earth, and changes in its pool size or composition could have a major impact on the global carbon cycle. Ocean acidification is a potential driver for these changes because it influences marine primary production and heterotrophic respiration. We simulated ocean acidification as expected for a business-as-usual emission scenario in the year 2100 in an unprecedented long-term mesocosm study. The large-scale experiments (50 m^3 each) covered a full seasonal cycle of marine production in a Swedish Fjord. Five mesocosms were artificially enriched in CO_2 to the partial pressure expected in the year 2100 (900 µatm), and five more served as controls (400 µatm). We applied ultrahigh-resolution mass spectrometry to monitor the succession of 7360 distinct DOM formulae over the course of the experiment. Plankton blooms had a clear effect on DOM concentration and molecular composition. This succession was reproducible across all 10 mesocosms, independent of CO_2 treatment. In contrast to the temporal trend, there were no significant differences in DOM concentration and composition between present-day and year 2100 CO_2 levels at any time point of the experiment. On the basis of our results, ocean acidification alone is unlikely to affect the seasonal accumulation of DOM in productive coastal environments.

2.2 Introduction

About half of the CO_2 emitted to the atmosphere by human fossil-fuel burning since preindustrial times has been absorbed by the oceans (Sabine et al., 2004), causing a continuous decrease in seawater pH by about 0.3 unit before the end of the 20th century (Caldeira and Wickett, 2003). This rapid change in seawater chemistry has a potential impact on the future marine biogeochemical carbon cycle (Caldeira and Wickett, 2003; Riebesell et al., 2009) through changes in marine primary production (Bellerby et al., 2003; Riebesell et al., 2007) and heterotrophic respiration (Grossart et al., 2006; Piontek et al., 2010). Marine dissolved organic matter (DOM) represents the largest active organic carbon pool within this cycle (~700 Gt) (Hansell et al., 2009). Changes in pool size or reactivity would affect the long-term carbon storage capability of the ocean's interior. However, the impact of ocean acidification on the marine DOM pool remains unknown, particularly on its molecular composition and long-term reactivity (Czerny et al., 2013; Engel et al., 2014, 2013; MacGilchrist et al., 2014).

A large fraction of oceanic net primary production is transferred to the DOM pool and respired to CO_2 via the microbial loop (Carlson et al., 2007; del Giorgio and Duarte, 2002). However, a subset of DOM is highly persistent against microbial degradation and resides in the deep ocean on time scales of hundreds to ten thousands of years (Hansell and Carlson, 1998; Hansell et al., 2009). The driving forces behind this recalcitrance are unknown (Dittmar, 2015), but most likely microbial processes govern the generation and transformation of recalcitrant DOM (Eppley and Peterson, 1979; Jiao et al., 2010; Ogawa et al., 2001; Osterholz et al., 2015). The recalcitrant fraction of DOM represents by far the largest proportion and is thus the most important in terms of carbon storage (Hansell, 2013).

Ocean acidification may stimulate microbial degradation of DOM (Grossart et al., 2006; Piontek et al., 2010). Therefore, it could induce lower carbon sequestration rates in the future ocean (Mari, 2008; Schippers et al., 2004). However, the concurrent stimulation of DOM production (Czerny et al., 2013; Engel et al., 2013) may offset the enhanced turnover, and the net effect of ocean acidification on bulk dissolved organic carbon (DOC) concentration may be insignificant on the short term (Engel et al., 2014, 2004; MacGilchrist et al., 2014).

However, DOM is a highly complex mixture of presumably millions of different compounds (Dittmar, 2015). Changes on the molecular level can bring about differences in reactivity and long-term accumulation of DOM in the ocean that are not detectable on the bulk concentration level in short-term experiments.

To investigate the effects of ocean acidification on the molecular composition of the marine DOM pool, we conducted a unique long-term mesocosm study in the Gullmar Fjord in Sweden. Ten mesocosm units, each enclosing volumes of 50 m^3, were used to monitor a natural plankton community in situ under pCO_2 (partial pressure of CO_2) levels projected for the end of this century. Five of these mesocosms were artificially enriched in CO_2 to the partial pressure expected in the year 2100 (900 µatm) (IPCC, 2013), and the other five served as controls (400 µatm). This experiment is unprecedented in terms of size and duration. We allowed for an extended acclimation time before the first algal bloom and monitored the full productive season over a time period at least twice as long as in any previous study.

We periodically monitored the DOM pool over the entire study through bulk DOC and total dissolved nitrogen (TDN) determinations as well as on a detailed molecular level through ultrahigh resolution mass spectrometry [Fourier-transform ion cyclotron resonance mass spectrometry (FT-ICR-MS)]. With this technique, the diversity of DOM can be resolved on a molecular formula level, and as such FT-ICR-MS is unprecedented in providing detailed molecular insights into the composition of DOM. The many thousand different molecular masses that can be resolved by FT-ICR-MS (Dittmar and Paeng, 2009; Koch et al., 2005) show a distinct succession over the course of phytoplankton blooms (Osterholz et al., 2015) and the technique is therefore well suited to obtain a most holistic overview of molecular DOM composition over the course of our experiments. As with any analytical technique, FT-ICR-MS has a defined analytical window, and compounds of low molecular mass (< 150 Da) and colloidal matter are outside of this window. Furthermore, highly labile compounds cycling on time scales of days were not targets by our sampling frequency and analytical techniques. Our experimental setup was intended to capture compounds that are produced in bloom situations (Osterholz et al., 2015) and turned over on time scales of weeks to months and

longer. This component of DOM is of highest importance in the context of carbon sequestration.

2.3 Results

2.3.1 General description of the mesocosms and bulk parameters

All 10 mesocosms exhibited a markedly reproducible succession of phytoplankton blooms and associated DOM production and consumption. Two sequential phytoplankton blooms were observed during the course of the experiment. The first bloom was sustained by inorganic nutrients and peaked around day 31 with an average chlorophyll *a* concentration of 6.8 µg liter^{-1} (Fig. 2.1a). TDN at the beginning of the study represented the combined concentrations of dissolved inorganic nitrogen (DIN) and dissolved organic nitrogen (DON) (Fig. 2.1b). DOC concentrations almost doubled from 149 ± 11 µmol L^{-1} on day −1, the day before the first CO_2 addition, to 256 ± 38 µmol L^{-1} on day 47 (mean ± SD, n = 10) (Fig. 2.1c) because of new production. The level is typical for the Gullmar Fjord at this time of the year (Waite et al., 2005).

Inorganic nitrogen was consumed during this first bloom phase, and TDN then was constituted only by DON. The second bloom was fueled by the recycling of elements from organic matter and occurred around day 53 with a lower chlorophyll *a* maximum of 4.3 µg liter^{-1} (Fig. 2.1a). During recycled production, DOC concentrations decreased to a minimum of 149 ± 6 µmol L^{-1} close to the end of the study. DOC/DON molar ratios started well above the classical Redfield ratio of 6.6, with decreasing values until the onset of the first phytoplankton bloom on day 20 (Fig. 2.1d). Superimposed onto these broad coherent trends, DOC concentrations consistently fluctuated from day to day in all 10 mesocosms. These irregular fluctuations are partly due to analytical uncertainty, which is inherent to bulk DOC analysis under such complex experimental settings. Most importantly, there was no statistically significant difference ($p < 0.01$) between the CO_2 treatments for all time points for chlorophyll *a*, DOC, DON, and TDN concentrations. The only exception was one sampling day (day 53), where TDN concentrations were apparently different between the two CO_2 treatments.

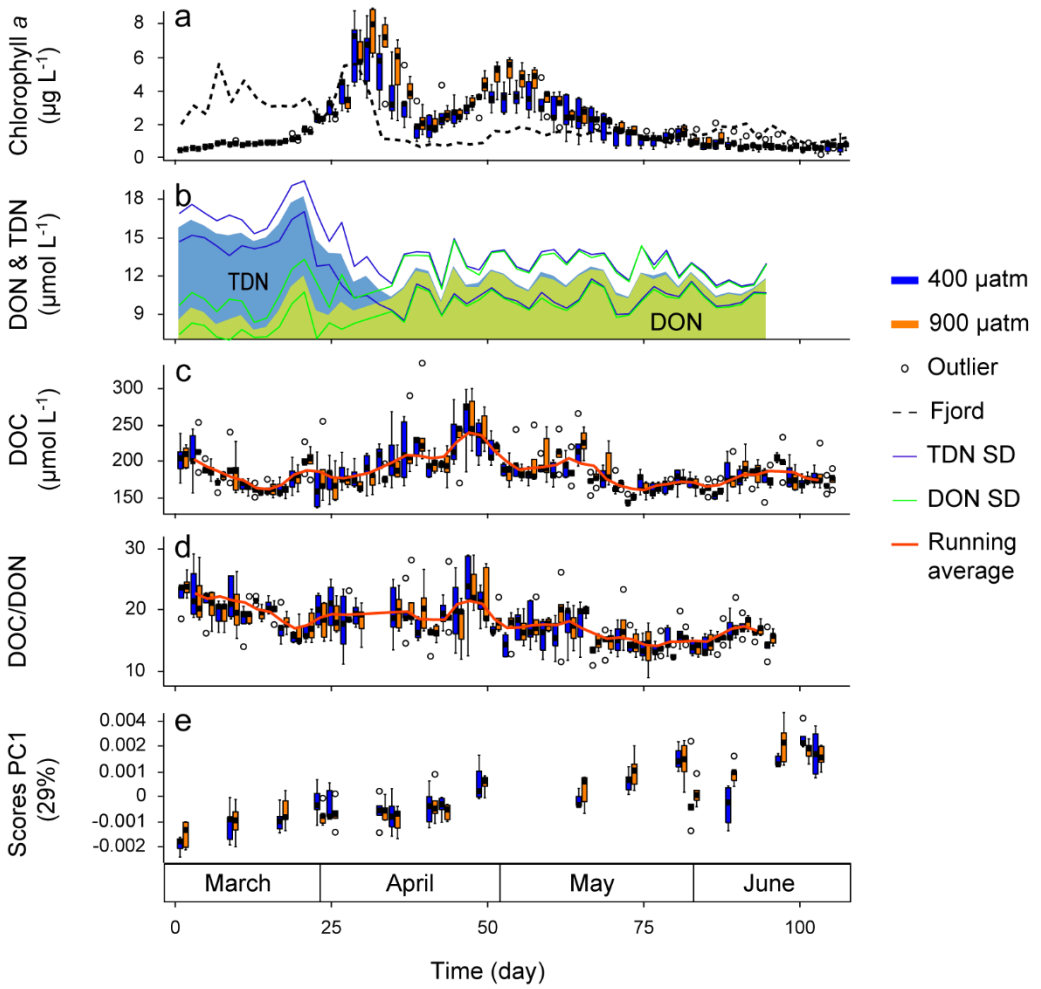

Figure 2.1 Time series of bulk and molecular data of the 10 mesocosms. Box plots include median, SD, maximum and minimum values, and outliers. Orange boxes are for the five mesocosms with high pCO_2; blue boxes are for the five control mesocosms. Dotted time series are for Gullmar Fjord ambient water. (a) Chlorophyll *a* concentration. (b) TDN and DON concentrations, displayed as average values for all 10 mesocosms. (c) DOC concentration. (d) DOC/DON molar ratio. (e) Results from the PCA (PC1) of 7360 molecular formulae and their MS signal intensities.

On a lower significance level ($p < 0.05$) there were only up to 4 days that showed differences for chlorophyll *a* (days 3, 49, 51, and 53), DOC (days 33, 61, and 73), DON (days −1, 53, and 79), and TDN (day 53) concentrations. These apparent differences did not show a consistent trend over time or between parameters. When considering several hypotheses in the same test the problem of multiplicity arises (Holm, 1979). If one accounts for this family-wise error rate, for example, with the Holm-Bonferroni correction (Holm, 1979), none of the apparent differences between CO_2 treatments is significant at any meaningful significance level.

2.3.2 DOM molecular composition

A total of 11,644 resolved masses of singly charged, intact compounds were detected with FT-ICR-MS (Fig. 2.2). Signal intensities followed a bell-shaped distribution along the mass axis with a weighted arithmetic mean of 391 ± 4 Da (average and SD for all samples). This overall pattern was the same for all samples, but individual masses differed among samples with respect to their presence and signal intensity. For multivariate statistical analysis, the same number (7360) of the most intense detected masses was considered for each sample.

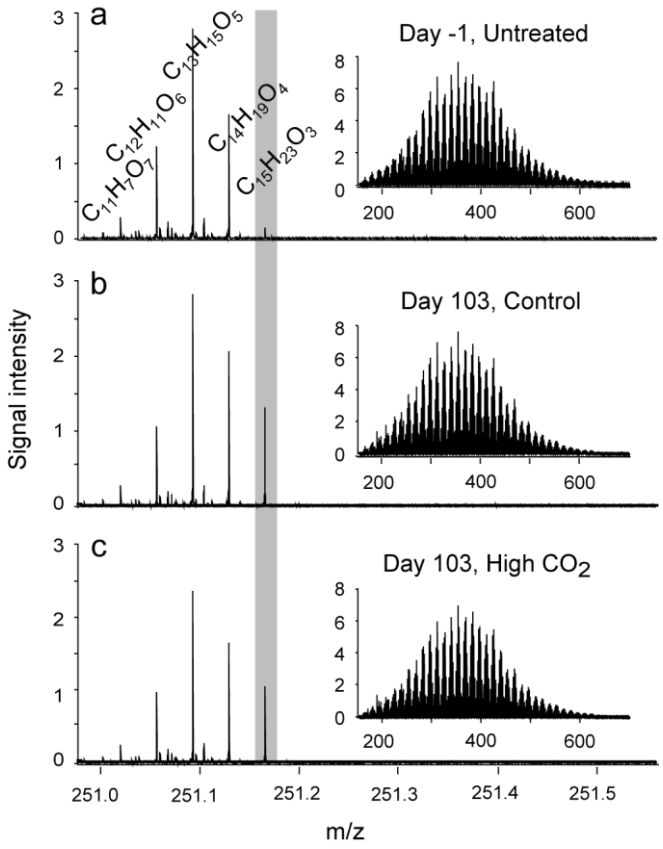

Figure 2.2 Examples of FT-ICR-MS spectra of mesocosm DOM at different time points and with different treatments. (a) Day −1 after closing mesocosm bags. (b) Day 103 ambient pCO_2 mesocosm. (c) Day 103 high pCO_2 mesocosm. Mass range is from 150 to 750 Da and zoomed into one exemplary nominal mass (251 Da). *m/z*, mass/charge ratio. The peak in the gray shaded area is exemplary of mass peaks that show a significant difference in intensities between day 1 and day 103 in a Student's *t* test ($p < 0.001$).

Using principal components analysis (PCA), we were able to summarize 29% of the total variability of the complex molecular information in a single component (PC1). This component showed a highly reproducible trend among the 10

independent mesocosm units over time (Fig. 2.1e). A Pearson correlation of the components from PCA with the environmental data revealed that PC1 was inversely correlated with chlorophyll *a* concentration ($p < 0.01$) but not with pCO_2 treatment (Table 2.1). A positive correlation of PC1 was observed with SiO_4^{4-}, PO_4^{3-}, NO_2^-, and NO_3^- concentrations ($p < 0.001$). However, none of the first 10 principal components pointed toward an influence of CO_2 manipulation. By comparing the distances to the respective group centroid (PerMANOVA), we obtained the same result, because there were no significant differences in the molecular data for samples from CO_2-enriched compared to control mesocosms.

Table 2.1 Pearson correlation of environmental parameters with the PCA scores. Significant correlations are noted by the level of significance (p-value); "-" denotes absence of any detectable correlation ($p > 0.05$).

	PC1 (25%)	PC2 (17%)
CO_2	-	-
DOC	-	-
NO_2^-/NO_3^-	3.07×10^{-9}	2.39×10^{-4}
PO_4^{3-}	2.09×10^{-9}	6.54×10^{-5}
SiO_4^{4-}	1.71×10^{-9}	3.38×10^{-5}
NH_4^+	-	3.49×10^{-2}
Chlorophyll *a*	6.25×10^{-3}	-

Individual molecular formula analysis of the relative signal intensities of the five replicate mesocosms showed similar results. Multiple Student's *t* tests were individually performed for each pCO_2 treatment at each time point, revealing an increasing number of molecular formulae that significantly ($p < 0.001$) differed from the starting conditions over time. In total, up to 16% of the considered molecular features showed a variation between day −1 and the last day of sampling (Fig. 2.3), which is the result of specific molecules being released or used by the resident microbial communities inside the mesocosms. We performed the same test for the molecular formulae from the different pCO_2 treatments. We observed only a small number of formulae that significantly differed, ranging only from 0 to 20 formulae for all time points (Fig. 2.4). The abovementioned family-wise error rate is of major relevance to our family of 7360 tests (molecular formulae). To compare our results with what random chance might produce (Nuzzo, 2014), we generated

artificial data sets of 7360 randomly generated numbers. Comparison of two random data sets showed a similar number of apparent differences to that observed between two CO_2 treatments (Figs. 2.3b and 2.4b). Hence, CO_2 levels did not affect the net molecular composition of the DOM pool covered by our analysis after a succession of phytoplankton blooms. This consistency among the mesocosms is striking, given the fact that in 5 of 10 mesocosms, pCO_2 was more than doubled, and that 7360 independent molecular features were considered of which > 1000 showed a consistent succession over time.

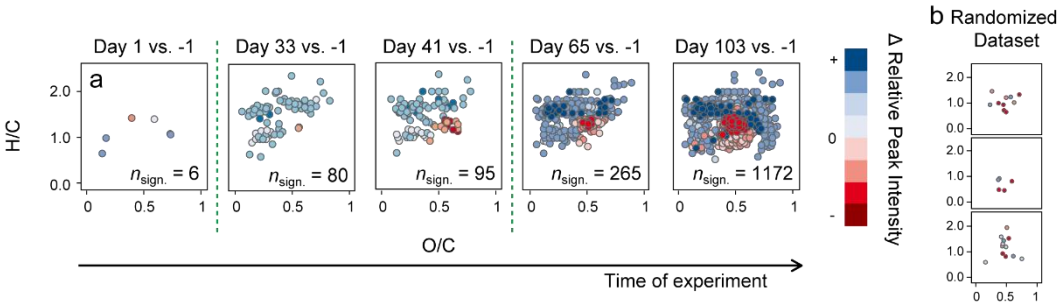

Figure 2.3 Molecular differences over time. (a) Exemplary van Krevelen diagrams showing only the molecular formulae (out of 7360) that significantly varied in their intensities over the course of the experiment compared to day −1 for all 10 mesocosm replicates ($p < 0.001$). The different colors represent differences in normalized relative peak intensity: blue dots indicate an increase in peak intensities, whereas red dots indicate a decrease in peak intensity. Green dashed lines represent time points of phytoplankton blooms. (b) The results are within the statistical error, determined by performing the same test on a randomized data set.

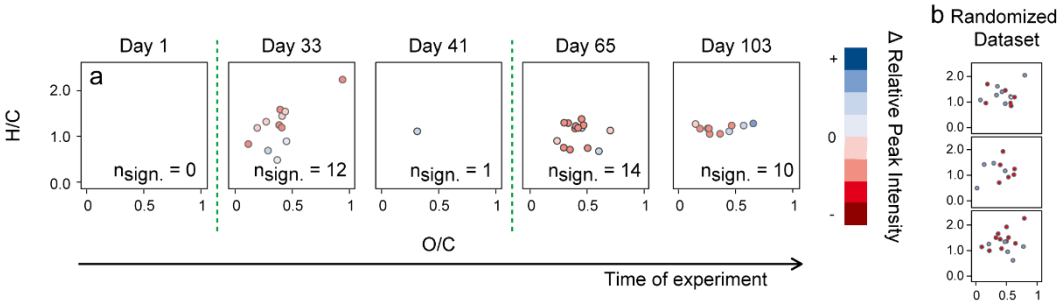

Figure 2.4 Molecular differences between different CO_2 treatments. (a) Exemplary van Krevelen diagrams showing only the molecular formulae (out of 7360) that significantly varied in their intensities between the five high PCO_2 and control mesocosm replicates, tested for the respective day ($p < 0.001$). The different colors represent differences in normalized relative peak intensity: blue dots indicate an increase in peak intensity, whereas red dots indicate a decrease in peak intensity. Green dashed lines represent time points of phytoplankton blooms. (b) The results are within the statistical error determined by performing the same test on a randomized data set.

2.4 Discussion

At first view, our results seem to contradict some previous observations. In a similar (though much shorter) experiment in Svalbard, elevated pCO_2 conditions enhanced primary production (Engel et al., 2013), and an associated accumulation of DOC was indirectly calculated with a budget approach (Czerny, 2013). These results were interpreted as evidence for enhanced DOC production and accumulation under high pCO_2 conditions (Riebesell et al., 2013a). However, bacterial and extracellular enzyme activities were also stimulated in this (Piontek et al., 2013) and other (Endres et al., 2013; Grossart et al., 2006) studies which may have enhanced the turnover of DOM. Consistent with this explanation, in a different mesocosm study in Norway (Endres et al., 2014), bacterial abundance was 28% higher in CO_2-manipulated mesocosms compared to controls, and DOC concentrations did not differ between treatments, even though pCO_2 levels in this experiment exceeded three times those in our approach. In other experiments, no differences were observed for DOC and DON concentrations under ocean acidification conditions (Engel et al., 2014, 2004; MacGilchrist et al., 2014). The apparent contradiction between the study in Svalbard (Riebesell et al., 2013a) and most other studies may possibly be due to a hidden pool of very quickly cycling DOM compounds that were turned over on short time scales (Czerny et al., 2013; Engel et al., 2013) and were not resolved by the sampling scheme applied in most studies, including ours. Enhanced production is likely closely coupled to removal of DOM components. Thus, ocean acidification may not have a detectable effect on the concentration of the most labile compounds, because enhanced production is quickly counteracted by stimulated consumption. Aggregation of polysaccharide-rich particles such as transparent exopolymer particles (TEP) may be another mechanism for fast removal of excess freshly produced DOM (Engel et al., 2014).

More importantly in the context of our study, CO_2 induced changes in the quick cycling of labile DOM, if present, did not affect the composition of the remaining DOM pool after a phytoplankton bloom phase. This may not be surprising considering the long turnover times of some of the components, but small scale mesocosm experiments have provided evidence that compounds that are molecularly undistinguishable from the most refractory DOM in the deep ocean can

be produced via microbial activity within months (Osterholz et al., 2015). Together, our findings are consistent with the scenario that ocean acidification has an insignificant impact on DOM that is turned over on time scales of weeks to months and longer. This component of DOM is of highest importance in the context of carbon sequestration because it has the potential to accumulate in the global ocean over historic time scales. Elevated pCO_2 levels did not affect the molecular composition of DOM despite a clear succession of molecular composition over time in response to microbial activity. This finding suggests that elevated pCO_2 levels have no major impact on the composition of DOM in a coastal setting through changes in the functioning of the microbial loop.

One major difference in the experimental design from previous mesocosm studies is that in our study the community had more time to acclimate to elevated pCO_2 before the seasonal increase in primary production. This possibly allowed the microbial community to establish a balance between DOM production and consumption, which may not have been achieved in earlier studies. This is supported by the fact that most coastal environments naturally exhibit fluctuations in pCO_2. The Gullmar Fjord is no exception. Furthermore, responses to the relatively moderate levels of pCO_2 that were chosen for our study could simply be too small to be detected.

In the most productive areas of the world oceans, the assimilation and release of CO_2 by planktonic communities causes a natural fluctuation of seawater pH on short time scales to which microbial communities are adapted. Our results indicate that microbial communities may also be resilient to gradual changes in seawater pH as predicted for the next century, at least with respect to the concentration and molecular composition of seasonally accumulated DOM. Overall, the results of our study strongly support the scenario that ocean acidification alone will not change the amount of coastal net primary production that is funneled into the recalcitrant DOM pool via microbial activity.

2.5 Materials and Methods

2.5.1 Experimental setup

The mesocosm study was performed between 8 March and 24 June 2013 (109 days) at the University of Gothenburg Sven Lovén Centre for Marine Sciences in Kristineberg, Sweden. Ten cylindrical Kiel Off-Shore Mesocosms for Future Ocean Simulations (KOSMOS) were deployed in the Gullmar Fjord at 58°16'N 11°29'E. Water depth at this site was about 50 m, and the average water temperature increased from 0.5 °C in March to 16 °C in June. The mesocosms consisted of floating frames with attached polyurethane bags of about 50 m^3 volume, 2 m diameter, and 17 m water depth. All bags were filled at the same time with seawater from the fjord, which was passed through a 3 mm net during filling to keep a natural plankton community, but excluding larger organisms. The average salinity was 29.3 inside the mesocosms. Details about the technical features and experimental setup of the KOSMOS are described by Riebesell et al. (2013) and Schulz et al. (2013). To simulate future ocean acidification conditions, five mesocosm replicates were manipulated to a target pCO_2 level of 900 µatm. The other five mesocosms were used as controls at ambient pCO_2 values of initially 400 µatm. The manipulation with carbon dioxide was done by stepwise addition of CO_2-saturated seawater. The pH ranged from 7.82 to 8.03 for the controls and from 7.46 to 7.85 for the enriched mesocosms. All mesocosms were open to the atmosphere, and thus, CO_2-enriched water had to be added at several time points to keep the pCO_2 level close to the target. The different treatments were randomly distributed over the mooring arrays. Mesocosm bags were frequently cleaned to avoid wall growth and allow natural light penetration through the water column.

2.5.2 Sample preparation and bulk analysis

Representative of mesocosms and the surrounding fjord water were collected from boats every other day at 0900 to 1100 local time, starting from the day before the first CO_2 manipulation (day −1). We used 5 L integrating water samplers (IWS; Hydrobios), giving a representative sample for the upper 15 m of the water column. pH was measured with a spectrophotometer (Agilent 8453) with 1 cm cuvettes at 25 °C following the protocol of Clayton and Byrne (1993). The data were corrected

to in situ temperature and reported on the total pH scale. Chlorophyll *a* concentrations were determined by filtration of 250 to 500 mL of sample onto GF/F filters (0.7 µm, Whatman). The filters were stored at −80 °C for 24 hours and homogenized in 90% acetone with glass beads in a cell mill. The centrifugate was analyzed fluorometrically for chlorophyll *a* (Welschmeyer, 1994).

For DOC and TDN analysis, samples were collected in duplicate and directly filtered from the IWS sampler via gravity filtration through 0.7 µm GF/F precombusted (400 °C, 4 hours) glass microfiber filters (Whatman) into precombusted 20 mL glass vials with acid-rinsed Teflon caps (Wheaton). Immediately after filtration, the samples were acidified with HCl (25%, analytical grade, Carl Roth) to pH 2. DOC and TDN concentrations were analyzed using a high-temperature catalytic oxidation method (Qian and Mopper, 1996) with a Shimadzu (Japan) TOC-VCPH/CPN Total Organic Carbon Analyzer, equipped with an ASI-V autosampler and a TNM-1 module for the determination of TDN. Measurement accuracy was controlled with the Deep Atlantic Seawater Reference material (DSR, D.A. Hansell, University of Miami, Miami, FL) for every run. The error for DOC and TDN analysis was, on average, 4 and 6%, respectively. To identify contaminated samples, we calculated the deviation between the replicates for each mesocosm every sampling day. If the DOC concentrations deviated by 30% or more between replicates, the one with higher DOC concentration was considered to be contaminated and excluded from the data set. The data were then pooled for control and high pCO_2 mesocosms and checked for outliers (Dixon-Dean test, $p < 0.05$). Average values were calculated for each mesocosm and time point from the remaining data. The same procedure was applied to the measured TDN concentrations. We calculated DON concentrations from TDN by subtracting the concentration of all DIN species from TDN. DIN is the sum of nitrate, nitrite, and ammonium concentrations that were measured using a segmented flow analyzer (SEAL QuAAtro). For graphical data presentation of chlorophyll *a*, DOC, and DOC/DON concentrations, values outside of 1.5 times the interquartile range above the upper and below the lower quartiles were displayed as outliers. A running average was calculated for DOC and DOC/DON concentrations by calculating the average of the combined values from the respective sampling day, the day before, and the day after.

Samples for molecular characterization were collected from the IWS sampler into 2 L acid-rinsed polycarbonate bottles (Nalgene). The samples were transported to shore and stored at in situ water temperatures in the dark until processing on the same day. After filtration through 0.7 µm GF/F glass microfiber filters (Whatman) with manual vacuum pumps (< 200 mbar), the samples were acidified with HCl (25%, analysis grade, Carl Roth) to pH 2. Samples were stored at 4 °C in the dark. The samples were extracted by solid-phase extraction (SPE) following the protocol of Dittmar et al. (2008). We used a commercially available modified styrene divinylbenzene polymer resin (PPL, 1 g, Agilent). Before use, the cartridges were soaked in methanol [high-performance liquid chromatography (HPLC) grade, Sigma-Aldrich] overnight and sequentially rinsed with methanol and 0.01 mol L^{-1} HCl in ultrapure water. After being loaded onto the cartridges, the samples were rinsed with 0.01 mol L^{-1} HCl to remove remaining salts and dried with nitrogen gas (analysis grade, Air Liquide). The extracted DOM was eluted with 6 mL of methanol and stored in precombusted glass vials at −20 °C. To determine extraction efficiency, aliquots of the methanol extract were dried and redissolved in ultrapure water. The average extraction efficiency was 45 ± 6% on a carbon basis. Especially colloidal matter and small ionic compounds may escape extraction and are likely lost from our analytical window. Procedural blanks were prepared by processing ultrapure water in the same way as the DOM samples. DOC concentrations in the resulting extracts were below the detection limit (Stubbins and Dittmar, 2012).

2.5.3 Molecular characterization

DOM consists of a multitude of compounds in very small concentrations, and thus, a separation of the single compounds surpasses the technical resolution of conventional analytical techniques (Dittmar et al., 2007; Koch et al., 2008; Woods et al., 2011). As a consequence, less than 7% of the compounds in DOM can be assigned to molecularly defined building blocks such as sugars and amino acids (Kaiser and Benner, 2009). Ultrahigh-resolution FT-ICR-MS has revolutionized the field of DOM research because it provides chemical information on thousands of individual molecules (Sleighter and Hatcher, 2007). More than tens of thousands of single compounds in DOM can be resolved in the mass spectra and assigned to

molecular formulae owing to the ultrahigh mass accuracy and resolution (Koch et al., 2005; Dittmar and Paeng, 2009).

MS analysis of SPE extracts was done with FT-ICR-MS on a 15 T Solarix system (Bruker Daltonics) equipped with an electrospray ionization source (ESI, Bruker Apollo II) applied in negative ionization mode. Methanol extracts were diluted with ultrapure water and methanol to give a final concentration of 20 mg C L^{-1} in a 1:1 mixture (v/v) of methanol (HPLC grade, Sigma-Aldrich) and ultrapure water. For each measurement, 500 scans were accumulated in a mass window of 150 to 2000 Da. Spectra were internally calibrated with a reference mass list, using the Bruker Daltonics Data Analysis software package. The mass error of the calibration was < 0.06 ppm for all samples. In addition to the exclusion criterion of a signal-to-noise (S/N) ratio of 4 or higher, small peaks with S/N ratios of < 20 that occurred in less than 20% of the samples were also excluded. All 209 samples from a total of 19 time points (mesocosms and fjord samples) were analyzed by FT-ICR-MS in random order. Four samples were excluded from further data evaluation because of contaminations. To test the reproducibility and stability of the FT-ICR-MS analysis, we used DOM extract of North Equatorial Pacific Intermediate Water (NEqPIW) as in-house reference sample (Green et al., 2014). We used MatLab routines developed by our working group for molecular formula assignment and further data processing. Only peaks with S/N ratios of 4 or higher that fulfilled the criteria stated by Koch et al. (2007) were considered. All molecules were detected as singly charged ions. Molecular formulae were assigned to these masses according to the criteria set by Koch et al. (2007) and Rossel et al. (2013), with consideration of the elements C, H, O, N, S, and P. As with any analytical technique, FT-ICR-MS has its analytical detection window. The analytical settings were chosen to detect as many compounds as possible to obtain the most informative picture of DOM molecular composition. Nevertheless, the principle of FT-ICR-MS prevents the detection of very small compounds (< 150 Da) or colloidal matter.

2.5.4 Statistical analysis of FT-ICR-MS data

For multivariate statistical analyses, we considered the same number of detected masses for each sample. For this selection, the peak intensities were sorted

in a ranked intensity order, independent for each sample, and the same number of masses with the most intense peaks was selected. Fjord samples were treated independently. The data were then normalized to the sum of peak intensities and finally used for statistical analysis. Variations in the molecular DOM composition were characterized by PCA. To identify links between the scores for the principal components and environmental parameters (type of CO_2 treatment and concentrations of chlorophyll *a*, ammonium, nitrate, nitrite, phosphate, silicate, and DOC), a second PCA was calculated from the data of time points, to which the respective environmental parameters were available. On this basis, a Pearson correlation (two-tailed) was done (Supplementary materials Fig. S2.1). Furthermore, we tested the data from both CO_2-enriched and control mesocosms over the entire time period by PerMANOVA (Anderson, 2006). The average distance to each group centroid was calculated on the basis of a matrix of Euclidean distances. This distance was equivalent to the average distance among all pairwise group member combinations and served as a measure of dispersion. The differences in dispersions of both groups were then tested for significance by permutation. Furthermore, the intensities of the molecular formulae of both groups were tested for differences at each individual sampling time point as well as at the start of the study by a Student's *t* test ($p < 0.001$). Randomized data were generated in the intensity ranges of the peaks occurring in the analyzed spectra. All statistical analyses were done with the software package R (version 3.0.2, package "vegan") (Oksanen et al., 2013). The MS signal intensity of each detected molecular formula, as well as DOC and chlorophyll *a* concentrations and molar DOC/DON ratios of samples from CO_2-enriched and control mesocosms, was tested for differences by Student's *t* test.

2.6 Acknowledgements

We thank the team of the Kristineberg mesocosm study in 2013 and particularly A. Ludwig for the logistical organization and coordination. We also thank the staff of the Sven Lovén Centre for Marine Sciences, University of Gothenburg, for hosting our team, and the captain and crew of R/V Alkor for support with transport and deployment of mesocosms. We thank S. Muellenmeister and I. Köster for help during sampling, and K. Klaproth, M. Friebe, and I. Ulber for technical support

with FT-ICR-MS and DOC/TDN analysis. We also thank A. Ludwig for the analysis of chlorophyll *a* concentrations, and L. G. Anderson and Y. Ericson for the analysis of dissolved inorganic carbon and total alkalinity. Nutrient concentrations were provided by E. Achterberg, M. Esposito, and J. Bellworthy. We thank E. Achterberg for comments on the manuscript.

Financial support for this study was provided by the German Ministry of Education and Research (BMBF, FKZ 03F0655D) through the BIOACID (Biological Impacts of Ocean ACIDification) project. Further financial support was provided by the Association of European Marine Biological Laboratories (ASSEMBLE, grant no. 227799) and the Heinz Neumüller Foundation.

2.7 References and Notes

Anderson, M.J., 2006. Distance-based tests for homogeneity of multivariate dispersions. Biometrics 62, 245−253.

Bellerby, R.G.J., Schulz, K.G., Riebesell, U., Neill, C., Nondal, G., Heegaard, E., et al., 2008. Marine ecosystem community carbon and nutrient uptake stoichiometry under varying ocean acidification during the PeECE III experiment. Biogeosciences 5, 1517−1527.

Caldeira, K., Wickett, M.E., 2003. Oceanography: Anthropogenic carbon and ocean pH. Nature 425, 365.

Carlson, C.A., Del Giorgio, P.A., Herndl, G.J., 2007. Microbes and the dissipation of energy and respiration: From cells to ecosystems. Oceanography 20, 89−100.

Clayton, T.D., Byrne, R.H., 1993. Spectrophotometric seawater pH measurements: Total hydrogen ion concentration scale calibration of *m*-cresol purple and at-sea results. Deep-Sea Res. Pt. I 40, 2115−2129.

Czerny, J., Schulz, K.G., Boxhammer, T., Bellerby, R.G.J., Büdenbender, J., Engel, A., et al., 2013. Implications of elevated CO_2 on pelagic carbon fluxes in an Arctic mesocosm study–An elemental mass balance approach. Biogeosciences 10, 3109−3125.

Del Giorgio, P.A., Duarte, C., 2002. Respiration in the open ocean. Nature 420, 379−384.

Dittmar, T., 2015. Reasons behind the long-term stability of dissolved organic matter, in: Hansell, D.A., Carlson, C.A., (Eds.), The biogeochemistry of marine dissolved organic matter, 2nd edition. Academic Press, Burlington, pp. 369−388.

Dittmar, T., Koch, B.P., Hertkorn, N., Kattner, G., 2008. A simple and efficient method for the solid-phase extraction of dissolved organic matter (SPE-DOM) from seawater. Limnol. Oceanogr. Methods 6, 230−235.

Dittmar, T., Paeng, J., 2009. A heat-induced molecular signature in marine dissolved organic matter. Nat. Geosci. 2, 175−179.

Dittmar, T., Whitehead, K., Minor, E.C., Koch, B.P., 2007. Tracing terrigenous dissolved organic matter and its photochemical decay in the ocean by using liquid chromatography/mass spectrometry. Mar. Chem. 107, 378−387.

Endres, S., Galgani, L., Riebesell, U., Schulz, K.G., Engel, A., 2014. Stimulated bacterial growth under elevated pCO_2: Results from an off-shore mesocosm study. PLOS One **9**, e99228.

Endres, S., Unger, J., Wannicke, N., Nausch, M., Voss, M., Engel, A., 2013. Response of *Nodularia spumigena* to pCO_2–Part 2: Exudation and extracellular enzyme activities. Biogeosciences 10, 567−582.

Engel, A., Borchard, C., Piontek, J., Schulz, K.G., Riebesell, U., Bellerby, R., 2013. CO_2 increases ^{14}C primary production in an Arctic plankton community. Biogeosciences 10, 1291−1308.

Engel, A., Delille, B., Jacquet, S., Riebesell, U., Rochelle-Newall, E., Terbrüggen, A., et al., 2004. Transparent exopolymer particles and dissolved organic carbon production by *Emiliania huxleyi* exposed to different CO_2 concentrations: A mesocosm experiment. Aquat. Microb. Ecol. 34, 93−104.

Engel, A., Piontek, J., Grossart, H.-P., Riebesell, U., Schulz, K.G., Sperling, M., 2014. Impact of CO_2 enrichment on organic matter dynamics during nutrient induced coastal phytoplankton blooms. J. Plankton Res. 36, 641−657.

Eppley, R.W., Peterson, B.J., 1979. Particulate organic matter flux and planktonic new production in the deep ocean. Nature 282, 677−689.

Green, N.W., Perdue, E.M., Aiken, G.R., Butler, K.D., Chen, H., Dittmar, T., et al., 2014. An intercomparison of three methods for the large-scale isolation of oceanic dissolved organic matter. Mar. Chem. 161, 14−19.

Grossart, H.-P., Allgaier, M., Passow, U., Riebesell, U., 2006. Testing the effect of CO_2 concentration on the dynamics of marine heterotrophic bacterioplankton. Limnol. Oceanogr. 51, 1−11.

Hansell, D.A., 2013. Recalcitrant dissolved organic carbon fractions. Ann. Rev. Mar. Sci. 5, 421−445.

Hansell, D.A., Carlson, C.A., 1998. Net community production of dissolved organic carbon. Global Biogeochem. Cycles 12, 443−453.

Hansell, D.A., Carlson, C.A., Repeta, D.J., Schlitzer, R., 2009. Dissolved organic matter in the ocean: A controversy stimulates new insights. Oceanography 22, 202−211.

Holm, S., 1979. A simple sequentially rejective multiple test procedure. Scand. J. Stat. 6, 65−70.

IPCC, 2013. Climate Change 2013: The Physical Science Basis. Contribution of Working Group 1 to the Fifth Assessment Report of the Intergovernmental Panel on Climate Change, in: Stocker, T.F., Qin, D., Plattner, G.-K., Tignor, M., Allen, S.K., Boschung, J., Nauels, A., Xia, Y., Bex, V., Midgley, P.M., (Eds.), Cambridge University Press, Cambridge and New York, p. 1096.

Jiao, N., Herndl, G.J., Hansell, D.A., Benner, R., Kattner, G., Wilhelm, S.W., et al., 2010. Microbial production of recalcitrant dissolved organic matter: Long-term carbon storage in the global ocean. Nat. Rev. Microbiol. 8, 593−599.

Kaiser, K., Benner, R., 2009. Biochemical composition and size distribution of organic matter at the Pacific and Atlantic time-series stations. Mar. Chem. 113, 63−77.

Koch, B.P., Dittmar, T., Witt, M., Kattner, G., 2007. Fundamentals of molecular formula assignment to ultrahigh resolution mass data of natural organic matter. Anal. Chem. 79, 1758−1763.

Koch, B.P., Ludwichowski, K.-U., Kattner, G., Dittmar, T., Witt, M., 2008. Advanced characterization of marine dissolved organic matter by combining reversed-phase liquid chromatography and FT-ICR-MS. Mar. Chem. 111, 233−241.

Koch, B.P., Witt, M., Engbrodt, R., Dittmar, T., Kattner, G., 2005. Molecular formulae of marine and terrigenous dissolved organic matter detected by electrospray ionization Fourier transform ion cyclotron resonance mass spectrometry. Geochim. Cosmochim. Acta 69, 3299−3308.

MacGilchrist, G.A., Shi, T., Tyrell, T., Richier, S., Moore, C.M., Dumousseaud, C., et al., 2014. Effects of enhanced pCO_2 levels on the production of dissolved organic carbon and transparent exopolymer particles in short-term bioassay experiments. Biogeosciences 11, 3695−3706.

Mari, X., 2008. Does ocean acidification induce an upward flux of marine aggregates? Biogeosciences 5, 1023−1031.

Nuzzo, R., 2014. Scientific method: Statistical errors. Nature 506, 150−152.

Ogawa, H., Amagai, Y., Koike, I., Kaiser, K., Benner, R., 2001. Production of refractory dissolved organic matter by bacteria. Science 292, 917−920.

Oksanen, J., Blanchet, F.G., Kindt, R., Legendre, P., Minchin, P.R., O'Hara, R.B., et al., 2013. Vegan: Community ecology package. R package version 2.0-10. http://CRAN.R-project.org/package=vegan.

Osterholz, H., Niggemann, J., Giebel, H.-A., Simon, M., Dittmar, T., 2015. Inefficient microbial production of refractory dissolved organic matter in the ocean. Nat. Commun. 6, 7422.

Piontek, J., Borchard, C., Sperling, M., Schulz, K.G., Riebesell, U., Engel, A., 2013. Response of bacterioplankton activity in an Arctic fjord system to elevated pCO_2: Results from a mesocosm perturbation study. Biogeosciences 10, 297−314.

Piontek, J., Lunau, M., Händel, N., Borchard, C., Wurst, M., Engel, A., 2010. Acidification increases microbial polysaccharide degradation in the ocean. Biogeosciences 7, 1615−1624.

Qian, J., Mopper, K., 1996. Automated high-performance, high-temperature combustion total organic carbon analyzer. Anal. Chem. 68, 3090−3097.

Riebesell, U., Czerny, J., von Bröckel, K., Boxhammer, T., Büdenbender, J., Deckelnick, M., et al., 2013. Technical note: A mobile sea-going mesocosm system– New opportunities for ocean change research. Biogeosciences 10, 1835−1847.

Riebesell, U., Gattuso, J.-P., Thingstad, T.F., Middelburg, J.J., 2013a. Arctic ocean acidification: Pelagic ecosystem and biogeochemical responses during a mesocosm study. Biogeosciences 10, 5619−5626.

Riebesell, U., Körtzinger, A., Oschlies, A., 2009. Sensitivities of marine carbon fluxes to ocean change. Proc. Natl. Acad. Sci. U.S.A. 106, 20602−20609.

Riebesell, U., Schulz, K.G., Bellerby, R.G.J., Botros, M., Fritsche, P., Meyerhöfer, M., et al., 2007. Enhanced biological carbon consumption in a high CO_2 ocean. Nature 450, 545−548.

Rossel, P.E., Vähätalo, A.V., Witt, M., Dittmar, T., 2013. Molecular composition of dissolved organic matter from a wetland plant (*Juncus effusus*) after photochemical and microbial decomposition (1.25 yr): Common features with deep sea dissolved organic matter. Org. Geochem. 60, 62−71.

Sabine, C.L., Feely, R.A., Gruber, N., Key, R.M., Lee, K., Bullister, J.L., et al., 2004. The oceanic sink for anthropogenic CO_2. Science 305, 367−371.

Schippers, P., Lürling, M., Scheffer, M., 2004. Increase of atmospheric CO_2 promotes phytoplankton productivity. Ecol. Lett. 7, 446−451.

Schulz, K.G., Bellerby, R.G.J., Brussaard, C.P.D., Büdenbender, J., Czerny, J., Engel, A., et al., 2013. Temporal biomass dynamics of an Arctic plankton bloom in response to increasing levels of atmospheric carbon dioxide. Biogeosciences 10, 161-180.

Sleigther, R.L., Hatcher, P.G., 2007. The application of electrospray ionization coupled to ultrahigh resolution mass spectrometry for the molecular characterization of natural organic matter. J. Mass. Spectrom. 42, 559−574.

Stubbins, A., Dittmar, T., 2012. Low volume quantification of dissolved organic carbon and dissolved nitrogen. Limnol. Oceanogr. Methods 10, 347−352 .

Waite, A.M., Gustafsson, Ö., Lindahl, O., Tiselius, P., 2005. Linking ecosystem dynamics and biogeochemistry: Sinking fractionation of organic carbon in a Swedish fjord. Limnol. Oceanogr. 50, 658−671.

Welschmeyer, N.A., 1994. Fluorometric analysis of chlorophyll *a* in the presence of chlorophyll *b* and pheopigments. Limnol. Oceanogr. 39, 1985−1992.

Woods, G.C., Simpson, M.J., Koerner, P.J., Napoli, A., Simpson, A.J., 2011. HILIC-NMR: Toward the identification of individual molecular components in dissolved organic matter. Environ. Sci. Technol. 45, 3880−3886.

2.8 Supplementary materials

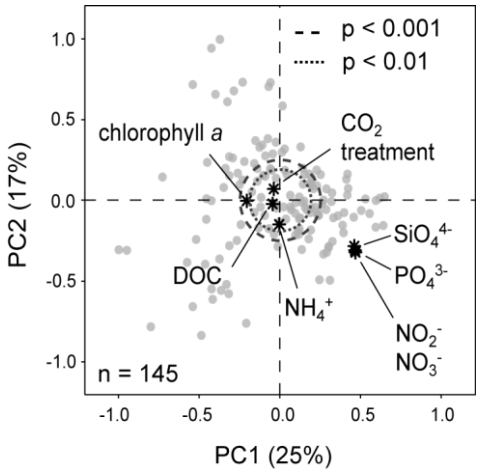

Figure S2.1 Pearson correlation of environmental parameters with the scores of the principal component analysis. Gray dots indicate the samples, black marks represent the correlation coefficients of environmental parameters with the respective principal component. The dashed circles mark the area inside which the correlation coefficients are not significant.

A Pearson correlation of the components from PCA with the environmental data (chlorophyll *a*, DOC concentration, CO_2-treatment, ammonium NH_4^+, silicate SiO_4^{4-}, phosphate PO_4^{3-}, nitrite NO_2^- and nitrate NO_3^-) revealed that PC1 correlated inversely with chlorophyll *a* concentration ($p < 0.01$, see Supplementary materials Fig. S2.1) but not with *P*CO_2 treatment. A positive correlation of PC1 was observed for SiO_4^{4-}, PO_4^{3-}, NO_2^-, NO_3^- ($p < 0.001$). Unlike the other nutrients, NH_4^+ did not correlate with PC1. The second principal component (PC2) did not correlate with chlorophyll *a* but with SiO_4^{4-}, PO_4^{3-}, NO_2^- and NO_3^- ($p < 0.001$). In other words, the molecular composition of DOM, represented by 7360 molecular features, significantly varied over time as a function of nutrient concentrations, and partially chlorophyll *a*.

Manuscript II:

Dissolved organic matter dynamics during an oligotrophic ocean acidification experiment using large-scale mesocosms

Maren Zark,[1] Nadine Kerstin Broda,[1] Ulf Riebesell,[2] Thorsten Dittmar[1]

This chapter corresponds to a full manuscript that was prepared for submission to *Limnology and Oceanography*.

[1] Institute for Chemistry and Biology of the Marine Environment (ICBM), Research Group for Marine Geochemistry (ICBM-MPI Bridging Group), Carl von Ossietzky University of Oldenburg, Carl-von-Ossietzky-Straße 9-11, 26129 Oldenburg, Germany.

[2] GEOMAR Helmholtz Centre for Ocean Research Kiel, Düsternbrooker Weg 20, 24105 Kiel, Germany.

The manuscript “Dissolved organic matter dynamics during an oligotrophic ocean acidification experiment using large scale mesocosms” (Manuscript II) addresses the impact of elevated CO_2 concentrations in an oligotrophic area in the subtropical North Atlantic Ocean. A mesocosm study was performed with target pCO_2 values ranging from 600 to 2000 µatm in order to determine threshold concentrations for potential CO_2 effects. Indications were observed for enhanced DOC accumulation but no changes in the molecular composition of DOM could be detected. All authors were involved in conceiving the study. M. Zark, U. Riebesell, and N. K. Broda took the samples. M. Zark and N. K. Broda conducted solid-phase extractions. FT-ICR-MS analysis was performed by M. Zark. Statistical analyses was done by M. Zark and T. Dittmar. M. Zark wrote the manuscript with comments from T. Dittmar and N. K. Broda.

The manuscript is close to submission to *Limnology and Oceanography* and presented with adjusted formatting according to the style of this thesis.

3.1 Abstract

Dissolved organic matter (DOM) represents one of the biggest active carbon pools on Earth. Despite the potential impacts on the global biogeochemical carbon cycle, effects of environmental stressors such as ocean acidification on the DOM pool are yet not well understood. It is likely that responses vary among different marine ecosystems depending on factors such as the resilience of the host microbial communities towards changes in pH. Previous experiments investigating ocean acidification effects on the DOM pool under natural conditions were mostly conducted in coastal areas. In this study, effects of ocean acidification on the DOM pool in the subtropical North Atlantic Ocean were investigated during an oligotrophic phase and after a succession of phytoplankton blooms that were initiated by artificial upwelling. We simulated future ocean conditions in large-scale mesocosms with step-wise increasing target pCO_2 levels from 600 to 2000 µatm and monitored the DOM molecular composition using ultrahigh-resolution mass spectrometry. The treatments were almost not distinguishable until the onset of a phase of recycled production towards the end of the experiment. Despite indications for enhanced DOC accumulation, we observed no significant effect of ocean acidification on the concentration and molecular composition of DOM. We further found a pool of similar compounds which were produced in all individual treatments during phytoplankton blooms and accumulate over time. Our results provide new insights into the dynamics of DOM production, under acidifying conditions and in general, in a natural oligotrophic ecosystem.

3.2 Introduction

The global oceans currently take up carbon dioxide at a magnitude of about 25% of total anthropogenic CO_2 emissions (Le Queré et al., 2013). Once dissolved in seawater, CO_2 forms carbonic acid. This process is commonly referred to as ocean acidification and assumed that CO_2 emissions continue to rise at current rates, surface ocean pH could be reduced by 0.7 units in total (Caldeira and Wickett, 2003). Ocean acidification may cause impacts on marine organisms, the structure of phytoplankton communities, and the biogeochemical cycling of elements (Dutkiewicz et al., 2015; Kroeker et al., 2010; Riebesell et al., 2007). One of the important players in the marine carbon cycle is dissolved organic matter (DOM), which holds a similar amount of carbon as all living biomass on earth (Hedges, 1992). This huge carbon pool is mainly produced by marine primary production and fuels the microbial loop, the bottom of the marine food web (Azam et al., 1983; Carlson et al., 2007). Changes in concentration or composition of this pool have the potential to severely impact the biogeochemical carbon cycle.

Due to stimulation of marine primary production under ocean acidification conditions (Riebesell, 2000), it is likely that enhanced carbon dioxide partial pressure (pCO_2) fuels dissolved organic carbon (DOC) production, which was also shown in previous experiments (Czerny et al., 2013; Engel et al., 2013). However, other findings point towards no effect or even decreased DOC production (Engel et al., 2014; MacGilchrist et al., 2014; Yoshimura et al., 2010) that could be explained by stimulated microbial degradation (Grossart et al., 2006; Piontek et al., 2010). In a long-term mesocosm study in a coastal environment off the coast of Sweden, ocean acidification effects on DOM composition were analyzed for the first time on a molecular fingerprint level. Elevated pCO_2 as projected for the end of the century had no effect on the DOM pool size and molecular composition (Zark et al., 2015). Assumingly, the occurrence of effects is closely coupled to the environmental settings and there may exist a threshold pCO_2 level for many responses. Further, the resilience of the microbial community plays an important role as pH is partly dependent on net community production and shows different variabilities among ecosystems (Joint et al., 2011). Microbes in an oligotrophic

ocean have experienced less variability in pH than in coastal regions and are presumably less adapted (Joint et al., 2011; Salisbury et al., 2008).

In this study, we aim to identify the effects of ocean acidification on the DOM molecular composition in an oligotrophic ecosystem. There, changes in DOM accumulation could lead to significant impacts on the marine carbon cycle since oligotrophic areas represent ~30% of the global oceanic primary production (Longhurst et al., 1995). It remains vague if the yet observed effects on DOM will be similar in these systems because most large scale field experiments were conducted under nutrient replete conditions (Maugendre et al., 2015a). We performed a large scale pelagic mesocosm experiment in the subtropical Atlantic Ocean. Nine sea-going mesocosm systems were deployed off the coast of Gran Canaria, two of them serving as control with ambient pCO_2 levels and the other seven were artificially enriched with CO_2. A gradient design was chosen from target levels of 600 µatm to a maximum 2000 µatm pCO_2 in order to test for threshold effects. The maximum amount of CO_2 added may be reached at some time point within the next centuries, depending on the amount of fossil fuel emissions in the future (Winkelmann et al., 2015). We monitored the changes in molecular DOM composition and concentration over the course of two phytoplankton blooms.

3.3 Materials and methods

3.3.1 Experimental set-up

The mesocosm study was performed from 28 September to 25 November 2014 (59 days) at the Plataforma Oceánica de Canarias (PLOCAN) on Gran Canaria, Spain. Nine cylindrical Kiel Off-Shore Mesocosms for Future Ocean Simulations (KOSMOS) were deployed in the Bay of Gando at 27° 55.679' N 15° 21.924 W (Fig. 3.1). Water depth at this site is approximately 20 m and the average water temperature decreased from 24.5 °C in September to 22.2 °C in November. Mesocosms consisted of floating frames with polyurethane bags of ca. 40 m^3 volume, 2 m diameter, and 15 m water depth. All bags were filled at the same time with seawater from the Atlantic. To keep a natural plankton community but exclude larger organisms the water was passed through a 3 mm net. Salinity was on average 37.4 inside the mesocosms and slightly increasing throughout the experiment due

to evaporation (average 39 L day^{-1}). Details about technical features and experimental setup of the KOSMOS are described in Riebesell et al. (2013) and Schulz et al. (2013).

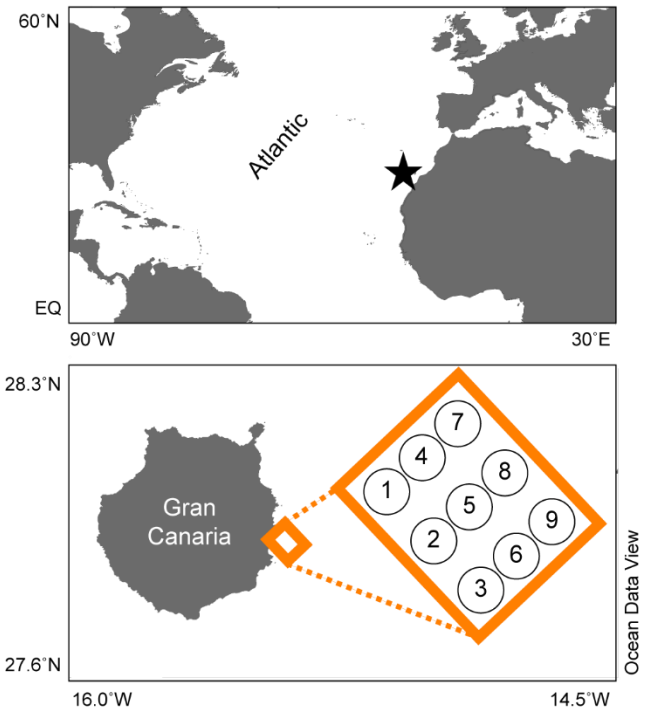

Figure 3.1 Map of study site in the Atlantic Ocean. Mesocosms were moored in the Bay of Gando, off the coast of Gran Canaria (Spain).

Mesocosms were manipulated with CO_2 to reach target pCO_2 levels of 600, 800, 1000, 1250, 1500, 1750, and 2000 µatm. The remaining two mesocosms were used as controls at ambient pCO_2 values of initially 400 µatm. Manipulation with carbon dioxide was done by stepwise addition of CO_2 saturated seawater. The pH ranged from 8.08 to 8.49 for the controls and from 7.69 to 8.43 for the enriched mesocosms. All mesocosms were open to the atmosphere and CO_2 enriched water had to be added at several time points to keep the pCO_2 level close to the target (days 0, 2, 4, 6, 21, and 38). The different treatments were randomly distributed over the mooring arrays. Mesocosm bags were cleaned frequently to avoid wall growth and allow natural light penetration through the water column. To simulate a naturally occurring upwelling event we added about 8000 L deep-sea water to each of the systems on day 23. The water was collected at day 22 from 650 m depth

(62 µmol L^{-1} DOC, 17 µmol L^{-1} combined NO_3^- and NO_2^-) with the help of a novel custom-built system using a large plastic bag. It has to be noted that the mesocosm with a treatment of 1500 µatm was damaged on day 26 and had to be partly excluded from the analysis.

3.3.2 Sample preparation and bulk analysis

Representative samples were collected for both, the mesocosms and the surrounding Atlantic water, every other day from boats between 0900 and 1100 local time, starting from the day after the mesocosm bags were closed (day -3). We used 5 L integrating water samplers (IWS, Hydrobios) giving a representative sample for the upper 13 m of the water column. The pH measurements were carried out spectrophotometrically (Agilent 8453) with 1 cm cuvettes at 25 °C after Clayton and Byrne (1993). The data were corrected to in-situ temperature and reported on the total pH scale. Chlorophyll *a* concentrations were determined by filtration of 250 – 500 mL of sample onto GF/F filters (0.7 µm, Whatman). Filters were stored at –80 °C for 24 h, homogenized in 90% acetone using glass beads in a cell mill. The centrifugate was analyzed fluorometrically for chlorophyll *a* (Welschmeyer, 1994).

For dissolved organic carbon (DOC) and total dissolved nitrogen (TDN) analysis, samples were collected into pre-rinsed 250 mL polycarbonate bottles (Nalgene) in triplicate. The samples were then filtered through a syringe with 0.7 µm GF/F pre-combusted (400 °C, 4 h) glass microfiber filters (Whatman) into pre-combusted 20 mL glass vials (400 °C, 4 h) with acid-rinsed Teflon caps (Wheaton). Directly after filtration, we acidified samples with HCl (25%, analysis grade, Carl Roth) to pH 2. The analysis of DOC and TDN concentrations was done via a high-temperature catalytic oxidation method (Qian and Mopper, 1996) using a Shimadzu TOC-VCPH/CPN Total Organic Carbon Analyzer, equipped with ASI-V auto sampler and TNM-1 module for the determination of TDN. The accuracy of the measurement was controlled with Florida Strait Water reference material (D.A. Hansell, University of Miami, Florida) for every run. The error for DOC and TDN analysis was on average 4 and 10%, respectively. Average concentrations were calculated for each mesocosm and time point from triplicates.

We calculated dissolved organic nitrogen (DON) concentrations from TDN by subtracting the concentration of all dissolved inorganic nitrogen species (DIN). DIN is the sum of nitrate, nitrite and ammonium concentrations that were measured using a segmented flow analyzer (SEAL QuAAtro).

Samples for molecular DOM characterization were collected from the IWS sampler into 2 L acid-rinsed polycarbonate bottles (Nalgene). The samples were transported to shore and stored at in situ water temperatures in the dark until processing on the same day. After filtration through 0.7 µm GF/F glass microfiber filters (Whatman) using manual vacuum pumps (< 200 mbar) we acidified samples with HCl (25%, analysis grade, Carl Roth) to pH 2. Samples were stored at 4 °C in the dark until solid phase extraction (SPE) after Dittmar et al. (2008). We used a commercially available modified styrene divinyl benzene polymer resin (PPL, 1 g, Agilent). Prior to use, cartridges were soaked in methanol (HPLC grade, Sigma-Aldrich) overnight, and rinsed sequentially with methanol and 0.01 mol L^{-1} HCl in ultrapure water. After loading the samples onto the cartridges they were rinsed with 0.01 mol L^{-1} HCl to remove remaining salts and dried with nitrogen gas (analysis grade, Air Liquide). The extracted DOM was eluted with 6 mL methanol and stored in pre-combusted glass vials at -20 °C. To determine extraction efficiency, aliquots of the methanol extract were dried and re-dissolved in ultrapure water. The average extraction efficiency was 34 ± 4% on a carbon basis. Especially colloidal matter and small ionic compounds may escape extraction and are likely lost from our analytical window. Procedural blanks were prepared by processing ultrapure water the same way as DOM samples. The detection limit for solid phase extractable DOC (SPE-DOC) was lower than the detection limit for regular DOC samples (Stubbins et al., 2012) due to concentration by a factor of hundred. SPE-DOC concentrations in the resulting blank extracts were slightly above detection limit but did not exceed a concentration level of 12.3 µmol L^{-1}.

3.3.3 Molecular characterization

Mass spectra were obtained on a 15 Tesla Solarix FT-ICR-MS system (Bruker Daltonics) equipped with an electrospray ionization source (ESI, Bruker Apollo II) applied in negative ionization mode. Methanol extracts were diluted with ultrapure

water and methanol to give a final concentration of 15 mg C L^{-1} in a 1:1 mixture (v/v) of methanol (HPLC grade, Sigma-Aldrich) and ultra-pure water. For each measurement we accumulated 500 scans in the mass window of 150 – 2000 Da. We calibrated spectra internally with a reference mass list using the Bruker Daltonics Data Analysis software package. The mass error of the calibration was < 0.06 ppm for all samples. To remove noise we applied a method detection limit following the guidelines of Riedel and Dittmar (2014). Compounds detected in procedural blanks were removed. We further found a group (n = 50) of likely contaminants that continuously increased in all mesocosms, some of them with molecular formulae corresponding to known constituents of sunscreen and detergents. They were excluded from statistical analysis because of the likelihood that the whole group was due to contamination of the mesocsms. In previous mesocosm experiments using the same setup no such contamination did occur (Zark et al., 2015). All data will be published in PANGAEA.

All 89 samples from a total of 10 time points (79 samples from mesocosms and 10 from the Atlantic) were analyzed via FT-ICR-MS in random order. To test the reproducibility and stability of the FT-ICR-MS analysis, we analyzed DOM extract of North Equatorial Pacific Intermediate Water (NEqPIW) twice per day (Green et al., 2014). MATLAB routines developed by our working group were applied for molecular formula assignment and further data processing. All molecules were detected as singly-charged ions and molecular formulae were assigned based on the criteria by Koch et al. (2007) and Rossel et al. (2013), under consideration of the elements C, H, O, N, S, and P.

3.3.4 Statistical analysis of FT-ICR-MS data

For multivariate analysis, we considered the same number of detected masses for each sample in order to exclude small noise signals. For this selection, the signal intensities were sorted in a ranked order, independent for each mesocosm, and the same number of masses with the most intense signals was selected. FT-ICR-MS statistical analyses were based on normalized peak magnitude. Variations in the molecular DOM composition were characterized by principal components analysis (PCA). Additionally, a Bray-Curtis based distance matrix was calculated from all

mesocosms and time points for a general comparison of the molecular diversity between samples. We further calculated Pearson product-moment correlation coefficients r for the correlation of each detected molecular formula with DOC and chlorophyll *a* concentration, based on individual signal intensities. The resulting coefficients for the individual molecular formulae were then used for a follow-up Pearson correlation between the mesocosm units for intercomparison of the DOM dynamics inside each system. All statistical analyses were performed with the software package R (Version 3.0.2, package "vegan", Oksanen et al. 2013).

3.4 Results

3.4.1 DOC production after a phytoplankton bloom induced by artificial upwelling

The temporal succession of phytoplankton blooms was similar for all 9 mesocosms and can be divided into four phases that were driven by different processes. Prior to the addition of CO_2, mesocosms showed similar conditions after a short equilibration period (Phase 0, Fig. 3.2a-c). After CO_2 enrichment, the first phase of the experiment was characterized by oligotrophic conditions (Phase I) with stable chlorophyll *a* concentrations (Fig. 3.2a). An increase in DOC concentrations was observed (Fig. 3.2b) from 88 ± 5 µmol L^{-1} on day -1 to 112 ± 5 µmol L^{-1} on day 23 (mean ± SD), which was not related to evaporation. This trend was assumingly caused by the lack of lateral mixing and not observed for the samples from the Atlantic where DOC can be removed by horizontal transport. Immediately after the start of Phase II, with addition of nutrient-rich deep-sea water, chlorophyll *a* rapidly increased in all mesocosms (Fig. 3.2a) until a maximum of 4.6 µg L^{-1} was reached on day 28. This concentration is within the range of regular chlorophyll *a* maxima in winter months and was thus typical for the subtropic oligotrophic Atlantic at this time of the year (Neuer et al., 2006). This first bloom was dominated by diatoms and dinoflagellates as the most abundant species (L. Bach, pers. comm.). A sharp decrease of DOC from day 23 to day 25 can be attributed to dilution with deep-sea water. DOC concentrations increased to a maximum of 149 ± 12 µmol L^{-1} after decay of the bloom on day 37 (Fig. 3.2b). Inorganic nutrients were again depleted from day 30 until the end of the experiment. At the beginning of Phase III

a second phytoplankton bloom developed, sustained from recycled production with a lower chlorophyll *a* concentration of 1.0 µg L^{-1} on day 37 (Fig. 3.2a).

Due to oligotrophic conditions, DON is represented by TDN at the beginning of the study (Supplementary materials Fig. S3.1). After addition of deep-sea water with a TDN concentration of 2.4 µmol L^{-1}, a maximum of 6 ± 1 µmol L^{-1} TDN was observed. On average, the TDN was lower in the oligotrophic Phase I than in the post-bloom Phase III. DOC/DON molar ratios started well above the classical Redfield ratio of 6.6 (Redfield, 1963) with a phase-average of 19.8 for Phase 0. The ratio then increased until the onset of the first phytoplankton bloom on day 25 when it reached a maximum of 41.6. This is consistent with the sharp increase in TDN (Supplementary materials Fig. S3.1). After the bloom, DOC/DON molar ratios were on average 30.7 (Phase III).

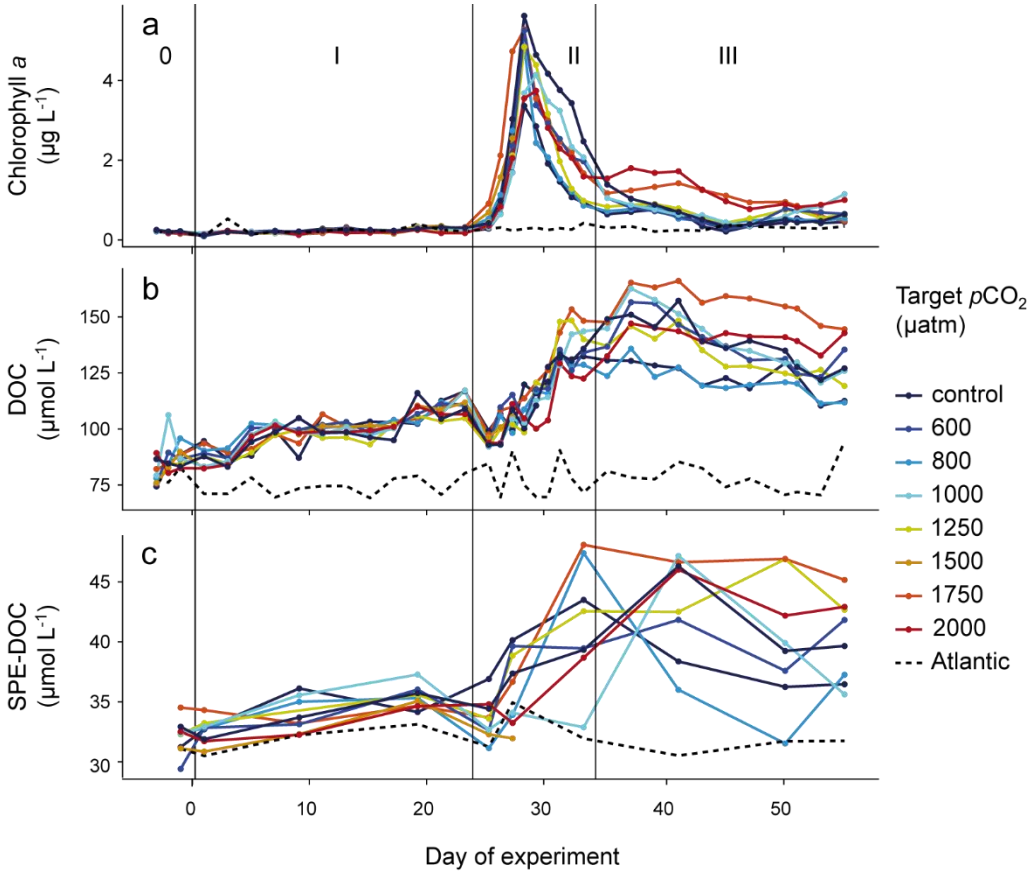

Figure 3.2 Time series of bulk parameters of the 9 mesocosm units. Colors display the respective target pCO_2 value. Dotted time series are for Atlantic water. (a) Chlorophyll *a* concentration. (b) DOC concentrations. (c) SPE-DOC concentration as a measure of the solid-phase extractable component in DOM. One outlier was excluded for SPE-DOC (1250 µatm, day 9).

Apart from these broad, superimposed trends, the two mesocosms with the highest pCO_2 treatments (2000 and 1750 µatm pCO_2) showed higher chlorophyll *a* and DOC concentrations during recycled production in Phase III (Supplementary materials Fig. S3.2). This trend is significant in a linear regression for both, DOC and chlorophyll *a* ($p < 0.05$). It has to be noted that presumably a harmful algae (*Heterosigma akashiwo*) developed in the high CO_2 treatments and may have accounted for the differences in both parameters (L. Bach, pers. comm.). There were no differences with CO_2 between treatments for Phase I and Phase II.

3.4.2 The succession of molecular DOM composition

We identified a total of 11,898 intact compounds with assigned molecular formulae from FT-ICR-MS analysis of mesocosm samples. For statistical analysis and in order to remove noise signals, only the most intense detected molecular formulae were considered for each sample resulting in a data set consisting of 7212 compounds. SPE-DOC concentrations in the collected DOM extracts reflect the same general trends as DOC (Fig. 3.2c) and our analysis can thus be considered representative for the fraction in DOM that showed variability during the experiment. Signal intensities followed an overall similar pattern with a bell-shaped distribution along the mass axis and an intensity weighted maximum at 372 Da. Using PCA, we were able to summarize 60% of the total variability of the complex molecular information in a single component (PC1). This component correlates significantly in a Pearson's product-moment correlation with DOC and showed a highly reproducible trend among all independent mesocosm units over time (Pearson, $r = 0.60$, $p < 0.0001$, $n = 79$). It thus represents the accumulating molecular signature (Supplementary materials Fig. S3.3). A positive correlation was observed for PC3 with CO_2 (Pearson, $r = 0.20$, $p < 0.05$, $n = 79$). This component, however, explains only 6% of the total observed variability.

The succession of DOM molecular composition was similar in all mesocosms until the end of Phase II despite different pCO_2 treatments. Only with the start of recycled production, mesocosms start to diverge in their molecular composition (Fig. 3.3). During oligotrophic Phase I and directly after injection of nutrients, no such trend was observed. The dissimilarity on a Bray-Curtis level increased in

Phase III, but without indications for a trend with pCO_2 levels. Comparing control to control mesocosms or control to high CO_2 mesocosms revealed the same amount of variability.

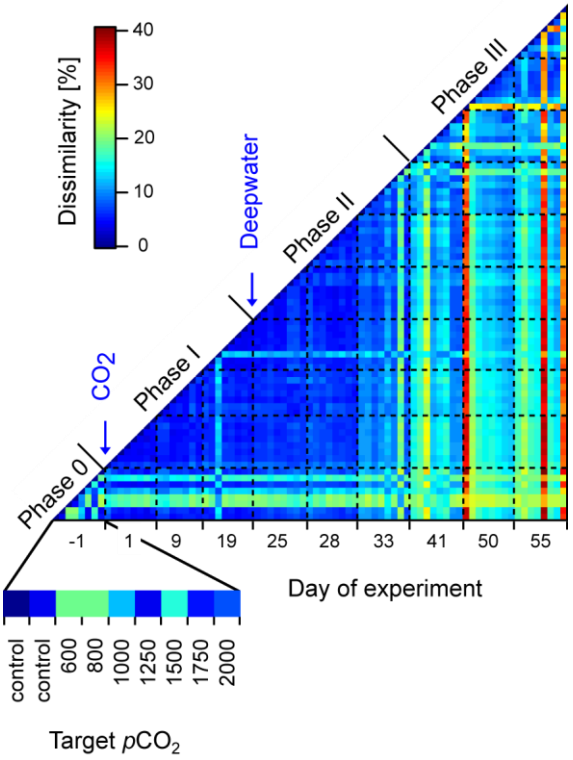

Figure 3.3 Molecular dissimilarity between mesocosms. The color scale displays the dissimilarity between two samples. Samples were first ordered by pCO_2 target levels and second by the respective day of the experiment.

In order to compare the succession of DOM on a molecular level between individual mesocosm units in more detail, we performed targeted analysis on specific compound groups using DOC and chlorophyll *a* concentrations as proxies. Molecular formulae that show close coupling to DOC concentrations in the succession of signal intensities are presumably accumulating over time while formulae matching the temporal trend of chlorophyll *a* concentrations are likely related to the highly dynamic fraction in DOM. A correlation of the normalized signal intensities with DOC concentrations for the individual mesocosms was in good agreement to the results from Bray-Curtis based dissimilarity analysis and similar compound groups correlated significantly (Pearson, $r < 0.549 / > -0.549$,

$p < 0.05$, $n = 10$) for all mesocosms (Fig. 3.4a) but no indications were observed for differences related to CO_2 levels. Correlation with chlorophyll *a* (Fig. 3.4b) showed a similar result (Pearson, $r < 0.549 / > -0.549$, $p < 0.05$, $n = 10$), but more compounds show positive significant correlation with DOC ($n = 3627$) than with chlorophyll *a* concentrations ($n = 1336$). In order to trace the succession pattern of the individual molecular formulae with significant changes over time, average relative signal intensities were calculated and plotted for the respective extraction day over time (Fig. 3.4c and d). Whereas the trend of molecular formulae correlating with DOC concentrations was in good accordance with the succession of average DOC concentration (Fig. 3.4c), molecular formulae showing correlation with chlorophyll *a* deviated to great extent from average chlorophyll *a* concentrations, even though the general pattern was matching.

Pearson's product-moment correlation coefficients r for individual molecular formulae that showed significant positive correlation with DOC were correlated in a second step between individual mesocosms (Fig. 3.5a) was highly significant (Pearson, $r < 0.75 / > 0.49$, $p < 0.0001$, $n = 3627$). A similar trend, however, was not observed for molecular formulae correlating significantly with chlorophyll *a* concentrations (Fig. 3.5b).

Finally we applied the decribed proxy approach to mass spectrometric data on the molecular DOM composition from a second mesocosm study that was performed in a Swedish Fjord (Zark et al., 2015). About 35% of the molecular formulae present in both studies (3972 common molecular formulae) showed significant correlation with DOC. For this common fraction, that presumably accumulates, we observed significant correlation between both studies (Pearson, $r = 0.47$, $p < 0.0001$, $n = 1353$), based on correlation coefficients r for each individual molecular formula with DOC as an average for the mesocosm units in the respective experiment.

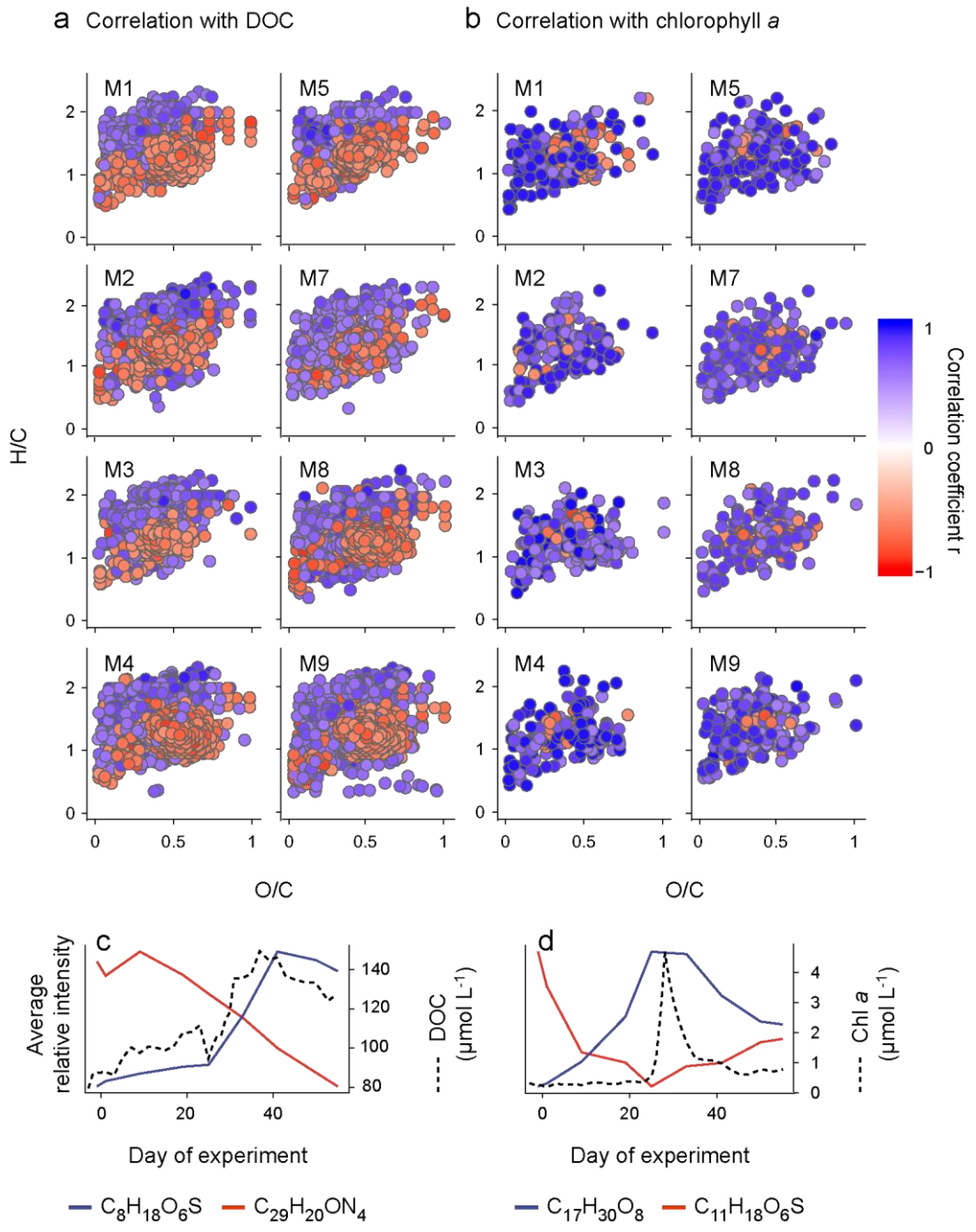

Figure 3.4 Trends of individual molecular compounds. (a) Pearson's product-moment correlation of DOC and (b) chlorophyll *a* concentrations with relative signal intensities for the individual mesocosm units. Displayed are only the molecular formulae (out of 7212) that significantly varied in their intensities ($p < 0.05$). Averaged relative peak intensities of the two molecular formulae showing the highest positive (blue) or negative (red) correlation over experiment time with (c) DOC and (d) chlorophyll *a*. The black dashed lines represent average concentrations of the respective parameters for all mesocosms.

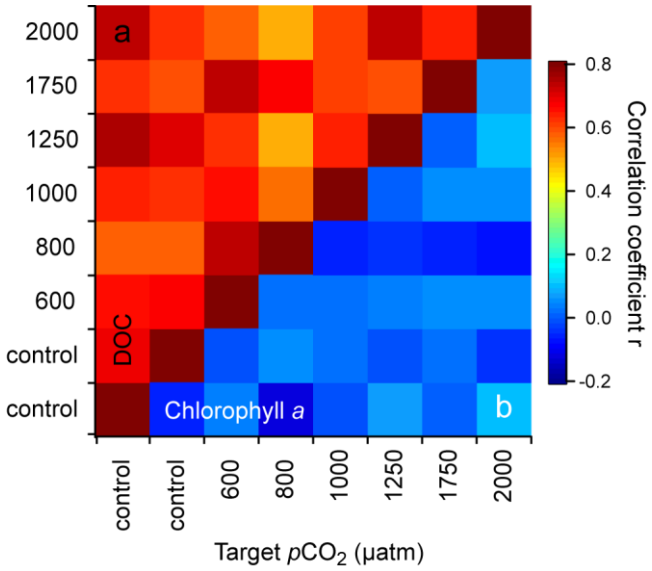

Figure 3.5 Production of similar compounds in all mesocosms. A Pearson's product-moment correlation illustrates the succession of molecular compounds with (a) DOC and (b) chlorophyll *a* concentrations between the individual treatments. The calculation is based on Pearson product-moment correlation coefficients r from the correlation of relative signal intensities of molecular formulae with concentrations of DOC or chlorophyll *a*. Only correlation coefficients from molecular formulae that showed significant correlation were considered (Pearson, $r < 0.549 / > -0.549$, $p < 0.05$, $n = 10$). Compounds correlating with DOC show the same succession for all mesocosms (Pearson, $r < 0.75 / > 0.49$, $p < 0.0001$, $n = 3627$). A similar trend was not observed for chlorophyll *a*.

3.5 Discussion

3.5.1 CO_2 threshold for effects on the marine DOM pool

In our study design we aimed towards the determination of a threshold for ocean acidification effects on DOM. At the beginning of the study, mesocosms were almost not distinguishable from each other and did not differ in bulk parameters and molecular composition between treatments until the onset of recycled production in Phase III. The concentrations of DOC and SPE-DOC started to diverge between treatments at the time when all nutrients added by deep-sea water were consumed. DOC concentrations were then highest in the two mesocosms with highest pCO_2 (1750 and 2000 µatm), however, the findings are not statistically robust due to the lack of replicates for the respective pCO_2 treatments. Nevertheless, they indicate that a threshold for effects on DOC concentrations emerges at $pCO_2 > 1250$ µatm. Doubtlessly, this estimate is very coarse considering the spatial limitations of the mesocosms as well as the fact that only a short time period was monitored compared to the time scales typically used

for projections, but consistent with mesocosm studies in Norway (Paul et al., 2015) and in the Arctic (Czerny et al., 2013; Engel et al., 2013) where higher DOC accumulation was observed under elevated pCO_2 target levels of up to 1650 µatm. In agreement, it was reported that lower maximum target levels of 1000 µatm pCO_2 showed no significant effects on DOC (MacGilchrist et al., 2014; Zark et al., 2015). These studies, however, were all conducted in coastal areas under eutrophic conditions. A different response was observed in studies that were conducted under oligotrophic conditions in the Mediterranean Sea where no effects were observed on chlorophyll *a* and DOC accumulation under moderate ocean acidification conditions with 1250 µatm pCO_2 levels (Maugendre et al., 2015b). Incubation studies using water from the oligotrophic Okhotsk Sea further show higher DOC removal under enhanced CO_2 (Yoshimura et al., 2010). Overall, the effect of pCO_2 on DOM seems to be ambiguous and highly dependent on the respective ecosystem.

3.5.2 C/N Stoichiometry

As a consequence of DOC accumulation under nutrient depletion, the stoichiometry of DOM is likely to shift. When more dissolved inorganic carbon (DIC) relative to inorganic nutrients is incorporated by phytoplankton, DOC/DON molar ratios increase above the classical Redfield ratio of 6.6 (Redfield et al., 1963) which is also known as carbon overconsumption (Toggweiler, 1993). The effect occurs under stress situations such as warming (Taucher et al., 2012) or acidification (Riebesell et al., 2007). We observed a characteristic scenario for the nutrient depleted Atlantic Ocean with high DOC/DON ratios on average 28.7 for all mesocosms (Kähler and Koeve, 2001). However, no higher DOC/DON ratios were observed for the two high CO_2 mesocosms with the onset of Phase III. This is presumably due to the fact that TDN measurements were close to the detection limit and the variance was accordingly high.

3.5.3 Production of a fraction of compounds with similar molecular formulae in all mesocosms

In a previous mesocosm study in a Swedish Fjord with maximum target pCO_2 levels of 1000 µatm, we observed no effects of elevated pCO_2 on the compounds being consumed or produced over time (Zark et al., 2015). The same was true for

this study in the subtropical North Atlantic Ocean. Even though indications for DOC accumulation were observed, the overall effect of CO_2 on DOM molecular composition, if present, is smaller than the variance between control replicates towards the end of the experiment, according to our measurements. Nevertheless it is possible that DOM compounds produced in excess, as a response to elevated CO_2 levels, aggregate very fast to form larger particles (Engel et al., 2014; Taucher et al., 2015) and, hence, leave no detectable imprint in the DOM resolved by our sampling frequency.

In order to assess the trends of individual compound fractions over time, we used DOC and chlorophyll *a* concentrations as proxies to improve our understanding of the underlying DOM dynamics. This approach is based on the assumption that we are basically observing two groups of compounds that either accumulate with DOC or that are quickly turned over, and thus correlating to chlorophyll *a* concentrations. Correlation with chlorophyll *a* concentrations was not pronounced with mostly negative correlations. This is not surprising as our sampling frequency was not intended to capture labile compounds. In the context of carbon sequestration, the fraction of DOM that is turned over on time scales of weeks or longer is of highest importance. This accumulating fraction is represented by compounds correlating significantly with DOC. We found that half of the occurring molecular formulae showed significant ($p < 0.0001$) correlation with DOC concentration similar for all mesocosm units over time. This finding is remarkable, given the fact that mesocosms were closed and that very small initial differences in starting parameters could potentially cause large divergences over time.

By applying the same approach to the molecular DOM data from the experiment in a Swedish Fjord (Zark et al., 2015) it was possible to show that there was a comparable fraction of molecular formulae in both, the oligotrophic North Atlantic Ocean and the coastal study, that significantly correlated with DOC in a similar way. From this observation it may be derived that compounds with the same elemental composition also show the same biogeochemical spatial and temporal dynamics. Considering the fact that individual molecular formulae in DOM are likely to respresent a number of different isomers (Zark et al., in preparation), it

seems possible that similar dynamics among ecosystems are the effect of an overall averaging of structural parameters. This hypothesis, however, remains speculative and molecular characterization of the dynamic fraction in DOM with higher temporal resolution is an important task for future mesocosm experiments.

3.6 Conclusion

DOM concentration and composition showed the same succession for all mesocosms in our experiment and effects of ocean acidification were only indicated. Elevated DOC concentrations were observed for the two high pCO_2 treatments compared to the treatments with lower pCO_2 target levels during the last phase of the experiment, whereas the molecular composition of the DOM pool did not change. The observed threshold for this effect was > 1250 µatm pCO_2. Most likely, a high number of compounds that were already present in the DOM pool before the artificial enrichment with excess CO_2 are produced in excess under acidifying conditions rather than different specific compound groups. However, the observed trends were not pronounced and can only serve as an indicator because our study was designed without replicates. If the observed excess DOC was available in a future high CO_2 ocean, it could function as a nutrient for new production. Alternatively, it could be sequestered and may thereby impact the future global carbon cycle. Finally, we found that compounds correlating significantly with DOC concentrations, as a proxy for the accumulating fraction in DOM, show surprisingly similar dynamics over the succession of the two phytoplankton blooms.

3.7 Acknowledgements

We thank the team of the Gran Canaria mesocosm study in 2014, in particular A. Ludwig for the logistical organization and coordination. We also thank the staff of the Plataforma Oceánica de Canarias (PLOCAN) for hosting our team and for technical assistance. The authors furthermore thank K. Klaproth, M. Friebe, and I. Ulber for technical support with FT-ICR-MS and DOC/TDN analysis. We acknowledge A. Ludwig for the analysis of chlorophyll *a* concentrations. Nutrient concentrations were kindly provided by E. Achterberg and M. Esposito. Financial support for this study was provided by the German Ministry of Education and

Research (BMBF, FKZ 03F0655D) through the BIOACID (Biological Impacts of Ocean ACIDification) project.

3.8 References

Azam, F., Fenchel, T., Field, J.G., Gray, J.S., Meyer-Reil, L.A., Thingstad, F., 1983. The ecological role of water-column microbes in the sea. Mar. Ecol. Prog. Ser. 10, 257−263.

Caldeira, K., Wickett, M.E., 2003. Anthropogenic carbon and ocean pH. Nature 425, 365.

Carlson, C.A., Del Giorgio, P.A., Herndl, G.J., 2007. Microbes and the dissipation of energy and respiration: from cells to ecosystems. Oceanography 20, 89−100.

Clayton, T.D., Byrne, R.H., 1993. Spectrophotometric seawater pH measurements: Total hydrogen ion concentration scale calibration of *m*-cresol purple and at-sea results. Deep-Sea Res. Pt. I 40, 2115−2129.

Czerny, J., Schulz, K.G., Boxhammer, T., Bellerby, R.G.J., Büdenbender, J., Engel, A., et al., 2013. Implications of elevated CO_2 on pelagic carbon fluxes in an Arctic mesocosm study - an elemental mass balance approach. Biogeosciences 10, 3109−3125.

Dittmar, T., Koch, B., Hertkorn, N., Kattner, G., 2008. A simple and efficient method for the solid-phase extraction of dissolved organic matter (SPE-DOM) from seawater. Limnol. Oceanogr. Methods 6, 230−235.

Dutkiewicz, S., Morris, J.J., Follows, M.J., Scott, J., Levitan, O., Dyhrman, S.T., et al., 2015. Impact of ocean acidification on the structure of future phytoplankton communities. Nature climate change 5, 1002−1006.

Engel, A., Borchard, C., Piontek, J., Schulz, K.G., Riebesell, U., Bellerby, R., 2013. CO_2 increases ^{14}C primary production in an Arctic plankton community. Biogeosciences 10, 1291−1308.

Engel, A., Piontek, J., Grossart, H.-P., Riebesell, U., Schulz, K.G., Sperling, M., 2014. Impact of CO_2 enrichment on organic matter dynamics during nutrient induced coastal phytoplankton blooms. J. Plankton Res. 36, 641−657.

Green, N.W., Perdue, E.M., Aiken, G.R., Butler, K.D., Chen, H., Dittmar, T., et al., 2014. An intercomparison of three methods for the large-scale isolation of oceanic dissolved organic matter. Mar. Chem. 161, 14−19.

Grossart, H.-P., Allgaier, M., Passow, U., Riebesell, U., 2006. Testing the effect of CO_2 concentration on the dynamics of marine heterotrophic bacterioplankton. Limnol. Oceanogr. 51, 1−11.

Hedges, J.I., 1992. Global biogeochemical cycles: progress and problems. Mar. Chem. 39, 67−93.

Koch, B.P., Dittmar, T., Witt, M., Kattner, G., 2007. Fundamentals of molecular formula assignment to ultrahigh resolution mass data of natural organic matter. Anal. Chem. 79, 1758−1763.

Joint, I., Doney, S.C., Karl, D.M., 2011. Will ocean acidification affect marine microbes? ISME J. 5, 1−7.

Kähler, P., Koeve, W., 2001. Marine dissolved organic matter: can its C:N ratio explain carbon overconsumption? Deep-Sea Res. Pt. I 48, 49−62.

Kroeker, K.J., Kordas, R.L., Crim, R.N., Singh, G.G., 2010. Meta-analysis reveals negative yet variable effects of ocean acidification on marine organisms. Ecol. Lett. 13, 1419−1434.

Le Queré, C., Peters, G.P., Andres, R.J., Andrew, R.M., Boden, T., Ciais, P., 2013. Global carbon budget 2013. Earth Syst. Sci. Data Discuss. 6, 689−760.

Longhurst, A., Sathyendranath, S., Platt, T., Caverhill, C., 1995. An estimate of global primary production in the ocean from satellite radiometer data. J. Plankt. Res. 17, 1245−1271.

MacGilchrist, G.A., Shi, T., Tyrell, T., Richier, S., Moore, C.M., Dumousseaud, C., et al., 2014. Effects of enhanced pCO_2 levels on the production of dissolved organic carbon and transparent exopolymer particles in short-term bioassay experiments. Biogeosciences 11, 3695−3706.

Maugendre L., Gattuso, J.-P., Louis, J., de Kluijver, A., Marro, S., Soetaert, K., et al., 2015a. Effect of ocean warming and acidification on a plankton

community in the NW Mediterranean Sea. ICES J. Mar. Sci. 72, 1744−1755.

Maugendre, L., Gattuso, J.-P., Poulton, A.J., Dellisanti, W., Gaubert, M., Guieu, et al., 2015b. No detectable effect of ocean acidification on plankton metabolism in the NW oligotrophic Mediterranean Sea: Results from two mesocosm studies. Estuar. Coast. Shelf S. 1−11, in press.

Neuer, S., Cianca, A., Helmke, P., Freudenthal, T., Davenport, R., Meggers, H., et al., 2007. Biogeochemistry and hydrography in the eastern subtropical North Atlantic gyre. Results from the European time-series station ESTOC. Prog. Oceanogr. 72, 1−29.

Oksanen, J., Blanchet, F.G., Kindt, R., Legendre, P., Minchin, P.R., O'Hara, R.B., et al., 2013. Vegan: Community ecology package. R package version 2.0-10. http://CRAN.R-project.org/package=vegan.

Paul, A.J., Bach, L.T., Schulz, K.-G., Boxhammer, T., Czerny, J., Achterberg, E.P., et al., 2015. Effect of elevated CO_2 on organic matter pools and fluxes in a summer Baltic Sea plankton community. Biogeosciences 12, 6181−6203.

Piontek, J., Lunau, M., Händel, N., Borchard, C., Wurst, M., Engel, A., 2010. Acidification increases microbial polysaccharide degradation in the ocean. Biogeosciences 7, 1615−1624.

Qian, J., Mopper, K., 1996. Automated high-performance, high-temperature combustion total organic carbon analyzer. Anal. Chem. 68, 3090−3097.

Redfield, A.C., Ketchum, B.H., Richards, F.A.,1963. The influence of organisms on the composition of seawater, in: Hill, M.N., (Ed.), The Sea, Vol. 2. Wiley, New York, pp. 26−77.

Riebesell, U., 2000. Carbon fix for a diatom. Nature 407, 959−960.

Riebesell, U., Czerny, J., von Bröckel, K., Boxhammer, T., Büdenbender, J., Deckelnick, M., et al., 2013. Technical note: A mobile sea-going mesocosm system - New opportunities for ocean change research. Biogeosciences 10, 1835−1847.

Riebesell, U., Schulz, K.G., Bellerby, R.G.J., Botros, M., Fritsche, P., Meyerhöfer, M., et al., 2007. Enhanced biological carbon consumption in a high CO_2 ocean. Nature 450, 545−549.

Riedel, T., Dittmar, T., 2014. A method detection limit for the analysis of natural organic matter via Fourier transform ion cyclotron resonance mass spectrometry. Anal. Chem. 86, 8876−8382.

Rossel, P.E., Vähätalo, A.V., Witt, M., Dittmar, T., 2013. Molecular composition of dissolved organic matter from a wetland plant (*Juncus effusus*) after photochemical and microbial decomposition (1.25 yr): Common features with deep sea dissolved organic matter. Org. Geochem. 60, 62−71.

Salisbury, J., Green, M., Hunt, C., Campbell, J., 2008. Coastal acidification by rivers: a threat to shellfish? Eos 89, 513.

Schulz, K.G., Bellerby, R.G.J., Brussaard, C.P.D., Büdenbender, J., Czerny, J., Engel, A., et al., 2013. Temporal biomass dynamics of an Arctic plankton bloom in response to increasing levels of atmospheric carbon dioxide. Biogeosciences 10, 161−180.

Stubbins, A. and T. Dittmar. 2012. Low volume quantification of dissolved organic carbon and dissolved nitrogen. Limnol. Oceanogr. Methods 10, 347−352.

Taucher, J., Jones, J., James, A., Brzezinski, M.A., Carlson, C.A., Riebesell, U., et al., 2015. Combined effects of CO_2 and temperature on carbon uptake and partitioning by the marine diatoms *Thalassiosira weissflogii* and *Dactyliosolen fragilissimus*. Limnol. Oceanogr. 60, 901−919.

Taucher, J., Schulz, K.G., Dittmar, T., Sommer, U., Oschlies, A., Riebesell, U., 2012. Enhanced carbon overconsumption in response to increasing temperatures during a mesocosm experiment. Biogeosciences 9, 3531−3545.

Toggweiler, J.R., 1993. Carbon overconsumption. Nature 363, 210−211.

Welschmeyer, N.A., 1994. Fluorometric analysis of chlorophyll *a* in the presence of chlorophyll *b* and pheopigments. Limnol. Oceanogr. 39, 1985−1992.

Winkelmann, R., Levermann, A., Ridgewell, A., Caldeira, K., 2015. Combustion of available fossil fuel resources sufficient to eliminate the Antarctic Ice Sheet. Sci. Adv. e1500589.

Yoshimura, T., Nishioka, J., Suzuki, K., Hattori, H., Kiyosawa, H., Watanabe, Y.W., 2010. Impacts of elevated CO_2 on organic carbon dynamics in nutrient depleted Okhotsk Sea surface waters. J. Exp. Mar. Biol. Ecol. 395, 191−198.

Zark, M., Christoffers, J., Dittmar, T. Experimental evidence for structural diversity of deep-ocean dissolved organic matter. Geophys. Res. Let., in preparation.

Zark, M., Riebesell, U., Dittmar, T., 2015. Effects of ocean acidification on marine dissolved organic matter are not detectable over the succession of phytoplankton blooms. Sci. Adv. e1500531.

3.9 Supplementary materials

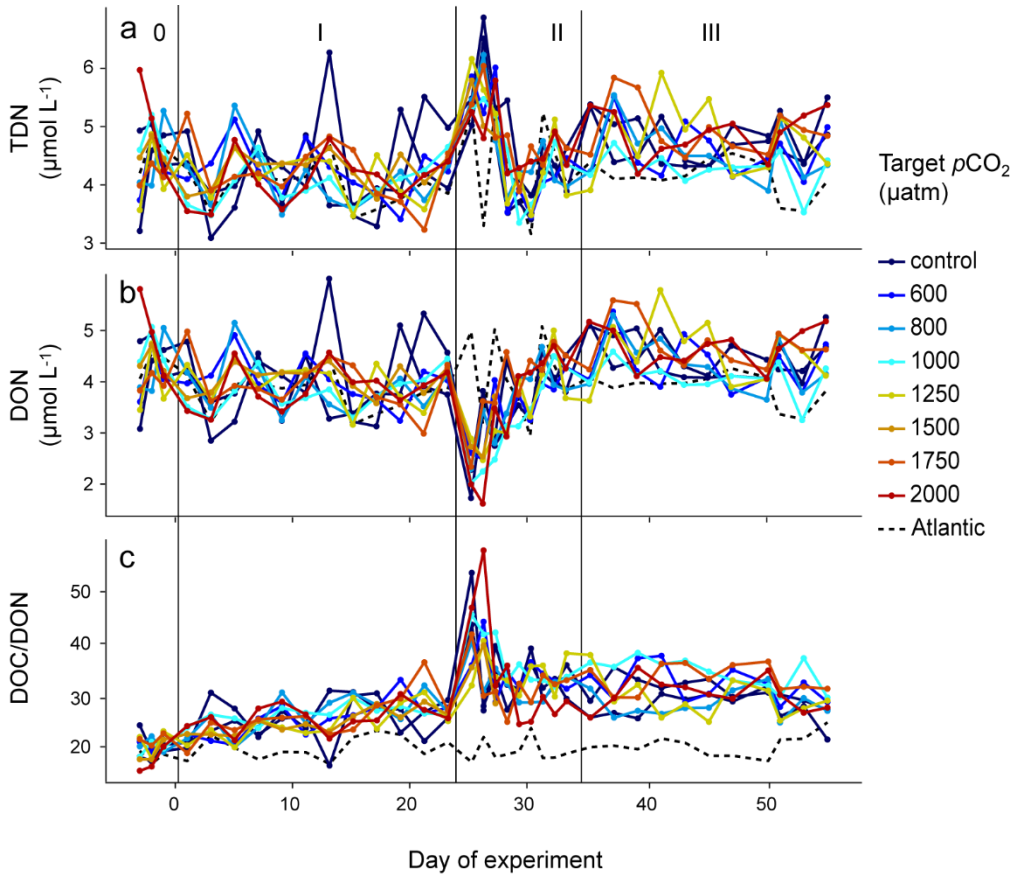

Figure S3.1 Time series of dissolved nitrogen species of the 9 mesocosms. (a) TDN and (b) DON average concentrations from triplicate measurements. (c) DOC/DON molar ratio. Dotted time series are for Atlantic seawater.

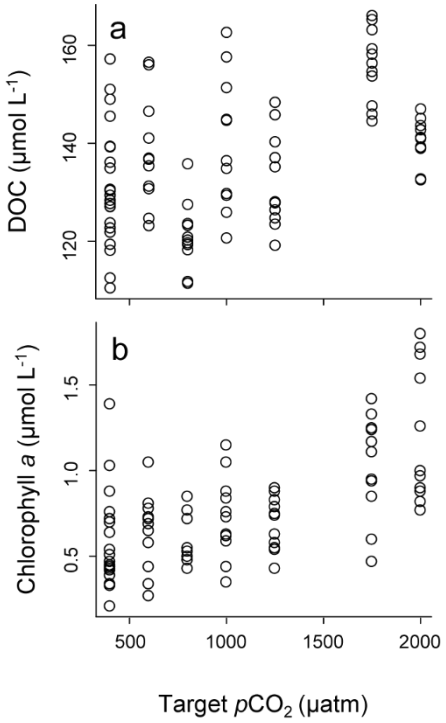

Figure S3.2 Carbon dioxide concentrations as driver for trends in bulk data during Phase III. (a) DOC and (b) chlorophyll *a* plotted for increasing target pCO_2 levels of experiment days 35-55 (post bloom).

A regression analysis of DOC and chlorophyll *a* concentrations with target pCO_2 levels of the respective mesocosms revealed a significant linear relation ($p < 0.05$) during post bloom Phase III. The trend was still significant if either the treatment with 1750 µatm or 2000 µatm was excluded ($p < 0.05$). However, the response is assumingly not linear but there is a threshold level of > 1250 µatm as the two treatments with highest CO_2 levels drive the trend. No significant ($p < 0.05$) linear relation was observed for DOC and chlorophyll *a* including all experiment days (day 1 to 55).

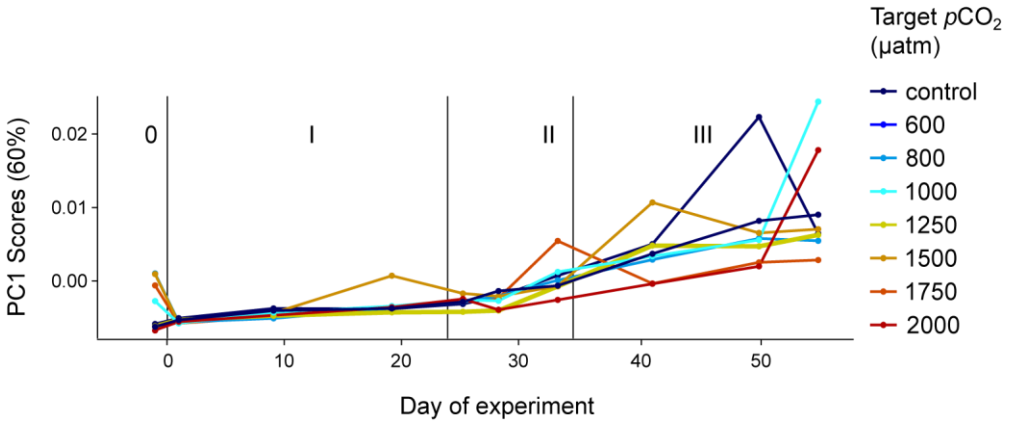

Figure S3.3 Time series of molecular composition of the 9 mesocosms. Results from the PCA (PC1) of 7212 molecular formulae and their MS signal intensities.

Manuscript III:

Universal molecular structures in natural dissolved organic matter

Maren Zark[1] and Thorsten Dittmar[1]

This chapter corresponds to a full manuscript that was submitted to *Proceedings of the National Academy of Science*.

[1] Institute for Chemistry and Biology of the Marine Environment (ICBM), Research Group for Marine Geochemistry (ICBM-MPI Bridging Group), Carl von Ossietzky University of Oldenburg, Carl-von-Ossietzky-Straße 9-11, 26129 Oldenburg, Germany.

The manuscript “Universal molecular structures in natural dissolved organic matter” (Manuscript III) aims at an intercomparison of the general structure of DOM between different aquatic environments. Based on tandem ultra high resolution mass spectrometry, we found that common molecular formulae detected in samples from most different water bodies are likely to exhibit similarities on the molecular structure level. Diversification of DOM over the course of degradation may ultimately lead to a large pool of compounds with undistinguishable molecular properties. This novel insight has application also for our understanding of long-term stability of DOM. The study was initiated by M. Zark and T. Dittmar. Field work, sample preparation, and tandem ultrahigh resolution mass spectrometry analysis was done by M. Zark. M. Zark and T. Dittmar performed statistical analysis and interpretation of fragment ion mass spectra. M. Zark wrote the manuscript with significant input from T. Dittmar.

This manuscript is submitted for publication in *Proceedings of the National Academy of Sciences (PNAS)* and presented with adjusted formatting according to the style of this thesis.

4.1 Abstract

The reasons behind the accumulation of the large pool of marine dissolved organic matter (DOM) and mechanisms of turnover are still largely elusive. Source and history leave imprints in the DOM molecular composition, and specific molecular traces from continental vegetation or bacterial biomass can be found in the deep ocean. At the same time, the bulk of DOM shares enormous molecular similarity, even at the highest accessible analytical resolution. Most of the thousands of molecular formulae that have been identified in DOM in the deep sea also occur in rivers, lakes, and wetlands. However, many vastly different isomers may exist for these molecular formulae, and the apparent molecular similarity of DOM across the globe might simply be due to analytical limitations. Here we show that similarity on a molecular formula level extends towards a molecular structural level. Fragmentation experiments in an ultrahigh-resolution Fourier-transform ion cyclotron resonance mass spectrometer (FT-ICR-MS) provided us with unprecedented detailed structural fingerprints of individual molecular formulae found in a range of marine and freshwater DOM samples. Identical DOM molecular formulae had undistinguishable structural fingerprints, independent of DOM source and history. Molecular formulae of DOM from culture experiments or defined model compounds, on the other hand, did not show this level of structural similarity. The presence of a large pool of compounds with common structural features in DOM could be the result of a cascade of similar degradation processes that ultimately leads to the formation of a common recalcitrant background, regardless of origin of the organic material.

4.2 Significance statement

Dissolved organic matter is one of the biggest active carbon pools on earth and to a great extent resistant towards degradation. Due to its size and persistence, changes in molecular composition could affect the global climate. Nevertheless, its chemical structure remains largely unknown and advances in the field of structure determination of dissolved organic matter are of utmost importance for a better understanding of its cycling and reactivity. We compared samples from very different aquatic environments with help of molecular fragmentation experiments in an ultrahigh-resolution mass spectrometer. We show that dissolved organic molecules in freshwater and marine systems share undistinguishable structural features. Based on this novel insight we propose that cascades of degradation processes ultimately form similar compounds.

4.3 Introduction

Marine dissolved organic matter (DOM) represents one of the largest active carbon reservoirs on earth, similar in size to atmospheric CO_2 (Hedges et al., 1992; Siegenthaler and Sarmiento, 1993). A major fraction is highly persistent against microbial oxidation and stored in the oceans for millennia (Hansell, 2013). Even small changes in molecular composition or concentration could affect the global carbon fluxes and, hence, the climate (Jiao et al., 2010; Legendre et al., 2015). However, DOM chemical structure remains largely unknown, despite the important role in the marine carbon cycle. The high number of individual components that are present in DOM and the very low concentrations in seawater (Arrieta et al., 2015) are among the challenges that analytical techniques have to take up in order to obtain structural information. Only less than 7% of marine dissolved organic carbon (DOC) can be assigned to molecular building blocks to date (Kaiser and Benner, 2012, 2009). A better knowledge of the structure of DOM is of utmost importance if we want to improve our understanding of the sources and transformations within the biogeochemical carbon cycle (Mopper et al., 2007). Elucidating the molecular structure could furthermore help to explain the reasons behind the long-term stability of DOM (Dittmar, 2015).

One of the most promising tools for the characterization of the highly diverse DOM pool is ultrahigh-resolution mass spectrometry, namely Fourier-transform ion cyclotron resonance mass spectrometry (FT-ICR-MS), coupled to soft ionization techniques, such as electrospray ionization (ESI). This combination of analytical techniques has the power to resolve and assign molecular formulae to individual components in DOM (Mopper et al., 2007). Surprisingly, thousands of molecular formulae in DOM found in the deep ocean are also present in rivers, lakes, wetlands and even degraded plant leachate and microbial cultures (Dittmar and Stubbins, 2014; Hansman et al., 2015; Koch et al., 2005; Lechtenfeld et al., 2015; Rossel et al., 2013). This is surprising regarding the different sources of organic material. It was hypothesized that the interaction of abiotic processes such as photodegradation (Stubbins et al., 2010) together with microbial mediated transformation of DOM (Jiao et al., 2010) leads source-independently to similar structural features which have an intrinsically refractory character (Koch et al., 2005; Rossel et al., 2013). These compounds are largely preserved and transported via conservative mixing throughout the water column to other water masses and the deep sea (Follett et al., 2014; Hansman et al., 2015). However, there is yet no proof that the pool of common formulae in natural DOM samples truly represents identical structures rather than a number of isomers, either structural or spatial, with the same elemental composition (Stenson, 2008). For instance the phenolic degradation products of lignin, one of the most abundant biopolymers on earth and exclusively produced by vascular plants on the continents, contain to some degree the same molecular formulae as non-phenolic compounds produced by marine biota (Liu et al., 2011). Thus, molecular formula information alone is often insufficient to constrain molecular structure, and source and fate of a given DOM compound.

Collision induced molecular fragmentation is a well-established mass spectrometric method for structure determination of single substances and was early applied also for the analysis of complex natural organic matter mixtures (Plancque et al., 2001). In combination with FT-ICR-MS it reveals structural information on individual molecular formulae. DOM predominantly shows neutral losses of carbon dioxide from decarboxylation of carboxyl groups and water neutral losses as a result of alcohol dehydration or formation of anhydrides for both, terrigenous (Leenheer et al., 2001; Stenson et al., 2003; Witt et al., 2009) and marine origin (Reemtsma et

al., 2008). The dominating occurrence of a small group of fragments was interpreted as a lower structural diversity than initially expected (Witt et al., 2009).

Not only the type of occurring fragment ions is structure-specific, also the relative abundance of fragments provides structural information. Combining qualitative and quantitative information from fragmentation mass spectra is therefore well suited for the structural analysis of DOM. Samples with resembling mass spectrometric fingerprints but different structures can be clearly distinguished by this approach. For example, DOM produced by marine microbial communities in culture experiments is very similar to DOM in the ocean regarding molecular formulae (Koch et al., 2014; Lechtenfeld et al., 2015), but fragmentation experiments revealed different molecular structures behind the same molecular formulae in such experiments (Osterholz et al., 2015a).

Aim of this study was to compare DOM from most different aquatic environments on a structural molecular level. The goal was not full structural elucidation of DOM, which to date is an impossible task. Instead, fragmentation experiments in an FT-ICR-MS provided us with detailed structural molecular fingerprints that allowed for structural similarity analysis of DOM of extremely different origin in the ocean and on land (Fig. 4.1). Antarctic Bottom Water (AABW) and North Atlantic Deep Water (NADW) are deep water masses with a refractory DOM signature (Hansell and Carlson, 1998) but different origin as NADW is formed in the North Atlantic and AABW in the Southern Ocean.

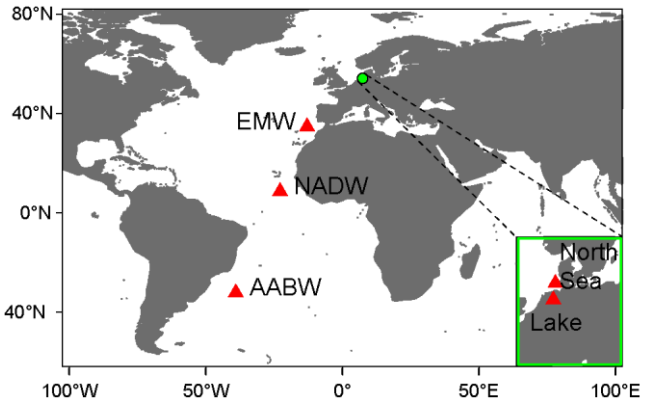

Figure 4.1 Map of sampling sites. The box highlighted in green shows the enlarged region of Northern Germany where water from the North Sea and from a eutrophic peat lake was collected.

Highly saline Eurafrican Mediterranean Water (EMW) from the outflow of the Mediterranean Sea is younger than oceanic deep water masses but also characterized by a refractory DOM signal (Santinelli et al., 2010). Further, a sample from the North Sea, a continental shelf sea in Europe, that contains a terrigenous component and freshly produced DOM (Osterholz et al., 2015b), was included in our comparison, as well as water from a eutrophic peat lake in North Germany that is presumably dominated by terrestrial vascular plant decomposition products (Wilkinson et al., 2013). To provide a proof of principle we additionally analyzed model compounds of the same molecular formula but with different chemical structures in the same way. We hypothesize that the pool of ubiquitously occurring molecules in DOM does not only share the same molecular formulae but shows high structural similarity

4.4 Results

4.4.1 Fragmentation of model compounds

Fragmentation FT-ICR-MS experiments of benzene tricarboxylic acid isomers, that have the same molecular formula ($C_9H_6O_6$) but slightly different structures (different positions of the carboxyl group), led to very different fragmentation patterns (Fig. 4.2). Three main fragment ions occurred as a result of multiple neutral losses of water and carbon dioxide at the mass to charge ratios (m/z) 191 (loss of 1 H_2O), 165 (loss of 1 CO_2) and 121 (loss of 2 CO_2). The intensity and appearance of these fragment ions was very characteristic for each isomer despite the same fragmentation conditions applied for each analysis. Thus, ESI FT-ICR-MS fragmentation patterns can be used as structural fingerprints to differentiate even slight deviations in molecular structure. This is consistent with previous findings on complex DOM molecular mixtures (Osterholz et al., 2015a).

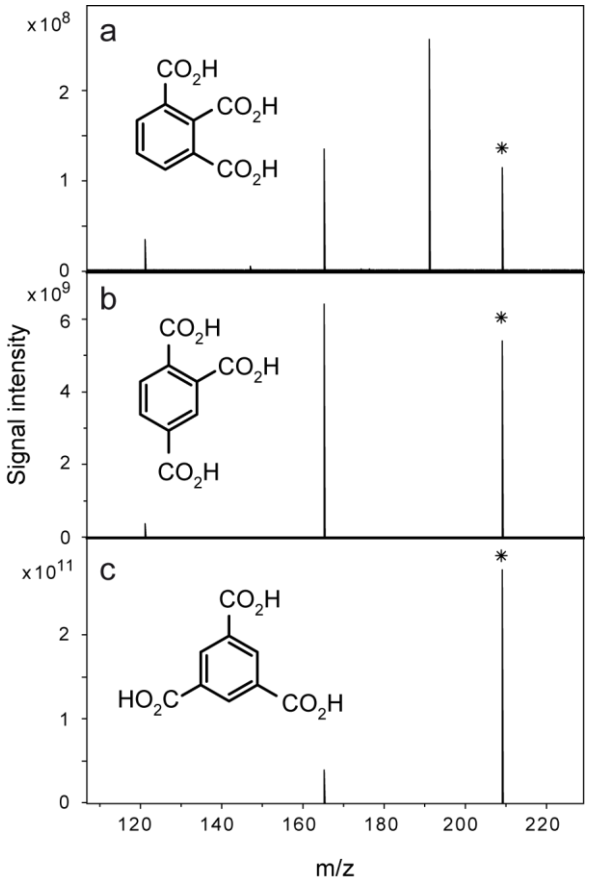

Figure 4.2 Fragmentation mass spectra of benzenetricarboxylic acid isomers with identical molecular formulae. The occurring fragment ions (m/z 121, 165, 191) with the same initial mass for the precursor ion (m/z 209) show different signal intensities according to the stereochemistry of the carboxylic groups attached to the benzene ring. The precursor ions are indicated by asterisks (*) in each spectrum.

4.4.2 Characterization of samples via FT-ICR-MS, molecular formula information

Prior to ESI FT-ICR-MS, samples have to be desalted and concentrated via solid phase extraction (Dittmar et al., 2008). Via this procedure, about 60% of DOM was recovered. A total of 11,153 resolved masses of singly charged, intact compounds were detected via FT-ICR-MS. Thereof, 6,676 masses could be assigned to molecular formulae. Most of the remaining detected masses were isotopologues of the same molecular formulae (analogs containing one ^{13}C, ^{15}N, and ^{18}O, and ^{34}S, respectively). Signal intensities followed a bell-shaped distribution along the mass axis from about 200 to 600 Da for all samples, but with different weighted arithmetic means (Fig. 4.3A).

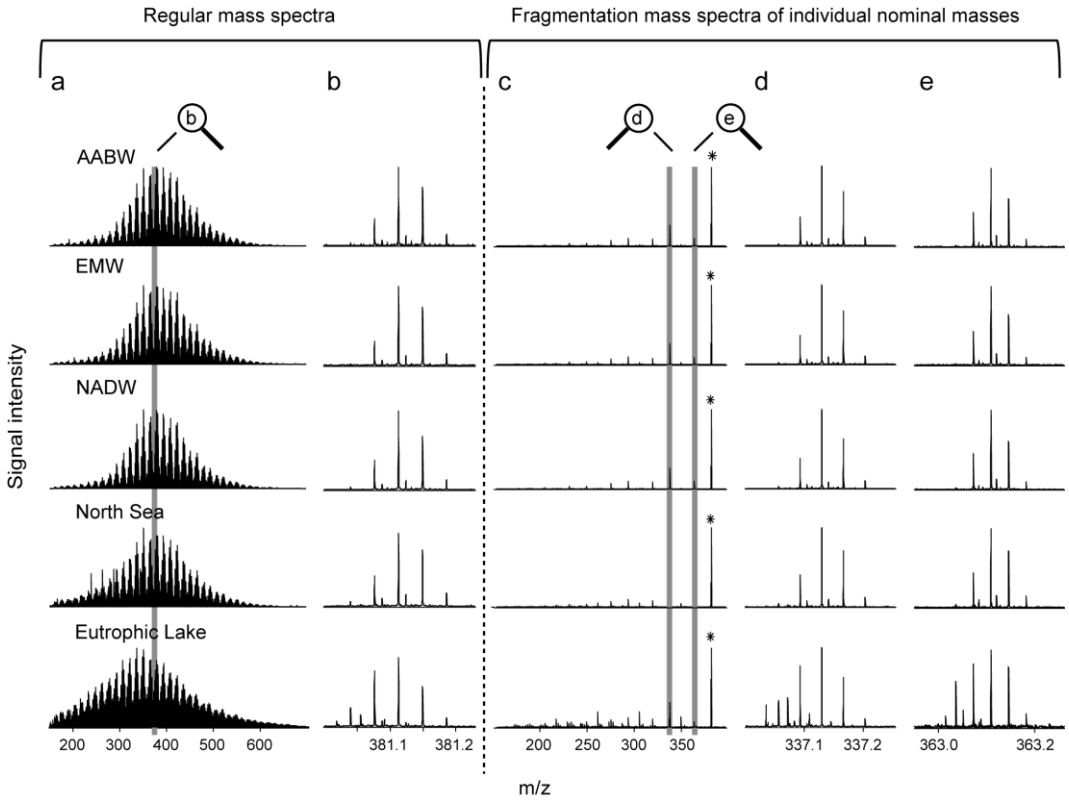

Figure 4.3 ESI FT-ICR mass spectra of DOM samples, broad band scans and fragmentation experiments. (a) Full range mass spectra showing bell-shape intensity distribution of detected masses. (b) Detected ions with nominal mass m/z 381 zoomed in from full range mass spectra, exemplary for the six fragmented nominal masses. (c) Full fragmentation patterns of m/z 381, exemplarily, which is indicated by asterisks (*). (d) Fragment ions resulting from the neutral loss of CO_2 and (e) from the neutral loss of H_2O, zoomed in from the respective mass range in full fragmentation pattern.

Subdividing compounds into molecular categories provided a helpful overview of likely structures behind the identified molecular formulae (Supplementary materials Table S4.1). Consistent with the respective origin, the eutrophic peat lake sample showed the highest number of molecular formulae of polyphenols (e.g. lignin-derived compounds) and combustion-derived, polycondensed aromates (black carbon) while EMW showed the highest percentage of highly unsaturated compounds.

For a more comprehensive comparison, we performed multivariate statistical analyses of the FT-ICR-MS signal intensities of the 6,676 identified molecular formulae. Principal components analysis (PCA) summarized 92% of the total variability of the complex molecular information in a single component (PC1). This component reflected the different origins of the samples as it correlated

significantly with salinity (Pearson, $r = -0.91$, $p < 0.05$, $n = 5$) and DOC concentration of the samples ($r = 0.90$, $p < 0.05$, $n = 5$).

Out of the 6676 detected molecular formulae 2531 were present in all of the five analyzed water samples. The percentage of this fraction of common molecular formulae relative to the total number of formulae was highest for EMW and lowest for the eutrophic peat lake (Table 4.1). A PCA of the common molecular formulae showed the same result as for all detected formulae as PC1 captured 92% of the total variability and correlated significantly with salinity (Pearson, $r = -0.95$, $p < 0.05$, $n = 5$) and DOC concentration ($r = 0.93$, $p < 0.05$, $n = 5$).

Furthermore, we performed a dissimilarity analysis (Bray-Curtis) based on occurring signal intensities from all detected molecular formulae in the original full range mass spectra (Fig. 4.5a). The highest dissimilarity was observed between Eurafrican Mediterranean Water and the eutrophic peat lake sample (47%). Also the common molecular formulae that were present in all samples showed a high degree of dissimilarity between the samples (34%, Fig. 4.5b).

Table 4.1 Physical and chemical properties of water samples from different sampling sites. Samples were pooled at equal parts from the respective positions and depths. All properties are for the pooled samples.

Sample	Longitude	Latitude	Depth [m]	SPE-DOC [µmol L^{-1}]	Salinity	# of detected formulae	Common formulae [%]	Aromatic structures* [%]
AABW	38° 60' W	30° 60' S	4100	23	34.7	3453	73	2.9
	39° 0' W	25° 60' S	4000					
EMW	12° 54' W	35° 14' N	1000	25	36.0	2897	87	2.6
	12° 37' W	38° 45' N	1000					
NADW	22° 46' W	9° 24' N	4000	26	34.9	3932	64	3.3
	22° 46' W	9° 24' N	3000					
	22° 46' W	9° 24' N	2500					
North Sea	7° 54' E	54° 11' N	0	118	32.7	4863	52	9.8
Lake	8° 1' E	53° 12' N	0	1906	0	5396	47	23.8

*Given are means weighted by corresponding signal intensities.

4.4.3 Characterization of samples via FT-ICR-MS, structural information

We chose six individual nominal masses (m/z 365, 379, 367, 381, 369, 383) for fragmentation experiments (Fig. 4.3b). These nominal masses represented a total of 217 molecular formulae of which 53 occurred in all of the five samples. The molecular formulae that were chosen for fragmentation represent all the major molecular categories (Supplementary materials Table S1), and they belong to different CH_2-homologues series. Thus, they are to some degree representative for the molecular diversity of DOM. The mass range around 370 Da was chosen, because the high signal intensities enable acquisition of the most detailed structural fingerprints. The collision induced fragmentation in the FT-ICR-MS resulted in a total of 1,953 distinct molecular fragments, of which 265 were produced from the common 53 molecular formulae that occurred in all samples.

The five natural DOM samples showed very similar fragmentation patterns (Fig. 4.3c). The most intensive fragment ions were identical and resulted from neutral losses of carbon dioxide (CO_2, Fig. 4.3d) and water (H_2O, Fig 4.3e). Other neutral losses were carbon monoxide (CO) and methanol (CH_3OH). The most intensive fragment ions at nominal mass minus 44 Da were results of one single carbon dioxide loss (Supplementary materials Fig. S4.1). A total of four successive CO_2 losses occurred in all samples. One direct water loss at nominal mass minus 18 Da was observed but no successive multiples thereof. Further water neutral losses occurred only in combination with CO_2 fragment ions.

To compare the structural features behind the common molecular formulae across all samples we performed linear regression analysis on the relative signal intensities of fragment ions that occurred from common masses. Relative fragment intensity (I_F/I_{Tot}) is here defined as the FT-ICR-MS signal intensity of the fragment ion (I_F) divided by the sum intensity of all major signals (I_{Tot}), which includes fragments and the original precursor ion. The deviation of the slope (Δsl) of the linear regression from an ideal slope of sl = 1 (representing identical fragment intensities) served as a measure for similarity. We found highly significant positive correlations ($r > 0.92$, $p < 0.0001$, $n = 265$) between the fragment intensities of all samples and only very minor deviations from a slope of one (Fig. 4.4).

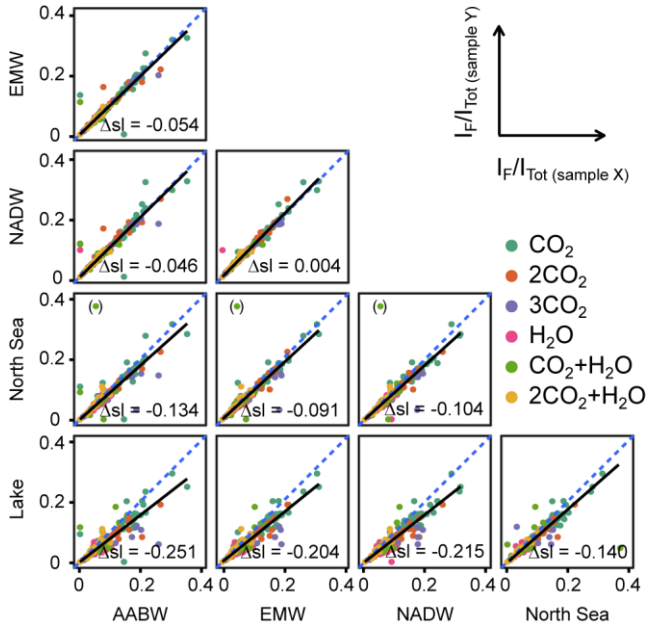

Figure 4.4 Structural relation of DOM samples from different environments. Linear regression analysis of relative fragment ion intensities from common molecular formulae shows the structural variance between two samples indicated by the significance of the correlation (all $p < 0.0001$, $n = 265$) and the deviation of the slope (sl) from ideal conformity (blue dashed lines). One outlier (in parentheses) was excluded from regression analysis.

These deviations (Δsl) ranged from 0.004 (NADW/EMW) to up to 0.251 (Lake/AABW, Fig. 4.4). This observation was confirmed by Bray-Curtis dissimilarity analysis. The fragment molecular patterns were highly similar among the samples, and the Bray-Curtis dissimilarity never exceeded 11% (Fig. 4.5c) which is within the range of our analytical variability.

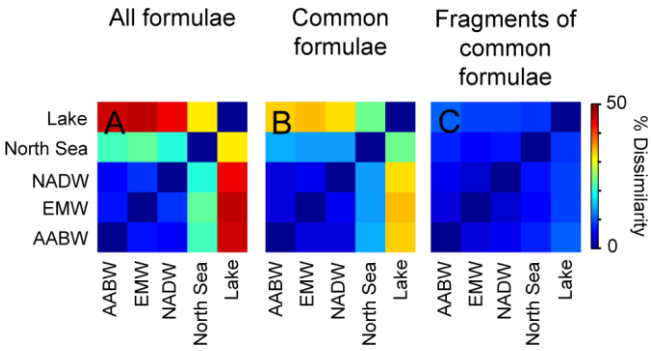

Figure 4.5 Dissimilarity of DOM from different environments on different levels of composition. Bray-Curtis dissimilarity based on relative peak intensities of (a) all detected molecular formulae in full range mass spectra ($n = 6676$), and (b) common molecular formulae in full range mass spectra ($n = 2531$). (c) Out of the 2531 common molecular formulae the 53 most intense were selected for fragmentation experiments. Bray-Curtis dissimilarity based on the resulting fragments shows high similarity ($n = 265$).

4.5 Discussion

The high similarity of fragmentation patterns is remarkable, considering the different origins of the samples. Regardless of origin, there is a component in DOM that has undistinguishable structural features, even when assessed by the most advanced analytical techniques. Compounds that shared the same molecular formula in vastly different aquatic environments also shared undistinguishable structural features. This similarity did not only apply to the type of functional groups, but also to their position in the given molecule. Our experiments with model compounds (Fig. 4.2) demonstrated that even minor difference in structure leads to vastly different fragmentation patterns in the FT-ICR-MS. This is also true for natural DOM. Osterholz et al. (2015a) recently showed that DOM produced by a natural planktonic community was different from marine DOM with respect to structural features, despite an almost complete overlap on a molecular formula level.

Carboxyl and hydroxyl groups were the main functional groups of DOM from all sampled water masses in our study. This is consistent with previous fragmentation experiments on riverine and coastal DOM (Liu et al., 2011; Stenson et al., 2003; Witt et al., 2009). The abundance of carboxyl and hydroxyl groups is also consistent with proposed molecular structures for marine DOM components (Hertkorn et al., 2006). DOM from the North Sea and more so the peat lake sample were both enriched in polyphenolic compounds, a unique compositional feature indicative for the presence of vascular plant debris. Because the respective molecular formulae were largely absent in the open ocean, the terrestrially influenced samples yielded additional fragmentation signals that originated exclusively from these polyphenols (Fig. 4.3c-e). Despite a clear terrigenous origin, functional groups that are typical for lignin (especially methoxy groups, Liu et al., 2011) were not observed in our experiments. This is likely due to the fact that these compounds are readily degraded (Dittmar and Lara, 2001) and were thus already removed on their journey from soils to the lake or into the coastal ocean.

We propose two possible scenarios that explain the observed structural similarities of common molecular formulae. The most intuitive explanation is that each molecular formula is represented by a single molecular structure which is

identical in all samples across the Atlantic and in the lake. Or, in sharp contrast, a very large number of isomers with different chemical structures might be present behind each molecular formula. Intrinsic averaging would result in undistinguishable fragmentation patterns. The latter explanation allows for different structures in the various samples, but, on average, the molecular structures behind a given molecular formula are undistinguishable as a result of averaging. Thus, the apparent structural similarity could be a property that emerges from an extraordinarily high molecular diversity behind each molecular formula. This explanation appears counterintuitive at first view, but recent findings from structure determination via nuclear magnetic resonance mass spectroscopy (NMR) reported more than thousand detectable structural units in marine DOM (Hertkorn et al., 2013). This together with recent evidence that single compounds in DOM occur in extraordinarily low concentrations in the deep ocean (Arrieta et al., 2015) supports the scenario of a high number of isomers behind each molecular formula. Further indication was provided by a database search for precursor ions based on fragment ions from fragmentation experiments on marine DOM (Cortés-Francisco and Caixach, 2015). This approach was not successful and no structure in the database could explain more than one of the observed fragment ions. This can either be explained by the lack of DOM compounds in the chosen database or by the fact that many structures are hidden behind each molecular formula.

The combined results provide evidence for the hypothesis that chains of degradation processes in aquatic environments ultimately leads to the formation of undistinguishable structural features, on land and in the ocean (Koch et al., 2005; Rossel et al., 2013). The virtual lack of common biomolecules and hydrolyzable functional groups in our samples (such as methoxy groups or esters) indicates that aqueous hydrolysis and the affinity of consumers towards common biomolecules is one of the communalities of degradation processes in all aquatic environments. The structural similarity of DOM, however, goes far beyond what can be explained by these processes. We propose that molecular diversification of DOM over the course of degradation ultimately leads to undistinguishable molecular properties.

The occurrence of a common pool of molecular formulae in most different aquatic environments has been known from several studies using ultrahigh-

resolution mass spectrometry. Our study represents the first comparison of comprehensive DOM molecular structural features in different aquatic environments, including the deep sea and a eutrophic peat lake. This novel insight has application also for our understanding of long-term stability of DOM. The underlying mechanisms behind the long-term turnover of DOM are possibly universal, at least for that component in DOM that is analytically undistinguishable across the globe. Simple dilution may be such mechanism (Arrieta et al., 2015).

4.6 Methods

4.6.1 Sampling sites and sample preparation

The samples were collected from five different sites (Fig. 4.1). Exact positions, volumes and water depths are displayed in Table 1. Antarctic Bottom Water (AABW), North Atlantic Deep Water (NADW) and Eurafrican Mediterranean Water (EMW) were collected onboard the German research vessel Polarstern on cruise leg ANT XXVIII/5 in 2012 using a rosette water sampler. The samples were pooled from two to three stations to obtain sufficient volume. We filtered water directly from the rosette sampler via gravity filtration. North Sea water samples were taken with a bucket from the sea surface between the two islands of Helgoland. A sample from a eutrophic peat lake, the Zwischenahner Meer in Bad Zwischenahn, Germany, was collected in January 2011 at the pier in Meyerhausen.

4.6.2 Dissolved organic matter extraction

Water was filtered (0.5-12 L, depending on the DOC concentration of the sample) into acid-rinsed polycarbonate bottles (Nalgene) through 0.7 µm GF/F glass microfiber filters (Whatman, pre-combusted 400 °C, 4 h). The filtrate was acidified with HCl (25%, analysis grade, Carl Roth) to pH 2 and stored at 4 °C in the dark. All samples were then extracted via solid phase extraction (SPE) using a styrene divinyl benzene polymer (PPL) as sorbent (Dittmar et al., 2008). Prior to use, the cartridges were soaked in methanol (HPLC grade, Sigma-Aldrich) overnight, and rinsed sequentially with methanol and 0.01 mol L^{-1} HCl in ultrapure water. After loading the samples onto the cartridges they were rinsed with 0.01 mol L^{-1} HCl to remove remaining salts and dried with argon gas (analysis

grade, Air Liquide). The extracted DOM was eluted with methanol. Procedural blanks were prepared by processing ultrapure water the same way as DOM samples. DOC concentrations in the resulting extracts were below the detection limit.

4.6.3 Dissolved Organic Carbon Analysis

Analysis of DOC concentrations was performed via high-temperature catalytic oxidation method (Qian and Mopper, 1996) using a Shimadzu (Japan) TOC-VCPH/CPN Total Organic Carbon Analyzer equipped with ASI-V auto sampler. We controlled the accuracy of the measurement with Florida Strait Water reference material (DSR, D.A. Hansell, University of Miami, Florida, USA) for every run. The error was below 2.8 µmol C L^{-1}.

4.6.4 ESI FT-ICR mass spectrometry analysis

We performed mass spectrometric analysis of SPE extracts via FT-ICR-MS on a solariX Fourier transform ion cyclotron resonance mass spectrometer with 15 Tesla magnet (Bruker Daltonics, USA). The system was equipped with an electrospray ionization source (ESI, Bruker Apollo II) applied in negative ionization mode. All instruments and the software were manufactured by Bruker Daltonik GmbH, Germany. Methanol extracts were mixed with ultrapure water 1:1 (v/v) for FT-ICR-MS analysis and diluted to a final DOC concentration of 20 mg C L^{-1}. For each measurement we accumulated 500 scans in the mass window of 150 – 2000 Da. We calibrated spectra internally with a reference mass list using Data Analysis software Version 4.0 SP4. The mass error of the calibration was < 0.06 ppm for all samples. We used MatLab routines developed by our working group for molecular formula assignment and further data processing. Only peaks with a signal-to-noise ratio of S/N = 5 or higher that fulfilled the criteria by Koch et al. (2007) and Rossel et al. (2013) were considered including the elements C, H, O, N, S, and P. All molecules were detected as singly-charged ions. To test the reproducibility and stability of the FT-ICR-MS analysis, SPE-DOM from North Equatorial Pacific Intermediate Water (NEqPIW) was analyzed with the same settings twice a day (Green et al., 2014). Finally, we normalized peak intensities of

the peaks with assigned molecular formula to the sum of peak intensities for multivariate statistical analysis.

Molecular categories according to criteria modified after Šantl-Temkiv et al. (2013) were calculated for all detected molecular formulae based on the modified aromaticity index AI_{mod} (Koch and Dittmar, 2006). The following groups were differentiated: combustion derived polycyclic aromats (Black Carbon; $AI_{mod} \geq 0.666$, no N, S, P), oxygen rich polyphenols ($0.666 > AI_{mod} < 0.5$, $O/C > 0.5$), oxygen poor polyphenols ($0.666 > AI_{mod} < 0.5$, $O/C \leq 0.5$), highly unsaturated compounds ($AI_{mod} < 0.5$, $H/C < 1.5$, $O/C < 0.9$), and aliphatic compounds ($2.0 \geq H/C \geq 1.5$, $O/C < 0.9$, no N).

4.6.5 ESI FT-ICR tandem mass spectrometry experiments

The mass spectrometric fragmentation experiments were performed using the same mass spectrometer as for the analysis of full range spectra. Fragmentation of DOM samples was carried out with methanol extracts that were mixed with ultrapure water 1:1 (v/v) to give a final concentration of 100 mg C L^{-1}. The three isomers of benzenetricarboxylic acid were analyzed at a concentration of 10 mg C L^{-1}. The detection range was set from m/z 125 - 2000. Six nominal masses (m/z 365, 379, 367, 381, 369, 383) were isolated for DOM (within a mass window of 0.4 Da) and 209 Da (window 0.2 Da) for benzenetricarboxylic acid, trapped and collided with inert argon gas in a quadrupole unit prior to ICR mass detection. The ion accumulation time was set to 2.0 s. For each spectrum 150 scans (300 scans for benzenetricarboxylic acid) were acquired with a data acquisition size of 4 Mword. The collision voltage was 15.0 V for all samples and 5.0 V for benzenetricarboxylic acid. The same parameters for data acquisition were used as for the isolation of the ions.

To calibrate fragmentation mass spectra we subtracted the exact masses of known occurring neutral losses of water, carbon dioxide, and combinations thereof (m/z 18.01056, 43.98983, 62.00039, 87.97966, 105.99022, 131.96949) from the masses of the ions detected on the respective isolated nominal mass. The resulting exact masses of potentially occurring fragment ions were then used for internal calibration. With this method, formula assignment to the fragment ions and

identification of the respective precursor ion became possible, based on the exact mass differences (Cortés-Francisco and Caixach, 2015; Osterholz et al., 2015a; Pohlabeln and Dittmar, 2015). Formula assignment was performed the same way as described for the full range mass spectra.

4.6.6 Statistical analysis of FT-ICR-MS data

For better comparison we calculated the relative peak intensity I_F/I_{Tot} for each individual fragment ion. Individual peak intensities were divided by the sum of the intensities of all major fragment peaks (corresponding to the neutral losses of CO_2, 2 CO_2, 3 CO_2, H_2O, $CO_2 + H_2O$, 2 $CO_2 + H_2O$, CH_3OH, $CO_2 + CH_3OH$, 2 $CO_2 + CH_3OH$) and the precursor ion peak intensity. Based on these relative peak intensities, a linear regression model was calculated (Fig. 4.4). For this analysis only fragment ions were considered, that were the result of fragmentation of common molecular formulae detected in the full range FT-ICR mass spectra across all samples. A common detection limit for all samples and individual precursor ions was defined as the minimum ratio of the signal of the respective precursor ion and analytical noise.

A Bray-Curtis dissimilarity matrix was calculated based on the normalized intensities of all masses detected in full range mass spectra, masses with common molecular formulae, and the normalized relative fragment intensities from fragmentation experiments (Fig. 4.5). Normalization was done by dividing the respective values to the sum of all peak intensities in the sample. For dissimilarity analysis of the common fragment intensities we considered the same data as for the linear regression model. All statistical analyses were performed with the software package R (Version 3.0.2, package “vegan”, Oksanen et al., 2013).

4.7 Acknowledgements

The authors thank the captain and the crew of RV Polarstern for technical assistance and Maren Seibt and René Ungermann for help during sampling onboard. Ina Ulber, Matthias Friebe and Kathrin Klaproth kindly provided technical assistance with DOC and FT-ICR-MS analyses. We furthermore acknowledge Jutta Niggemann for providing the North Sea samples and Silke Bölts for the sampling

of the eutrophic peat lake. Part of this work was supported by the Deutsche Forschungsgemeinschaft (DFG) in the framework of the “Schwerpunktprogramm Antarktisforschung” (NI 1366/1-1 SPP 1158).

4.8 References

Arrieta, J.M., Mayol, E., Hansman, R., Herndl, G.J., Dittmar, T., Duarte, C., 2015. Dilution limits dissolved organic carbon utilization in the deep ocean. Science 348, 331−333.

Cortés-Francisco, N., Caixach, J., 2015. Fragmentation studies for the structural characterization of marine dissolved organic matter. Anal. Bioanal. Chem. 407, 2455−2462.

Dittmar, T., 2015. Reasons behind the long-term stability of dissolved organic matter, in: Hansell, D.A., Carlson, C.A., (Eds.), The biogeochemistry of marine dissolved organic matter, 2nd edition. Academic Press, Burlington, pp. 369−388.

Dittmar, T., Koch, B., Hertkorn, N., Kattner, G., 2008. A simple and efficient method for the solid-phase extraction of dissolved organic matter (SPE-DOM) from seawater. Limnol. Oceanogr. Methods 6, 230−235.

Dittmar, T., Lara, R.J., 2001. Molecular evidence for lignin degradation in sulfate reducing mangrove sediments (Amazônia, Brazil). Geochim. Cosmochim. Ac. 65, 1403−1414.

Follett, C.L., Repeta, D.J., Rothman, D.H., Xu, L., Santinelli, C., 2014. Hidden cycle of dissolved organic carbon in the deep ocean. Proc. Natl. Acad. Sci. U S A 111, 16706−16711.

Dittmar, T., Stubbins, A., 2014. Dissolved organic matter in aquatic systems, in: Birrer, B., Falkowski, P., Freeman, K., (Eds.), Treatise of Geochemistry, 2nd edition. Academic Press, Oxford, pp. 125−156.

Green, N.W., Perdue, E.M., Aiken, G.R., Butler, K.D., Chen, H., Dittmar, T., et al., 2014. An intercomparison of three methods for the large-scale isolation of oceanic dissolved organic matter. Mar. Chem. 161, 14−19.

Hansell, D.A., 2013. Recalcitrant dissolved organic carbon fractions. Annu. Rev. Mar. Sci. 5, 421−445.

Hansell, D.A., Carlson, C.A., 1998. Deep-ocean gradients in the concentration of dissolved organic carbon. Nature 395, 263−266.

Hansman, R.L., Dittmar, T., Herndl, G.J., 2015. Conservation of dissolved organic matter molecular composition during mixing of the deep water masses of the northeast Atlantic Ocean. Mar. Chem. 177, 288−297.

Hedges, J.I., Hatcher, P.G., Ertel, J.R., Meyers-Schulte, K., 1992. A comparison of dissolved humic substances from seawater with Amazon River counterparts by ^{13}C-NMR spectrometry. Geochim. Cosmochim. Ac. 56, 1753−1757.

Hertkorn, N., Benner, R., Frommberger, M., Schmitt-Kopplin, P., Witt, M., Kaiser, K., et al., 2006. Characterization of a major refractory component of marine dissolved organic matter. Geochim. Cosmochim. Ac. 70, 2990−3010.

Hertkorn, N., Harir, M., Koch, B.P., Michalke, B., Schmitt-Kopplin, P., 2013. High-field NMR spectroscopy and FTICR mass spectrometry: powerful discovery tools for the molecular level characterization of marine dissolved organic matter. Biogeosciences 10, 1583−1624.

Jiao, N., Herndl, G.J., Hansell, D.A., Benner, R., Kattner, G., Wilhelm, S.W., et al., 2010. Microbial production of recalcitrant dissolved organic matter: long-term carbon storage in the global ocean. Nat. Rev. Microbiol. 8, 593−599.

Kaiser, K., Benner, R., 2012. Organic matter transformations in the upper mesopelagic zone of the North Pacific: Chemical composition and linkages to microbial community structure. J. Geophys. Res. Oceans 117, C01023.

Kaiser, K., Benner, R., 2009. Biochemical composition and size distribution of organic matter at the Pacific and Atlantic time-series stations. Mar. Chem. 113, 63−77.

Koch, B.P., Dittmar, T., 2006. From mass to structure: an aromaticity index for high-resolution mass data of natural organic matter. Rapid. Commun. Mass. Spectrom. 20, 926−932.

Koch, B.P., Dittmar, T., Witt, M., Kattner, G., 2007. Fundamentals of molecular formula assignment to ultrahigh resolution mass data of natural organic matter. Anal. Chem. 79, 1758−1763.

Koch, B.P., Kattner, G., Witt, M., Passow, U., 2014. Molecular insights into the microbial formation of marine dissolved organic matter: recalcitrant or labile? Biogeosciences 11, 4173−4190.

Koch, B.P., Witt, M., Engbrodt, R., Dittmar, T., Kattner, G., 2005. Molecular formulae of marine and terrigenous dissolved organic matter detected by electrospray ionization Fourier transform ion cyclotron resonance mass spectrometry. Geochim. Cosmochim. Ac. 69, 3299−3308.

Lechtenfeld, O.J., Hertkorn, N., Shen, Y., Witt, M., Benner, R., 2015. Marine sequestration of carbon in bacterial metabolites. Nat. Commun. 6, 6711.

Leenheer, J.A., Rostad, C.E., Gates, P.M., Furlong, E.T., Ferrer, I., 2001. Molecular resolution and fragmentation of fulvic acid by electrospray ionization/multistage tandem mass spectrometry. Anal. Chem. 73, 1461−1471.

Legendre, L., Rivkin, R.B., Weinbauer, M.G., Guidi, L., Uitz, J., 2015. The microbial carbon pump concept: potential biogeochemical significance in the globally changing ocean. Prog. Oceanogr. 134, 432−450.

Liu, Z., Sleighter, R.L., Zhong, J., Hatcher, P.G., 2011. The chemical changes of DOM from black waters to coastal marine waters by HPLC combined with ultrahigh resolution mass spectrometry. Estuar. Coast. Shelf. Sci. 92, 205−216.

Mopper, K., Stubbins, A., Ritchie, J.D., Bialk, H.M., Hatcher, P.G., 2007. Advanced instrumental approaches for characterization of marine dissolved organic matter: Extraction techniques, mass spectrometry, and nuclear magnetic resonance spectroscopy. Chem. Rev. 107, 419−442.

Oksanen, J., Blanchet, F.G., Kindt, R., Legendre, P., Minchin, P.R., O'Hara, R.B., et al., 2013. Vegan: Community ecology package. R package version 2.0-10. http://CRAN.R-project.org/package=vegan.

Osterholz, H., Niggemann, J., Giebel, H.-A., Simon, M., Dittmar, T., 2015a. Inefficient microbial production of refractory dissolved organic matter in the ocean. Nat. Commun. 6, 7422.

Osterholz, H., Singer, G., Wemheuer, B., Daniel, R., Simon, M., Niggemann, J., Dittmar, T., 2015b. Deciphering associations between dissolved organic molecules and bacterial communities in a pelagic marine system. ISME J., in press.

Plancque, G., Amekraz, B., Moulin, V., Toulhoat, P., Moulin, C., 2001. Molecular structure of fulvic acids by electrospray with quadrupole time-of-flight mass spectrometry. Rapid. Commun. Mass. Spectrom. 15, 827−835.

Pohlabeln, A.M., Dittmar, T., 2015. Novel insights into the molecular structure of non-volatile marine dissolved organic sulfur. Mar. Chem. 168, 86−94.

Qian, J., Mopper, K., 1996. Automated high-performance, high-temperature combustion total organic carbon analyzer. Anal. Chem. 68, 3090−3097.

Reemtsma, T., These, A., Linscheid, M., Leenheer, J., Spitzy, A., 2008. Molecular and structural characterization of dissolved organic matter from the deep ocean by FTICR-MS, including hydrophilic nitrogenous organic molecules. Environ. Sci. Technol. 42, 1430−1437.

Rossel, P.E., Vähätalo, A.V., Witt, M., Dittmar, T., 2013. Molecular composition of dissolved organic matter from a wetland plant (*Juncus effusus*) after photochemical and microbial decomposition (1.25 yr): Common features with deep sea dissolved organic matter. Org. Geochem. 60, 62−71.

Santinelli, C., Nannicini, L., Seritti, A., 2010. DOC dynamics in the meso and bathypelagic layers of the Mediterranean Sea. Deep-Sea Res. Part 2 Top. Stud. Oceanogr. 57, 1446−1459.

Šantl-Temkiv, T., Finster, K., Dittmar, T., Hansen, B.M., Thyrhaug, R., Nielsen, N.W., et al., 2013. Hailstones: A window into the microbial and chemical inventory of a storm cloud. PLoS ONE 8, e53550.

Siegenthaler, U., Sarmiento, J.L., 1993. Atmospheric carbon dioxide and the ocean. Nature 365, 119−125.

Stenson, A.C., 2008. Reversed-phase chromatography fractionation tailored to mass spectral characterization of humic substances. Environ. Sci. Technol. 42, 2060−2065.

Stenson, A.C., Marshall, A.G., Cooper, W.T., 2003. Exact masses and chemical formulae of individual Suwannee River fulvic acids from ultrahigh resolution electrospray ionization Fourier transform ion cyclotron resonance mass spectrometry. Anal. Chem. 75, 1275−1284.

Stubbins, A., Spencer, R.G.M., Chen, H., Hatcher, P.G., Mopper, K., Hernes, P., et al., 2010. Illuminated darkness: Molecular signatures of Congo River dissolved organic matter and its photochemical alteration as revealed by ultrahigh precision mass spectrometry. Limnol. Oceanogr. 55, 1467−1477.

Wilkinson, G.M., Pace, M.L., Cole, J.J., 2013. Terrestrial dominance of organic matter in north temperate lakes. Global Biogeochem. Cycles 27, 43−51.

Witt, M., Fuchser, J., Koch, B.P., 2009. Fragmentation studies of fulvic acids using collision induced dissociation Fourier transform ion cyclotron resonance mass spectrometry. Anal. Chem. 81, 2688−2694.

4.9 Supplementary materials

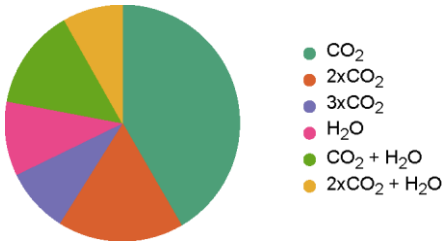

Figure S4.1: Relative abundances of main fragment ions from fragmentation experiments on DOM samples. Relative fragment intensities are displayed as percentage of total intensity of the fragment ions resulting from the neutral losses of carbon dioxide, water, and combinations thereof.

Table S4.1: Molecular characteristics of DOM derived from detected molecular formulae.

Sample	Mean mass* [m/z]	Black Carbon* [%]	Poly-phenols O-rich* [%]	Poly-phenols O-poor* [%]	Highly unsaturated* [%]	Aliphatic* [%]
AABW	404	0.07	0.27	2.60	91.07	4.94
EMW	404	0.04	0.23	2.35	91.54	5.05
NADW	402	0.07	0.35	2.87	90.75	4.82
North Sea	383	1.32	1.90	6.58	81.69	5.77
Lake	383	4.61	5.99	13.23	70.39	2.74

*Given are means weighted by corresponding signal intensities.

Manuscript IV:

Experimental evidence for structural diversity of deep-ocean dissolved organic matter

Maren Zark,[1] Jens Christoffers,[2] and Thorsten Dittmar[1]

This chapter corresponds to a full manuscript prepared for submission to *Geophysical Research Letters*.

[1] Institute for Chemistry and Biology of the Marine Environment (ICBM), Research Group for Marine Geochemistry (ICBM-MPI Bridging Group), Carl von Ossietzky University of Oldenburg, Carl-von-Ossietzky-Straße 9-11, 26129 Oldenburg, Germany.

[2] Institute for Chemistry (IfC), Carl von Ossietzky University of Oldenburg, Carl-von-Ossietzky-Straße 9-11, 26129 Oldenburg, Germany.

The manuscript “Experimental evidence for structural diversity of deep-ocean dissolved organic matter” (Manuscript IV) is focused on the question whether molecular formulae detected in deep-ocean DOM represent single or multiple chemical structures. By estimating the number of carboxyl groups from performing FT-ICR-MS fragmentation experiments we found indications for a high number of feasible isomers for each detected molecular formula in the DOM mixture, pointing towards high molecular diversity. The study was initiated by all authors. Field work, sample preparation, tandem ultrahigh resolution mass spectrometry analysis and statistical analysis was done by M. Zark and T. Dittmar. All authors performed interpretation of fragment ion mass spectra. M. Zark wrote the manuscript with significant input from T. Dittmar.

This manuscript is close to submission to *Geophysical Research Letters* and presented with adjusted formatting according to the style of this thesis.

Key Points

- Molecular formulae detected in DOM via FT-ICR-MS can be used to derive structural information on the occurring chemical compounds.
- Individual molecular formulae detected in deep-ocean DOM represent a number of isomers with similar elemental composition but different chemical structures.

5.1 Abstract

More than 642 Pg C are stored as refractory dissolved organic matter (DOM) in the global oceans and persist microbial degradation for thousands of years. Recent findings point towards dilution as the driver for long-term storage and individual substrate concentrations are assumingly too low for efficient microbial growth due to a highly diverse mixture of compounds. The number of identified molecular formulae from ultrahigh resolution FT-ICR-MS alone, however, is not sufficient to explain the proposed high diversity. The objective of this paper was to assess whether molecular formulae detected in deep-ocean DOM could be represented by a multitude of compounds with identical elemental composition. We performed tandem FT-ICR-MS on 63 individual molecular formulae isolated from deep-ocean DOM, which is considered representative for the refractory DOM fraction based on its great age. Our results suggest that the detected molecular formulae represent a high number of individual isomers with different chemical structures.

5.2 Introduction

Marine dissolved organic matter (DOM) represents a major carbon pool, similar in size to the amount of atmospheric carbon dioxide (Hansell et al., 2009; Hedges, 1992). Based on the reactivity within the water column, it can be divided into different fractions (Carlson and Ducklow, 1995; Hansell, 2013; Lancelot et al., 1993). Labile DOM is produced in the upper ocean layer by marine primary production (Carlson, 2002) and has very short turnover times of minutes up to days (Hansell et al., 2009). It serves as the driver for biological processes in the upper ocean, e.g. the microbial loop, ultimately fueling the entire marine food web (Carlson et al., 2007; Del Giorgio et al., 1997). The major fraction of marine DOM is bioresistant and persists in the oceans with a radiocarbon age of ~6000 yrs (Bauer et al., 1992; Williams and Druffel, 1987). This refractory DOM fraction occurs in homogenous concentrations throughout the water column where it is conserved comparable to salinity (Hansell and Carlson, 2013). It accounts for almost the entire dissolved organic carbon (DOC) content below 1000 m water depth (Hansell, 2013) and deep-ocean water is thus considered to be most representative for the refractory DOM fraction.

The fact that dissolved organic molecules that potentially offer energy and nutrients to marine microorganisms are not readily respired remains a conundrum. It was postulated that refractory DOM inheres intrinsic stability because it consists of mainly stable molecular structures that cannot be decomposed by microorganisms (Dittmar, 2015; Kattner et al., 2011). However, only very little is known about the structure of DOM and only less than a few percent of deep-sea DOM can be assigned to molecular structures (Kaiser and Benner, 2012, 2009) while the major part remains uncharacterized (Dittmar and Paeng, 2009; Hertkorn et al., 2006). This view is contradictory to the recent finding that the inhibition of microbial decomposition is revoked under elevated concentrations of deep-ocean DOM, suggesting that the persistence of DOM is independent from molecular structure (Arrieta et al., 2015). Accordingly, the concentration of individual DOM compounds may be below the chemoreceptive threshold for energy efficient uptake by marine microorganisms (Benner and Biddanda, 1998; Kattner et al., 2011).

Analyses using ultrahigh-resolution Fourier-transform ion cyclotron resonance mass spectrometry (FT-ICR-MS) detected more than 5000 individual molecular formulae in DOM (Dittmar and Stubbins, 2014; Hertkorn et al., 2006; Koch et al., 2005). However, as FT-ICR-MS resolves compounds with the same elemental composition many structural isomers may be represented by each detected molecular formula and the number of compounds present in refractory DOM could be several magnitudes higher (Dittmar, 2015).

To test whether molecular formulae detected in deep-ocean DOM represent individual compounds or a high number of molecular structures, we performed fragmentation experiments on model compounds and deep-ocean DOM via tandem FT-ICR-MS. In these intricate and time-intense experiments, compounds with the same molecular formula are physically isolated within the mass spectrometer and fragmented via controlled collision with argon. The molecular formulae of the fragments provide important hints on structural features of the original, unfragmented molecule and fragments resulting from neutral losses of CO_2 can be related to carboxyl functional groups (Witt et al., 2009).

5.3 Methods

5.3.1 Sample preparation

North Equatorial Pacific Intermediate Water (NEqPIW) was collected at the National Energy Laboratory of Hawaii Authority and processed as described in Green et al. (2014). In brief, water samples were filtered sequentially with 1 µm polypropylene filters (Causagard, Infiltec) and 0.2 µm polyether sulfone filters (Causa-PES, Infiltec). The DOC content was quantified via high-temperature catalytic oxidation method (Qian and Mopper, 1996) on a Shimadzu TOC-VCPH/CPN analyzer. Reference samples were analyzed with every run (Hansell DA, University of Miami, Florida) and the accuracy of the method is 2.8 ± 0.3 µmol C L^{-1}. Standard errors are typically < 2.5% (Stubbins and Dittmar, 2012). DOM was extracted for desalination via solid phase extraction (SPE) using a PPL resin (Bond-Elut, Agilent) and then eluted with methanol (HPLC grade, Sigma-Aldrich) as described in Dittmar et al. (2008). The extraction efficiency was 61% on a carbon basis (Green et al., 2014). For FT-ICR-MS analysis we diluted the

obtained extract to yield a final concentration of 20 mg C L^{-1} in a 1:1 mixture (v/v) of methanol (HPLC grade, Sigma-Aldrich) and ultrapure water. A broad band mass spectrum was obtained using a solariX Fourier-transform ion cyclotron resonance mass spectrometer with 15 Tesla magnet system (Bruker Daltonics) applied in ESI negative mode. After internal calibration, mass accuracies were < 0.2 Da and molecular formulae were assigned to the detected masses based on rules published in Koch et al. (2007).

5.3.2 Fragmentation experiments

Fragmentation experiments were carried out using the same Bruker solariX system. A total of 22 organic acids (Supplementary materials Table S5.1) on a mass range from 137 - 401 Da were analyzed as model compounds in solutions of 10 mg C L^{-1} in 1:1 (v/v) methanol (HPLC grade, Sigma-Aldrich) and ultrapure water. The individual ions were isolated and fragmented via controlled collision with argon. Ionization was ESI-negative and collision energy set to 15 V. 300 broad band scans were accumulated per run with 2 s ion accumulation time and data acquisition size was set to 4 Mword. Extracts of deep-ocean DOM were diluted to a final concentration of 100 mg C L^{-1} in 1:1 (v/v) methanol and ultrapure water. The fragmentation experiments were carried out under the same conditions as for organic acids but with 500 broad band scans. We isolated 12 individual nominal masses from the mass range 325 - 421 Da (Fig. 5.1a). Calibration of mass spectra was carried out externally with a mass list containing abundant CO_2 and H_2O neutral losses and combinations thereof following guidelines by Zark et al. (submitted). Several molecular formulae exist per nominal mass, but all fragments could be unambiguously associated to their respective original molecular formulae after assigning molecular formulae to the fragments (Cortés-Francisco and Caixach, 2015). We obtained fragmentation patterns for a total of 63 molecular formulae.

5.3.3 Number of carboxyl groups for a given molecular formula

We estimated the number of carboxyl groups from experimental evidence based on cumulative fragment intensities and from theoretical assumptions based on the assigned molecular formula of each component. Therefore, we calculated the

total signal intensity of fragments related to carboxyl groups (I_{COOH}) by adding up the signal intensities of molecular fragments resulting from the loss of CO_2, or multiples thereof (CO_2, $CO_2 + H_2O$, $CO_2 + CH_3OH$, $2\ CO_2$, $2\ CO_2 + H_2O$, $2\ CO_2 + CH_3OH$, $3\ CO_2$). Further, the total intensity of all fragments resulting from a specific molecular formula (I_{Tot}) was calculated by adding up the signal intensities from all abundant fragments (neutral losses H_2O, CH_3OH, CO_2, $CO_2 + H_2O$, $CO_2 + CH_3OH$, $2\ CO_2$, $2\ CO_2 + H_2O$, $2\ CO_2 + CH_3OH$, $3\ CO_2$) and the precursor ion. The estimated number of carboxyl groups [#COOH] can be assessed experimentally from the ratio I_{COOH}/I_{Tot} or theoretically from the molecular formula, based on O/H elemental ratio. For the transformation of the respective ratio to the number of carboxyl groups we assumed that compounds with minimum values for I_{COOH}/I_{Tot} and O/H do not contain carboxyl groups. We further assume that the maximum fragment intensity and elemental O/H ratio is associated to a maximum possible number of carboxyl groups [$\#COOH_{max}$]. Considering that always two oxygen atoms are bound for each carboxyl group, this maximum number is five for molecular formulae from deep-sea DOM (six for organic acids) because there was no molecular formula containing more than 11 (12) oxygen atoms. The calculation can be summarized as follows, with $x = I_{COOH}/I_{Tot}$ for the experimentally inferred number of carboxyl groups and x = O/H for the theoretical estimate.

$$[\#COOH] = \frac{(x_{min} - x)}{(x_{min} - x_{max})}\ [\#COOH_{max}]$$

Error bars consider the errors of signal intensities from individual fragment ions (noise + 5% signal intensity) and were calculated based on Gaussian error propagation. The range of possible numbers of carboxyl groups was derived for each compound from the number of oxygen atoms in the respective molecular formula (e.g. 5 oxygen atoms = 1 or 2 carboxyl groups).

5.4 Results and Discussion

From fragmentation experiments via FT-ICR-MS mostly neutral losses of one or multiples of CO_2 were observed (Figure 5.1b). This is evidence for abundant carboxylic functional groups (COOH) (Witt et al., 2009). Several other neutral losses concurred with a loss of CO_2, most prominently the loss of H_2O (derived

from hydroxyl or carboxyl groups). Overall, fragmentation patterns showed the same type of neutral losses for all isolated nominal masses (Supplementary materials Figure S5.1). The apparent high similarity of fragmentation patterns is remarkable, considering the fact that each molecular formula has a different elemental composition and, hence, different chemical structure. This suggests the occurrence of a large fraction of compounds with common structural features in deep-ocean DOM (Zark et al., submitted).

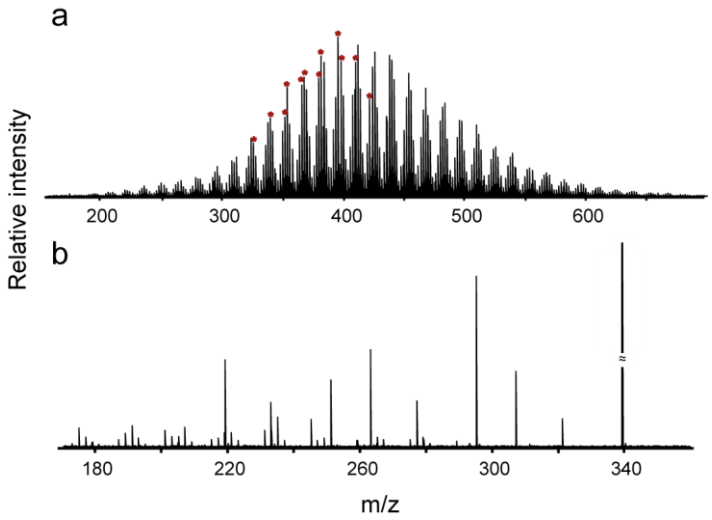

Figure 5.1 Results from ultrahigh resolution FT-ICR-MS fragmentation experiments of selected nominal masses detected within deep-ocean DOM. (a) Full range FT-ICR mass spectrum of extracted water from the deep ocean (electrospray ionization, negative mode), representative for refractory DOM. Red asterisks (*) mark nominal masses isolated for fragmentation experiments. (b) Fragmentation mass spectrum obtained from tandem FT-ICR-MS analysis shows the fragment ions for the nominal mass 339 Da. The fingerprint is similar to the other fragmented nominal masses regarding the type of occurring neutral losses

In a new approach to assess the chemical structure of the components in DOM in more detail, we estimated the number of carboxyl functional groups from both, molecular formulae (elemental composition) and from fragmentation experiments (chemical structures). In a given molecular formula, O/H ratios served as a measure for the number of carboxyl functional groups derived from elemental composition, while the weighted relative signal intensity of combined fragment ions related to CO_2 neutral loss (I_{COOH}/I_{Tot}) served as a measure for the number of carboxyl functional groups derived from molecular structure. This approach is based on two

assumptions. First, compounds in DOM containing no carboxyl groups presumably show no CO_2 losses whereas the maximum number is constraint by the maximum number of oxygen atoms in the molecular formulae. Second, the probability of containing carboxyl groups increases with oxygen density (O/C ratio) and decreases with saturation (H/C ratio) in a molecular formula. Consequently, the number of carboxyl groups is likely to increase linearly with the O/H ratio. For single substances, the estimated number of carboxyl groups from fragmentation experiments is expected to show high offset from the real number. The tendency of a specific compound to show neutral losses of CO_2 is largely dependent on the degree of intramolecular stabilization of the resulting fragment ion, and may thus be highly variable for compounds with different structures. Signal intensities of ions produced via fragmentation are therefore dependent on the number of carboxyl functional groups in the respective precursor ion, but ultimately determined by its chemical structure.

In order to test these theoretical assumptions, we fragmented 22 individual organic acids with different numbers of carboxyl functional groups as model compounds. The numbers estimated from O/H ratios (Figure 5.2a) showed good linear relation ($R^2 = 0.90$) to the real number of carboxyl groups in a given model compound, whereas the estimate based on fragment intensities I_{COOH}/I_{Tot} (Figure 5.2b) was not ($R^2 = 0.33$). Accordingly, high variability is observed between experimentally and theoretically inferred numbers of carboxyl groups (Fig. 5.2c) for single substances.

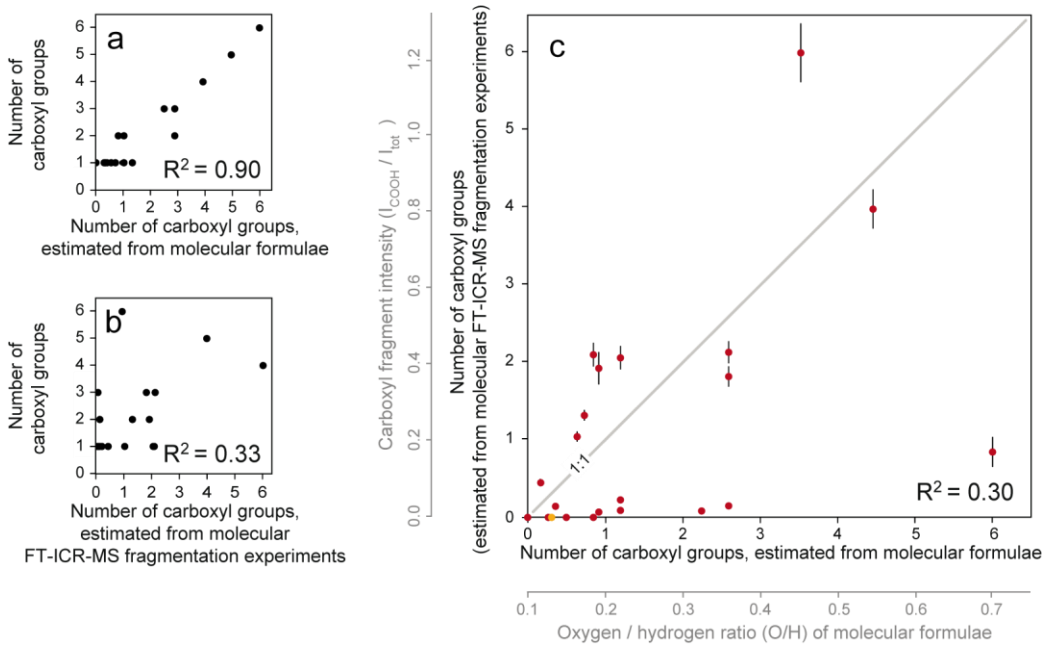

Figure 5.2 Fragmentation of individual organic acids as model compounds. Estimated numbers of carboxyl groups from a) elemental composition (O/H ratios), show good correlation with the true number, whereas the estimate from b) chemical structures via FT-ICR-MS fragmentation experiments (I_{COOH}/I_{Tot}) showed no clear relation. c) The combined estimated numbers are highly variable for model compounds, according to different structural properties. Each dot in the plot represents one molecular formula (n = 22). Yellow dots are molecular formulae containing nitrogen, red dots contain only carbon, hydrogen and oxygen. For clarity, we transformed the measured data (grey axes) into the estimated number of carboxyl groups for a given molecular formula (black axes).

We tested the developed approach with a natural deep-ocean DOM sample. A total of 63 signals with assigned molecular formulae were fragmented via tandem FT-ICR-MS. Different to the model compounds, a strong linear correlation ($R^2 = 0.94$) was observed for the number of carboxyl groups estimated from chemical structure and molecular formulae information (Figure 5.3). This is surprising as it implies that structural properties can be derived from molecular formula information alone. As a consequence of this highly linear correlation, it can be inferred that individual molecular formulae in deep-ocean DOM are not represented by single structures, because in case that each molecular formula corresponds to a single structure, the variability of total fragment intensities would be higher as it was shown with fragmentation of the 22 model compounds (Fig. 5.2c).

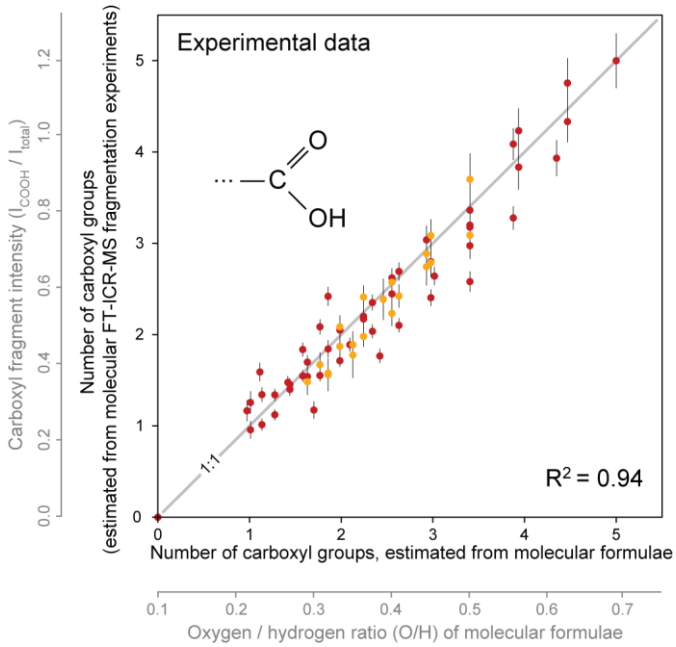

Figure 5.3 Number of carboxyl groups in deep-sea DOM compounds estimated from FT-ICR fragmentation experiments. The relative intensities of fragments with neutral CO_2 losses (I_{COOH}/I_{Tot}) correlate highly significantly with the O/H ratios of the respective molecular formulae. Each dot in the plot represents one molecular formula (n = 63). Yellow dots are molecular formulae containing nitrogen, red dots contain only carbon, hydrogen and oxygen. For clarity, we transformed the measured data (grey axes) into the number of estimated carboxyl groups for a given molecular formula (black axes).

If each molecular formula is represented by a stochastic subsample of all possible, stable structural isomers, however, the number of carboxyl groups associated to a molecular formula should represent average structural properties of these isomers. This average number should follow predictable patterns derived from molecular formulae information alone, similar to what we observed in our study (Figure 5.3). The strong correlation between the two fully independent parameters, one derived from molecular formulae (O/H) and one from FT-ICR-MS fragmentation (I_{COOH}/I_{tot}), is strong evidence for many isomers on each molecular formula. In addition, the obtained weighed fragment ion intensities I_{COOH}/I_{Tot} indicated a non-integer number of carboxyl functional groups. This is surprising at first view because any given molecule cannot contain a fraction of a carboxyl group and signal intensities of fragments should follow a stepwise pattern for single structures (Fig. 5.4). However, if each FT-ICR-MS peak is represented by multiple isomers, then a non-integer average number of carboxyl groups is the logical

consequence. Compounds containing nitrogen followed the same trend as the other compounds.

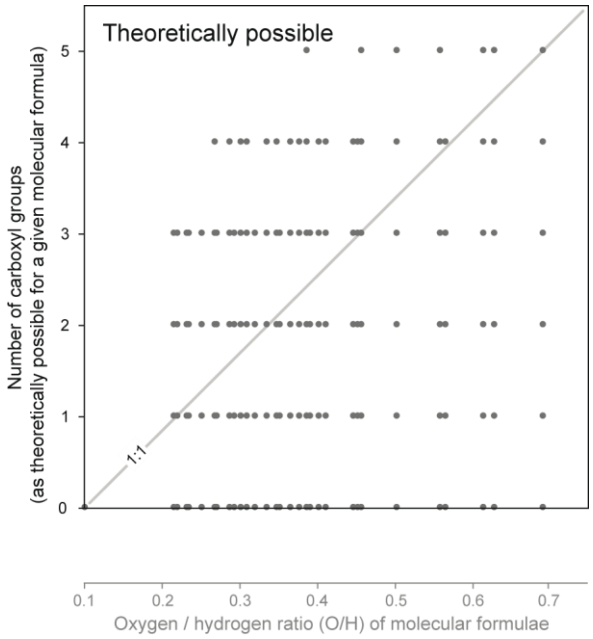

Figure 5.4 Range of possible numbers of carboxyl groups for a respective O/H ratio. The integer numbers of theoretically possible carboxyl groups are represented by grey dots and were inferred from the oxgen content in a given molecular formula.

Recent findings from NMR spectroscopy (Hertkorn et al., 2013) reported a high number of different structural units detected in DOM and are hence consistent with a high structural diversity in DOM. This, together with the fact that more than 10,000 individual molecular formulae were detected in FT-ICR-MS experiments (Dittmar and Stubbins, 2014; Hertkorn et al., 2006; Koch et al., 2005) for different DOM samples, indicates that the diversity of DOM could be as high as millions of different compounds (Dittmar, 2015) leading to exceedingly low concentrations of the individual components. Arrieta et al. (2015) found that natural bacterial communities can make use of DOM substrates in sufficiently high concentrations. The results provide strong evidence that extreme substrate dilution is supporting the stability of DOM compounds. Hence, refractory DOM is likely to represent an overall homogenous background signal with a high number of individual compounds. This finding is consistent with experimental observations on DOM samples from a range of different water masses (Hansman et al., 2015; Zark et al.,

submitted). Our results confirm the findings by Arrieta et al. (2015), and represent first experimental evidence for the low abundance of individual compounds within a highly diverse mixture, based on structural analysis of individual components.

In conclusion, our analyses revealed that structural information on DOM compounds can be inferred from simple elemental composition. This is not the case for single structures as it was demonstrated by fragmentation of model compounds and likely due to averaging of structural properties among a great number of isomers. The combined results provide strong experimental evidence for the fact that individual molecular formulae in deep-ocean DOM are represented by a high number of isomers with identical elemental composition.

5.5 Acknowledgements

We thank Ina Ulber and Matthias Friebe for technical assistance with sample preparation and analysis of DOC concentrations. We further thank Kathrin Klaproth for assistance with FT-ICR-MS analysis.

5.6 References

Arrieta, J.M., Mayol, E., Hansman, R.L., Herndl, G.J., Dittmar, T., Duarte, C.M., 2015. Dilution limits dissolved organic carbon utilization in the deep ocean. Science 348, 331−333.

Bauer, J.E., Williams, P.M., Druffel, E.R.M., 1992. ^{14}C activity of dissolved organic carbon fractions in the north-central Pacific and Sargasso Sea. Nature 357, 667−670.

Benner, R., Biddanda, B., 1998. Photochemical transformations of surface and deep marine dissolved organic matter: effects on bacterial growth. Limnol. Oceanogr. 43, 1373−1378.

Carlson, C.A., 2002. Production and removal processes, in: Carlson, D.A., Hansell, C.A., (Eds.), The biogeochemistry of marine dissolved organic matter. Academic Press, San Diego, pp. 91−151.

Carlson, C.A., Del Giorgio, P.A., Herndl, G.J., 2007. Microbes and the dissipation of energy and respiration: from cells to ecosystems. Oceanography 20, 89−100.

Carlson, C.A., Ducklow, H.W., 1995. Dissolved organic carbon in the upper ocean of the central equatorial Pacific Ocean, 1992: daily and finescale vertical variations. Deep-Sea Res. Pt. II, 42, 639−656.

Cortés-Francisco, N., Caixach, J., 2015. Fragmentation studies for the structural characterization of marine dissolved rganic matter. Anal. Bioanal. Chem. 407, 2455−2462.

Del Giorgio, P.A., Cole, J.J., Cimbleris, A., 1997. Respiration rates in bacteria exceed phytoplankton production in unproductive aquatic systems. Nature 385, 148−151.

Dittmar, T., Koch, B.P., Hertkorn, N., Kattner, G., 2008. A simple and efficient method for the solid-phase extraction of dissolved organic matter (SPE-DOM) from seawater. Limnol. Oceanogr.: Methods 6, 230−235.

Dittmar, T., Paeng, J., 2009. A heat-induced molecular signature in marine dissolved organic matter. Nat. Geosci. 2, 175−179.

Dittmar, T., Stubbins, A., 2014. Dissolved organic matter in aquatic systems, in: Birrer, B., Falkowski, P., Freeman, K., (Eds.), Treatise of Geochemistry, 2nd edition. Academic Press, Oxford, pp. 125−156.

Dittmar, T., 2015. Reasons behind the long-term stability of dissolved organic matter, in: Hansell, D.A., Carlson, C.A., (Eds.), The biogeochemistry of marine dissolved organic matter, 2nd edition. Academic Press, Burlington, pp. 369−388.

Green, N.W., Perdue, E.M., Aiken, G.R., Butler, K.D., Chen, H., Dittmar, T., et al., 2014. An intercomparison of three methods for the large-scale isolation of oceanic dissolved organic matter. Mar. Chem. 161, 14−19.

Hansell, D.A., 2013. Recalcitrant dissolved organic carbon fractions. Annu. Rev. Mar. Sci. 5, 421–445.

Hansell, D.A., Carlson, C.A., 2013. Localized refractory dissolved organic carbon sinks in the deep ocean. Global Biogeochem. Cycles 27, 705−710.

Hansell, D.A., Carlson, C.A., Repeta, D.J., Schlitzer, R., 2009. Dissolved organic matter in the ocean: a controversy stimulates new insights. Oceanography 22, 202−211.

Hansman, R.L., Dittmar, T., Herndl, G., 2015. Conservation of dissolved organic matter molecular composition during mixing of the deep water masses of the northeast Atlantic Ocean. Mar. Chem. 177, 288−297.

Hedges, J.I., 1992. Global biogeochemical cycles: progress and problems. Mar. Chem. 39, 67−93.

Hertkorn, N., Benner, R., Frommberger, M., Schmitt-Kopplin, P., Witt, M., Kaiser, K., et al., 2006. Characterization of a major refractory component of marine dissolved organic matter. Geochim. Cosmochim. Ac., 70, 2990−3010.

Hertkorn, N., Harir, M., Koch, B.P., Michalke, B., Schmitt-Kopplin, P., 2013. High-field NMR spectroscopy and FTICR mass spectrometry: powerful discovery tools fort he molecular level characterization of marine dissolved organic matter. Biogeosciences 10, 1583−1624.

Kaiser, K., Benner, R., 2009. Biochemical composition and size distribution of organic matter at the Pacific and Atlantic time-series stations. Mar. Chem. 113, 63−77.

Kaiser, K., Benner, R., 2012. Organic matter transformations in the upper mesopelagic zone of the North Pacific: chemical composition and linkages to microbial community structure. J. Geophys. Res. Oceans 117, C01023.

Kattner, G., Simon, M., Koch, B.P., 2011. Molecular characterization of dissolved organic matter and constraints for prokaryotic utilization, in: Jiao, N., Azam, F., Sanders, S., (Eds.), Microbial carbon pump in the ocean. American Association for the Advancement of Science, pp. 60−61.

Koch, B.P., Witt, M., Engbrodt, R., Dittmar, T., Kattner, G., 2005. Molecular formulae of marine and terrigenous dissolved organic matter detected by electrospray ionization Fourier transform ion cyclotron resonance mass spectrometry. Geochim. Cosmochm. Ac. 13, 3299−3308.

Koch, B.P., Dittmar, T., Witt, M., Kattner, G., 2007. Fundamentals of molecular formula assignment to ultrahigh resolution mass data of natural organic matter. Anal. Chem. 79, 1758−1763.

Lancelot, C., Fasham, M., Legendre, L., Radach, G., Scott, M., Kirchman, L., 1993. Dissolved organic matter in biogeochemical models of the ocean, in: Evans, G., Fasham, M.J.R., (Eds.), Towards a model of ocean biogeochemical processes. Springer, pp. 209−225.

Qian, J., Mopper, K., 1996. Automated high-performance, high-temperature combustion total organic carbon analyzer. Anal. Chem. 68, 3090−3097.

Stubbins, A., Dittmar, T., 2012. Low volume quantification of dissolved organic carbon and dissolved nitrogen. Limnol. Oceanogr.: Methods 10, 347−352.

Williams, P.M., Druffel, E.R.M., 1987. Radiocarbon in dissolved organic matter in the central North Pacific Ocean. Nature 330, 246−248.

Witt, M., Fuchser, J., Koch, B.P., 2009. Fragmentation studies of fulvic acids using collision induced dissociation Fourier transform ion cyclotron resonance mass spectrometry. Anal. Chem. 81, 2688−2694.

Zark, M., Dittmar, T. Universal molecular structures in natural dissolved organic matter. Proc. Natl. Acad. Sci. U S A, submitted.

5.7 Supplementary materials

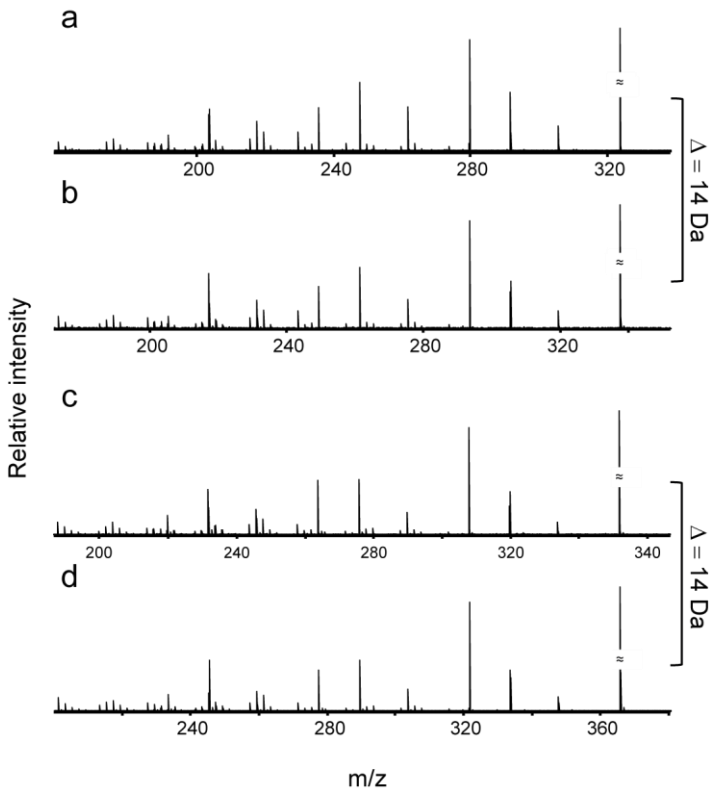

Figure S5.1 Fingerprint FT-ICR fragmentation mass spectra for nominal masses isolated from deep-ocean DOM. Fragment ions are displayed in their relative intensity for the nominal masses (a) 325 Da, (b) 339 Da, (c) 351 Da, and (d) 365 Da.

Table S5.1 Organic acids fragmented as model compounds via tandem FT-ICR-MS analysis with numbers of carboxyl groups present in the model compound, and estimated numbers from fragmentation [$\#COOH_{Frag}$] and from molecular formula information [$\#COOH_{O/H}$].

Compound name	Formula	Carboxyl groups	$\#COOH_{Frag}$	$\#COOH_{O/H}$
myristic acid	$C_{14}H_{28}O_2$	1	1.92	0.00
adipinic acid	$C_6H_{10}O_4$	2	0.00	1.02
mandelic acid	$C_8H_8O_3$	1	0.00	0.94
4-phenylbutyric acid	$C_{10}H_{12}O_2$	1	0.45	0.30
α-phenylcinnamic acid	$C_{15}H_{12}O_2$	1	1.04	0.30
2-benzoylbenzoic acid	$C_{14}H_{10}O_3$	1	0.15	0.71
tartaric acid	$C_4H_6O_6$	2	0.08	2.89
citric acid	$C_6H_8O_7$	3	1.32	2.50
pimelic acid	$C_7H_{12}O_4$	2	0.00	0.81
cinnamic acid	$C_9H_8O_2$	1	0.07	0.56
4-hydroxy-3-methoxycinnamic acid	$C_{10}H_{10}O_4$	1	2.06	1.02
4-hydroxybenzoic acid	$C_7H_6O_3$	1	0.09	1.33
vanillic acid	$C_8H_8O_4$	1	0.23	1.33
4-hydroxy-3,5-dimethoxy benzoic acid	$C_9H_{10}O_5$	1	1.82	1.33
1,2,3-benzenetricarboxylic acid	$C_9H_6O_6$	3	2.13	2.89
1,3,5-benzenetricarboxylic acid	$C_9H_6O_6$	3	6.00	2.89
1,2,4,5-benzenetetracarboxylic acid	$C_{10}H_6O_8$	4	3.98	3.93
benzenepentacarboxylic acid	$C_{11}H_6O_{10}$	5	0.95	4.96
mellitic acid	$C_{17}H_6O_{12}$	6	0.14	6.00
9-anthracenecarboxylic acid	$C_{15}H_{10}O_2$	1	0.00	0.40
phenylalanine	$C_9H_{11}NO_2$	1	2.10	0.34
4-hydroxycinnamic acid	$C_9H_8O_3$	1	0.00	0.94

6. Concluding remarks and perspectives

6.1 Conclusion

The focus of this thesis was to achieve a better understanding of the impact of ocean acidification on the dissolved organic matter pool in different marine environments. We investigated ocean acidification induced changes of the DOM pool on the concentration and molecular composition level in two large scale mesocosm studies. One study was performed in a coastal area in a Swedish fjord and the other in the oligotrophic subtropical Atlantic Ocean off Gran Canaria. Additional fragmentation experiments on DOM aimed at a better understanding of the molecular structure of DOM. The results of this thesis work provide some answers to the previously stated research questions and can be summarized as following:

(1) What are the regional and overall impacts of ocean acidification on DOM accumulation and molecular composition?

The results obtained in the two mesocosm studies in a Swedish fjord in 2013 (Manuscript I) and off Gran Canaria in 2014 (Manuscript II) indicate that ocean acidification will have no detectable effects under a business-as-usual scenario described in the latest IPCC report (IPCC, 2013) until the end of the century. The absence of significant effects was the same for both environments under elevated target pCO_2 conditions up to 1000 µatm. Starting at pCO_2 target levels of 1250 µatm we observed indications for enhanced DOC accumulation under ocean acidification conditions. However, this observation was not significant due to the lack of replicates. Further, as these levels were not covered in the experimental design of the study conducted in Sweden, we cannot determine the difference between threshold concentrations for both environments. No effects were observed in both studies on the molecular composition over the succession of phytoplankton blooms. There were clear imprints of new production on the composition but the produced and consumed compound were the same for all pCO_2 treatments. Overall, the effects of elevated pCO_2 on the DOM pool are presumably small over the succession of phytoplankton blooms in a natural environment.

Together with many collaborators, we performed the longest mesocosm study this far and successfully covered a full cycle of new production over two phytoplankton blooms. Out of the challenges that were stated by Riebesell and Gattuso in a recent publication for future ocean acidification research, both performed mesocosm studies addressed point (2), namely expanding experiments from single species to community levels, and (3), covering not only acclimation of organisms but adaption (Riebesell and Gattuso, 2015).

Point (1) of the challenges, the expansion of experiments from single to multiple drivers, however, was not yet investigated. As temperature was observed to be a stronger driver than reduced seawater pH in many studies (Paul et al., 2015; Taucher et al., 2015), it could also have a stronger influence on the molecular DOM composition. This could be an important factor for future predictions of the global carbon cycle as warming is expected to accompany ocean acidification on the same time scales. A rise in the average ocean surface temperature between 1 and 5 °C is expected for this century according to the latest IPCC report (IPCC, 2013). Therefore, it is important to include this driver in further investigations. Further, experiments with more replicates would presumably improve our current knowledge to a great extent because there is a high need for reproducible and robust data that can be used for future ocean models. However, this might not be feasible in the near future due to high costs.

(2) Are there natural differences in DOM molecular composition among aquatic environments in terms of its chemical structure?

The results obtained from fragmentation FT-ICR-MS experiments on DOM from very different environments (Manuscript III) indicate an overall high structural similarity. Fragmentation of 63 individual nominal masses lead to similar fingerprint patterns for all DOM samples with some additional small fragments that were site-specific. Hence, the underlying conditions are comparable for future effects of, e.g., ocean acidification on DOM molecular composition. Nevertheless, local differences in the microbial community structure and the other physical factors presumably play an important role in this sense.

(3) To what extent do common molecular formulae detected in FT-ICR-MS represent identical chemical structures in the different oceanic environments?

The fragmentation experiments described in Manuscript III showed that common DOM molecular formulae have undistinguishable structural fingerprints across the globe, providing strong evidence for the hypothesis that similarity on a molecular formula level also extends towards a molecular structural level. We propose that molecular diversification of DOM over the course of degradation ultimately leads to a large pool of compounds with undistinguishable molecular properties. This presumably refractory, common fraction of DOM compounds is hence potentially affected in a similar way by environmental stressors such as ocean acidification.

(4) Are detected molecular formulae representing single structures or a higher number of different isomers?

In a novel approach using tandem FT-ICR-MS analysis of deep-ocean DOM, the number of carboxyl groups was inferred from the intensity of fragment ions related to neutral losses of CO_2 (Manuscript IV). The results suggest that the detected molecular formulae are represented rather by a high number of isomers than single structures. As high diversity leads to averaging of structural properties on the bulk level it seems consistent that similar fragmentation pattern were observed for the 63 fragmented nominal messes in deep-ocean DOM (Manuscript IV) and in DOM samples from different aquatic environments (Manuscript III). The combined studies support the molecular diversity hypothesis, proposing that the long-term turnover of deep-sea DOM is related to dilution of substrates to concentrations too low for energy efficient uptake by microbes.

This finding is especially important in the context of potential climate feedbacks that could emerge as a response to molecular changes of the DOM pool by environmental stressors such as ocean acidification. If the refractory character of the major fraction of DOM was due to very stable structures rather than high dilution of compounds, structural changes induced by changing physical or biological conditions, similar to the fast decomposition of DOM in permafrost for

example (Dorrepaal et al., 2009), could lead to rapid remineralization. Due to the great size of the refractory carbon fraction, this process could potentially cause major perturbations of the earth's climate (Sexton et al., 2011). Our results, in contrast, suggest that only individual in-excess produced compounds become accessible by marine microorganisms until the inital background-level of concentrations is restored.

6.2 Future perspectives

In order to further advance our understanding of the cycling of DOM, it will be important to perform an integrated assessment including other data sets that were obtained by collaborators within the two mesocosm experiments. It will be crucial to disentangle the relationships between microbial communities and the DOM composition under future elevated CO_2 concentrations in order to gain insights into the interplay of closely coupled production and consumption. So far, we have considered DOM and the microbial communities as separate units. This approach does not take into account that microorganisms and substrate compounds interact (Romano et al., 2014; Shabarova et al., 2014). In a next step, multivariate statistical tools may be appropriate to detect functional linkages between the microbial community and the production and turnover of DOM in the mesocosm experiments. Next-generation sequencing approaches performed to elucidate the microbial community during the mesocosm studies provide the necessary high-resolution insights into the structure of the potential DOM consumers. The interpretation of detected operational taxonomic units (OTUs) together with FT-ICR-MS data on the molecular composition of the DOM pool would be an appropriate tool for further in-depth analyses of the interplay of organisms with the DOM "geometabolome", whose individual components differ in reactivity and their functional role (Osterholz et al., 2015).

Finally, it will be important to implement the obtained information into existing future ocean models. By close interdisciplinary collaboration together with ecosystem modelers it could be possible to integrate microbial community function and DOM cycling into existing models in order to assess the future changes of the global DOM pool and the co-occurring effects on the global carbon cycle.

6.3 References

Dorrepaal, E., Toet, S., van Logtestijn, R.S.P., Swart, E., van de Weg, M.J., Callaghan, T.V., Aerts, R., 2009. Carbon respiration from subsurface peat accelerated by climate warming in the subarctic. Nature 460, 616−619.

IPCC, 2013. Climate Change 2013: The Physical Science Basis. Contribution of Working Group 1 to the Fifth Assessment Report of the Intergovernmental Panel on Climate Change, in: Stocker, T.F., Qin, D., Plattner, G.-K., Tignor, M., Allen, S.K., Boschung, J., Nauels, A., Xia, Y., Bex, V., Midgley, P.M., (Eds.), Cambridge University Press, Cambridge and New York, p. 1096.

Osterholz, H., Singer, G., Wemheuer, B., Daniel, R., Simon, M., Niggemann, J., et al., 2015. Deciphering associations between dissolved organic molecules and bacterial communities in a pelagic marine system. ISME J., in press.

Paul, C., Matthiessen, B., Sommer, U., 2015. Warming, but not enhanced CO_2 concentration, quantitatively and qualitatively affects phytoplankton biomass. Mar. Ecol. Prog. Ser. 528, 39−51.

Riebesell, U., Gattuso, J.-P., 2015. Lessons learned from ocean acidification research. Nature Clim. Change 5, 12−14.

Romano, S., Dittmar, T., Bondarev, V., Weber, R.J.M., Viant, M.R., Schulz-Vogt, H.N., 2014. Exo-metabolome of *Pseudovibrio* sp. FO-BEG1 analyzed by ultra-high resolution mass spectrometry and the effect of phosphate limitation. PLoS One 9, e96038.

Sexton, P.F., Norris, R.D., Wilson, P.A., Pälike, H., Westerhold, T., Röhl, U., et al., 2011. Eocene global warming events driven by ventilation of oceanic dissolved organic carbon. Nature 471, 349−352.

Shabarova, T., Villiger, J., Morenkov, O., Niggemann, J., Dittmar, T., Pernthaler, J., 2014. Bacterial community structure and dissolved organic matter in repeatedly flooded subsurface karst water pools. FEMS Microbiol. Ecol. 89, 111−126.

Taucher, J., Jones, J., James, A., Brzezinski, M.A., Carlson, C.A., Riebesell, U., et al., 2015. Combined effects of CO_2 and temperature on carbon uptake and

partitioning by the marine diatoms *Thalassiosira weissflogii* and *Dactyliosolen fragilissimus*. Limnol. Oceanogr. 60, 901−919.

Curriculum vitae

Name: Maren Zark (*née Stumm*)

Date of birth: March 12, 1987

Place of birth: Rotenburg Wümme, Germany

Education

2006 – 2009	B.Sc. in Chemistry, University of Oldenburg (Germany)
2009 – 2011	M.Sc. in Chemistry, University of Oldenburg (Germany)
2010 – 2011	Graduate student exchange (6 months), University of Wyoming (USA)
Since 09/2012	Ph.D. student Research Group for Marine Geochemistry (ICBM-MPI Bridging Group), University of Oldenburg (Germany)

Scholarships

2010	"Step Out" Scholarship for International Internships, University of Oldenburg
2013	PhD Scholarship, Heinz Neumüller Foundation

Publications, peer-reviewed

Zark, M., Riebesell, U., Dittmar, T., 2015. Effects of ocean acidification on marine dissolved organic matter are not detectable over the succession of phytoplankton blooms. Science Advances 1, e1500531.

Zark, M., Dittmar, T. Universal molecular structures in natural dissolved organic matter. Proc. Natl. Acad. Sci. U S A, submitted.

Zark, M., Broda, N.K., Riebesell, U., Dittmar, T. Dissolved organic matter dynamics during an oligotrophic ocean acidification experiment using large scale mesocosms. Limnol. Oceanogr., in preparation.

Zark, M., Christoffers, J., Dittmar, T. Experimental evidence for structural diversity of deep-ocean dissolved organic matter. Geophys. Res. Lett., in preparation.

Bach, L.T., Taucher, J., Boxhammer, T., Ludwig, A., The Kristineberg KOSMOS Consortium, Achterberg, E., Alguero-Muniz, M., Anderson, L., Bellworthy, J., Büdenbender, J., Czerny, J., Ericson, Y., Esposito, M., Fischer, M., Haunost, M., Hellemann, D., Horn, H., Hornick, T., Meyer, J., Sswat, M., **Zark, M.**, Riebesell, U. Influence of ocean acidification on a natural winter-to-summer plankton succession: First insights from a long-term mesocosm study draw attention to periods of nutrient limitation. PLoS ONE, in preparation.

Other publications

Zark, M., Dittmar, T., Riebesell, U., 2015. Dissolved organic matter molecular composition and concentrations from a large scale mesocosm study KOSMOS 2013 (Kristineberg) on ocean acidification. Dataset #846137, doi:10.1594/PANGAEA.846137).

Zark, M., Broda, N.K., Riebesell, U., Dittmar, T. Molecular dissolved organic matter composition in the oligotrophic Atlantic Ocean off Gran Canaria during a mesocosm study on ocean acidification (KOSMOS 2014). PANGAEA Data Publication, in preparation.

Seibt, M., Stratmann, T., **Stumm, M.**, 2013. Dissolved organic matter (DOM) – small in size but large in impact: basis to life in the world's ocean, in: Einsporn, M.H., Wiedling, J., Beilfuss, S., (Eds.), Recent impulses to marine science and engineering – From coast to deep sea: multiscale approaches to marine sciences. DGM publishing company, Hamburg, pp. 18−28.

Conference contributions

Bergen, B., Endres, S., Engel, A., **Zark, M.**, Dittmar, T., Sommer, U., Jürgens, K. Effect of acidification and warming on planktonic bacterial communities during two seasonal phytoplankton bloom mesocosms. SAME14, Uppsala, Sweden, August 2015 (Poster).

Zark, M., Riebesell, U., Dittmar, T. Effects of ocean acidification on formation and turnover of DOM in a Swedish Fjord. Association for the Sciences of Limnology and Oceanography (ASLO), Granada, Spain, February 2015 (Talk).

Stumm, M., Christoffers, J., Dittmar, T. First steps towards structure determination of marine dissolved organic matter (DOM). YOUMARES 3 German Young Marine Scientist Meeting, Lübeck, Germany, September 2012 (Talk).

Author’s declaration

I hereby declare that I wrote this thesis on my own and without any unnamed sources or aid. Where I have quoted from the work of others, the source is always given. I confirm that I followed the general principles of good scientific work and publishing, as they are specified in the guidelines of good scientific practice of the Carl von Ossietzky University of Oldenburg

Eidesstattliche Erklärung

Hiermit versichere ich, dass ich diese Arbeit selbstständig verfasst und keine anderen als die angegebenen Quellen und Hilfsmittel benutzt habe. Außerdem versichere ich, dass ich die allgemeinen Prinzipien wissenschaftlicher Arbeit und Veröffentlichung, wie sie in den Leitlinien guter wissenschaftlicher Praxis der Carl von Ossietzky Universität Oldenburg festgelegt sind, befolgt habe.

Oldenburg, den 17.12.2015

(Maren Zark)